UNIVERSITY OF CALIFORNIA, SAN DIEGO

Multi-scale dynamics of coral reef complex systems: building the path towards models of peopled reefscapes

A dissertation submitted in partial satisfaction of the
requirements for the degree
Doctor of Philosophy

in

Oceanography

by

Marlene Brito-Millan

Committee in charge:

Professor Stuart A Sandin, Co-Chair
Professor Brad Werner, Co-Chair
Professor Gordon C McCord
Professor Dylan E McNamara
Professor Jennifer E Smith
Professor Daniel Widener

2017

The dissertation of Marlene Brito-Millan is approved, and it is acceptable in quality and form for publication on microfilm and electronically:

_____

_____

_____

_____

_____
Co-Chair

_____
Co-Chair

University of California, San Diego

2017

DEDICATION

To the long lineage of inspiring, revolutionary mothers in my family,
especially to my great grandmother, the Mexican revolutionary,
Maria Ocampo Garcia

EPIGRAPH

Remember that no matter what it looks like, we are safe, secure, protected and guided by our ancestors whose love we breathe...

TABLE OF CONTENTS

LIST OF FIGURES

LIST OF TABLES

ACKNOWLEDGMENTS

Este doctorado no hubiera sido posible sin el apoyo de mis co-asesores, mi familia y mi comunidad. Mis co-asesores pacientemente me guiaron en esta jornada académica y siempre se los agradeceré porque han cambiado mi vida y la de mi familia por siempre. El entusiasmo inquebrantable y la confianza de Stuart en mi capacidad en el campo me abrió las puertas al mundo cautivador de sistemas de arrecifes coralinos. La paciencia, fortaleza, sabiduría, y humildad de Brad fueron fundamental en mi formación como científica interdisciplinaria que trae una perspectiva radical y llena de esperanza en las voces de la gente marginalizada, porque son l@s que más apasionadamente luchan y reclaman nuestra humanidad colectiva.

Mi pareja, Carlos, tuvo que hacerla de papa soltero de nuestros hijos especialmente en los últimos meses. Aunque fue un reto difícil para ti en estar solo y para mí al estar lejos de ustedes, ¡Si se pudo¡ Te amo. A mi suegra querida, Doña Eva, le agradezco su entrega y apoyo con cuidar a mi niño, Atzin, para que pudiera enfocarme en mi examen de candidatura. Mi mamá y papá que trabajaron duro en fábricas para poder darme la posibilidad de llegar hasta aquí, nunca dudando de mi capacidad y animándome a cada paso. Gracias, los amo. Mi hermana, Cynthia, siempre fue mi fuerte reanimándome en los momentos que pensaba yo no poder más. ¡Te amo hermana, eres una inspiración¡ A mi hermano, Angel, le doy gracias por su ejemplo de persistencia y dedicación sin dejar de vivir y disfrutar. A mis amig@s y ment@res les agradezco de todo corazón...Elisa Maldonado, Jessica Blanton, Leslie Quintanilla, América Martinez, Eva Sanchez, Tessa Pierce, Janin Guzman Morales, Manuel Belmonte, Rishi Sugla, Osinachi Ajoku, Amrah Salomon, Erendira Aceves Bueno, Melvin Jimenez, Isabel Canto, Michael Navarro, Hao Ye, Geoff Gearheart, Nadia Rubio-Cisneros, Anai Novoa, Jessica Ng, Adriana Barraza, Gaby Reza, Lucy Terrazas, Fernanda Rios, Cristiane Palaretti, Anne Friere de Carvalho, Kate Furby, Emily Kelly, Beverly French, Abby Cannon y Jill Harris. Gracias a todos ustedes mis compañer@s en la lucha por un mundo transformado, porque con ustedes dejé de sentirme sola en la academia y pude reenfocar las cosas que en realidad valen para mí que son nuestros lazos y las luchas que nos

solidarizan. Mis hijos, Atzin y Amayru, y mis sobrinas, Jocelyn y Marlene, siempre fueron y serán mi gran sacrificio y mi esperanza por un futuro donde juntos podamos cosechar este logro y las puertas que nos abre. Juntos seguiremos en la lucha para "*construir mundos diferentes donde quepan muchos mundos verdaderos con verdades*" (-Escuelita Zapatista de Oventic).

-

This doctorate would not have been possible without the support of my co-advisors, my family, and my community. My co-advisors patiently guided me on this academic journey and I will always be thankful as you have changed my and my family's life forever. Stuart's unwavering enthusiasm and trust in my capacity in the field opened up the doors to the captivating world of coral reef systems. Brad's patience, strength, wisdom, and humility were fundamental in my formation as an interdisciplinary scientist that brings a radical perspective full of hope in the voices of the most marginalized peoples because they are the most passionate in the struggle reclaiming our collective humanity.

My partner, Carlos, had to become a single father of our two children especially these last few months. Even though being alone was a difficult challenge for you and being away from you all was heart wrenching for me, we did it! I love you. To my mother-in-law, Doña Eva, I thank you for your dedication and support with taking care of my son, Atzin, so that I could focus on advancing to candidacy. My mother and father, who worked hard in factories to provide me with the possibility of making it this far without ever doubting my capacity and encouraging me at every step, thank you. I love you both. My sister, Cynthia, always was a source of strength that reignited me in the moments that I thought I could not go on. I love you sister, you are an inspiration. My brother, Angel, thank you for your example of persistence and dedication without stopping the fun things that make you feel alive. To my friends and mentors, I thank you with all my heart: Elisa Maldonado, Jessica Blanton, Leslie Quintanilla, América Martinez, Eva Sanchez, Tessa Pierce, Janin Guzman Morales, Manuel Belmonte, Rishi Sugla, Osinachi Ajoku, Amrah Salomon, Erendira Aceves Bueno, Melvin Jimenez, Isabel Canto, Michael Navarro, Geoff Gearheart, Nadia Rubio-Cisneros, Anai Novoa, Jessica Ng,

Adriana Barraza, Gaby Reza, Lucy Terrazas, Fernanda Rios, Cristiane Palaretti, Anne Freire de Carvalho, Kate Furby, Emily Kelly, Beverly French, Abby Cannon and Jill Harris. Thank you to all my homies in the struggle for a transformed world because with you I stopped feeling alone in academia and was able to re-focus on the things that really matter to me, which are our ties and the struggles that solidarize us. My children, Atzin and Amayru, and my nieces, Jocelyn and Marlene, always were and are my greatest sacrifice and my hope for a future where together we can bring to fruit this accomplishment and the doors that it opens. Together let us continue in the struggle to "construir mundos diferentes donde quepan muchos mundos verdaderos con verdades" (-Escuelita Zapatista de Oventic).

Chapter 2, in full, is material being prepared for submission to Marine Ecological Progress Series: Brito-Millan, M, MJA Vermeij, EA Alcantar, and SA Sandin. Aspects of coral colony size-dependent change and fission-fusion dynamics. The dissertation author was the primary investigator and author of this paper.

Chapter 3, in full, is material prepared for submission to Proceedings of the Royal Society B: Brito-Millan, M, BT Werner, SA Sandin, and D McNamara. Influence of Aggregation on Benthic Coral Reef Spatio-temporal Dynamics. The dissertation author was the primary investigator and author of this paper.

Chapter 4, in full, is material being prepared for submission to Physical Review E: Brito-Millan, M and BT Werner. A continuum model for coral reef benthic dynamics.The dissertation author was the primary investigator and author of this paper.

VITA

2006	**Bachelor of Science, Northeastern Illinois University**
2008	UC San Diego Fellow
2010	NSF Graduate Research Fellow, Ford Foundation Predoctoral Fellow
2014	**Master of Science, University of California, San Diego**
2015	UC President's Dissertation Year Fellow
2017	**Doctor of Philosophy, University of California, San Diego**

ABSTRACT OF THE DISSERTATION

Multi-scale dynamics of coral reef complex systems: building the path towards models of peopled reefscapes

by

Marlene Brito-Millan

Doctor of Philosophy in Oceanography

University of California, San Diego, 2017

Professor Stuart A Sandin, Co-Chair
Professor Brad Werner, Co-Chair

Coral reef benthic communities form a critical part of coral reef systems linked to human societies. Using a complex systems approach that highlights interdependencies between substrate-bound organisms competing for space and ecological patterns that constrain demographic and competitive processes, the coral reef benthic system is dynamically characterized from the coral colony scale to the island scale with numerical models and data analysis techniques.

In Chapter 2, I quantify and analyze reef-building coral colony change with colony areal coverage and longevity. Using over 4,300 Caribbean colonies measured over 4.5 years, proportional change in area of smaller colonies was found to be greater than for larger ones, following expectations of allometrically constrained

growth. In terms of longevity, larger colonies lived longer than smaller ones, an effect that was lessened by colony fission and fusion, indicating these processes could confer a survival advantage. Overall, the results support a critical dependence of coral colony demography on size and morphology.

In Chapter 3, I analyze the effect of spatial patterning on reefscape change over decadal time spans. Using a cellular model that simulates the interactions between four benthic functional groups, I find that reefscape (dm-km) dynamics can be categorized robustly with four distinct stages, including a transient stage dominated by nonlinear competitive dynamics. Increasing levels of colony spatial aggregation (clumpiness) results in a longer duration transient stage, prolonging arrival to the steady state. Results have potential implications for reef monitoring and restoration; for example, high initial aggregation slows loss in degraded reefs and low initial aggregation accelerates growth in healthy reefs.

In Chapter 4, I describe derivation of a novel island-scale continuum coral reef model based on the cellular model used in Chapter 3. Numerical solutions of the resulting twelve coupled nonlinear partial differential equations (describing change of functional group fractional covers, nondimensional boundary lengths between functional groups, mean colony size and fish biomass density) match key aspects of the cellular model, as well as producing emergent patterns that go beyond what is observed in the cellular model.

In Chapter 5, I describe a novel framework for using these results to build models of coupled societal-reef systems.

Chapter 1

Introduction

The vast majority of coral reef systems, one of the most biologically rich habitats on the planet, are peopled seascapes. Given that the boundaries of systems are defined by their dynamics [Werner, 2003], coral reef systems, over decadal time scales, include the living, accreting benthic community foundational to the reef, the nekton in the water column shaping the reef, and the people and societies nonlinearly connected to the reef. The dynamical patterns that emerge across these interacting subcomponents suggest that coral reefs are rich, hierarchical complex systems [Dizon and Yap, 2006, Hatcher, 1997, Pandolfi, 2002]. Treating the fully coupled societal-coral reef system, including the people strongly linked to the ecosystem, is fundamental for quantifying its cross-scale interdependencies, emergent patterns, and time evolution of this rich complex system.

1.1 Coral reefs are complex systems

Complex systems consist of networks of many mutually interacting components of which the collective behavior is both attributable to and gives rise to multi-scale structural and dynamical patterns that are not inferable from one particular level of description [Parrott, 2002]. In other words, the components affect and are affected by the larger, more complicated levels of the system in which they are embedded [Dizon and Yap, 2006]. Emergent behaviors, often structured by regular or ordered patterns, arise from a myriad of interactions between components,

scale separation (i.e., the presence of distinct inherent time scales in which different elements operate) and nonlinearities rooted in the many relationships involving feedbacks at multiple levels of a system [Mena et al., 2011] Therefore, emergent behaviors are properties that are distinct from behaviors found in particular subsystems (human or ecological), but rather emerge from the interactions between them. For example, the world's diverse tapestry of human cultures (culture being a society's emergent sets of beliefs, knowledge, practices, values, ideas, language, and world-views) has emerged from the different ways that people relate to each other and to the environment in which they are embedded [Pizzirani, 2016].

Complex coral reef systems encompass numerous links within and among the ecological system, the physical system, and the human system [Michener et al., 2003]. Coral reefs, like other ecosystems, are affected by endogenous self-organizing processes (in the absence of disturbance) as well as exogenous dynamics (as they are open systems) that operate gradually (continuous) or abruptly (sudden). Ecologically, coral reef communities can be viewed as ensembles of interacting components. These components include the various functional groups on a reef (from bacteria, to plankton, to macroalgae, to the hard corals, and the large predators). From the interactions within and between these functional groups (e.g., coral-zooxanthellae symbiosis, competition, trophic interactions, synchronized reproduction and dispersal), arise broad scale, discernible patterns resulting from nonlinear and largely unpredictable mechanisms owing to the thousands of species that inhabit coral reefs worldwide, and from the range of unique, local environments that act on them [Dizon and Yap, 2006]. These patterns include, for example, the dominance of similar coral taxa and growth forms in the same geomorphological zones of reefs despite tremendous variability in larval dispersal and recruitment, species physical tolerances, reproductive modes, or the nature of interactions established[Done, 1999]. At the benthic community level, the emergent behaviors in which these patterns are manifested include coral fractional cover, coral size frequency distributions, composition of morphological types, and/or abundance of calcifying versus non-calcifying organisms [Preece and Johnson, 1993, Murdoch and Aronson, 1999].

One of the fundamental aspects of the complex systems approach is inves-

tigating the dynamics of a system given a set of rules and initial conditions, as opposed to determining the rules that produce an end state [Mena et al., 2011] This approach is eloquently summarized by Werner and Hicks [Werner and Hicks, 2014] as an approach that:

> *...entails characterizing complexity (a system property) using hierarchies of multiple levels of description to describe system behavior, differentiated by time scale, or the time it takes the system at that level of description to respond to a small push or pull (a perturbation). Studies of complex systems then are aimed at exploring how a system works by describing: the behavior at each level of description; the interrelations between adjacent levels of description; and the relationships between each level and the external environment lying outside the system [Werner, 1999, Werner, 2003]. This approach has the advantage that the detailed, complicated and simple aspects of complex systems can all be analyzed within a single framework.*

Therefore, employing a complexity approach provides a critical comprehensive framework for the study of coupled human-reef systems.

1.2 Integrating discipline-based approaches

Despite the interconnected nature of coral reefs, most approaches for studying and characterizing this multi-scale complex system are discipline-focused. For example, the fields of coral reef ecology and biology focus mainly on quantifying the structural composition and dynamics of the *natural* components of the reef system (without humans), specifically studying organisms and communities of the coral reef benthos and associated nekton from the scales of microns to kilometers [Vermeij and Sandin, 2008, Barott et al., 2011]. Independently, anthropologists and other social scientists focus on characterizing the *human* component, including describing the nature of human relations within societies as well as with their coastal environment, but without a systematic comprehensive quantification of *natural* environment [Alkire, 1978, Ruddle, 1988]. Researchers in other fields, including oceanography, geology, and paleoclimatology, have studied reefs at larger scales to describe properties and circulation patterns of water masses or to recon-

struct ocean and atmospheric conditions on evolutionary time scales [Gove et al., 2013, Carilli, 2014].

In the last couple of decades, studies have been conducted to quantitatively explore the dynamics of coral reef systems across disciplinary lines between environmental and social sciences, although many investigations are limited by a focus on scenario models that predict the impact of fisheries exploitation on reefs [Shafer, 2007, Kramer, 2008, Kittinger et al., 2011, Melbourne-Thomas et al., 2011a]. People are rarely included as autonomous agents with cultural traditions that are, in a sense, historical repositories of an inherent capacity to adapt, as shown in archaeological studies [Rivera-Collazo et al., 2015]. Representing societies as composed of agents that demonstrate autonomous behavior and an ability to sense their environment and to respond to it can inform which aspects of human behavior are related to the emergence of patterns within the coupled system [Montes De Oca Munguia et al., 2009, Iwamura et al., 2016]. The emergent collective dynamics of individual agents then can be used to analyze coupling to reefscape patterns [Parker et al., 2003, Jager and Mosler, 2007]. Both the absence of integrated cross-disciplinary approaches that characterize the ecological and anthropological aspects simultaneously and the lack of a comprehensive quantitative, analytical approach highlight the need for characterizing the coupled system within a common dynamical framework.

1.3 Space in coral reef systems

Fierce competition for space in an approximate two-dimensional benthic environment guides and constrains the development of coral reef structures and patterns. Coral colonies exhibit various life history strategies aimed at optimizing space occupancy and acquisition, which they manifest in their morphological characteristics as well as in their individual patterns of growth, mortality, and survivorship. Spatial constraints on ecosystem dynamics are recognized to critically affect overall population dynamics of sedentary organisms and that of their predators in both terrestrial and marine systems [Jackson, 1977, Schmitz,

2010]. Spatial patterning of the coral reef benthos has been explicitly treated using homogenous mean-field models (such as with Leslie transition matrices), energy flow models, ordinary differential equations, cellular simulation models, and hybrid cellular-continuous models [McClanahan, 1995, Hughes, 1996, Mumby, 2006, Fung, 2009, Sandin and McNamara, 2011]. Because coral reef benthic organisms are cemented to the bottom, approaches that capture neighborhood arrangements around individuals also can capture spatial configuration effects on the vital rates of individuals (i.e., growth, death, birth, etc.), which has significant relevance to population dynamics [Dieckmann et al., 2000]. Additionally, the question of how to accurately represent the spatially-constrained dynamics of coral reef benthic organisms on the larger scale (dm to km), where reefs are coupled to human societies, remains unanswered. Specifically, how does including spatially explicit interactions inform intermediate to large scale pattern formation, which influences fish and therefore human coupling?

1.4 Indigenous societal-coral reef coupled systems

The nature of human-coral reef relationships is highly variable across time and space and often rooted in historical context, coastal heritage, and place-based socio-cultural traditions [Alkire, 1978, Johannes, 1981, Liu et al., 2007, Shackeroff et al., 2009, Kittinger et al., 2012]. In quantitative human-landscape simulation models, it isn't until coupling human and landscape submodels that feedbacks (reciprocal interactions between distinct levels of description) and emergent physical and economic behaviors arise [Acevedo et al., 2008, Kramer, 2008, McNamara and Werner, 2008, Melbourne-Thomas et al., 2011b]. For coral reef systems, representations of people are mainly included as one-way external drivers of unbounded fisheries exploitation or as indirect causes of degradation from rampant development and pollution spillover [Hughes et al., 2003, Fabricius, 2005, Knowlton and Jackson, 2008]. However, in traditional subsistence-based indigenous societies, people and reefs are strongly interwoven and often considered inseparable [Alkire, 1978, Dickie, 2005, Petersen, 2009a]. Expanding the representation of hu-

mans beyond the standard market-integrated society is a necessary step towards acknowledging the diversity of coupled human-landscape relationships across the globe, and exploring ways of optimizing those relationships in the context of environmental change.

1.5 Outline of the Dissertation

The main goal of my research is to contribute to building the ecological model infrastructure required for comprehensively investigating the dynamics of fully coupled indigenous human-reef systems. Using an interdisciplinary complex systems approach, I focus on quantifying coral reef ecological dynamics that culminate in the development of a continuum model representing the reef at the temporal and spatial scales relevant to human societies (i.e., years to decades and decimeters to kilometers).

At the coral colony scale (Chapter 2), I describe the influence of initial size and dynamical fate (e.g., fission and fusion) processes on coral colony change. Coral colonies exhibit various life history strategies aimed at maximizing space occupancy and acquisition, which they manifest in their morphological characteristics, as well as, in their individual patterns of growth, mortality, and survivorship. I highlight the limitations of over-reliance on fractional cover alone in light of significant size-dependent changes in coral colonies, suggesting that coral colony size distributions and morphological composition exert order one influence on societal-scale coral demographic processes.

At the reefscape scale (dm-km) (Chapter 3), where feedbacks between spatio-temporal patterns and dynamics of the reef influence the nonlinear relationship to human societies, I investigated the effect of coral colony spatial configuration patterns (e.g., uniform, random, or clumped) on short- to intermediate-time-scale system behavior. A dynamical analysis of a modeled coral reef benthic system revealed that four temporal stages emerged: a repelling stage moving away from an unstable initial condition, a transient stage dominated by strong nonlinear coral-macroalgae interactions, an attracting stage where the reef decays towards a

steady-state attractor, and the attractor. Overall, spatial patterning was found to influence rates of reef change in different reef health scenarios, with high aggregation patterns resulting in coral cover loss in degraded systems and low aggregation configurations accelerating coral growth in healthy systems.

Chapter 4 details a first attempt to explicitly develop an intermediate scale continuum model of the reefscape based on the small-scale interactions represented in a cellular model of coral reef benthic dynamics. Twelve variables varying in both space and time represent the state of the system: fractional cover of four main functional groups on the reef (coral, macroalgae, turf algae, and crustose coralline algae), length of six non-dimensional boundary lengths between the four functional groups, mean coral colony size, and biomass density of fish population coupled to the benthic community. Key aspects of the cellular model match the numerical solutions of the equations. Intermediate- to long- scale emergent patterns that go beyond what is observed in the cellular model were obtained. Analysis of the equations provides a means to trace the origins of observed time scales and the nonlinear behavior underlying transient stages.

In the concluding chapter (5), I contextualize the ecological analyses of Chapters 2 to 4 within the overarching aim of moving towards a societal-reef coupled model. I include a conceptual synthesis of subsistence-based Micronesian fishing cultures linked to coral reef systems and a summary of an initial attempt to construct an agent-based model loosely parameterized after such societies. The initial coupling of this indigenous societal model to the continuum coral reef ecosystem model from chapter 4 is introduced along with a brief discussion of future research directions within the context of climate change and adaptive capacities of coupled human-environmental systems.

Chapter 2

Coral colony size-dependent change and fission-fusion dynamics

2.1 Abstract

Coral population dynamics are linked to colony growth and mortality processes constrained by the intrinsic biology of colonial organisms. Specifically, colony traits, such as size and morphology, can impose geometric constraints on the demographic growth potential of coral colonies. The type of life history strategy employed by a coral, whether weedy or stress-tolerant, and its clonal-based patterns of fission and fusion can also influence how it changes. To quantify size-dependent and morphologically-based patterns of coral colony change, over 4,300 southern Caribbean coral colonies belonging to four coral groups (*Madracis mirabilis*, massives, *Agaricia agaricites*, and *Millepora* spp) were digitally tracked for 4.5 years (biannual timestep). A size-class based analysis revealed that small colonies had significantly more positive log proportional areal change than larger sizes, which is in line with geometrically-constrained growth that predicts greater areal growth in colonies with higher perimeter:area ratios. Fission and fusion dynamics, which occurred in 16.4 % of colonies, also had a significant effect on colony proportional change (i.e. fission resulted in net negative changes and fusion in net positive changes) while eliminating the size-dependent longevity trend in all coral types

except for *M. mirabilis*. *M. mirabilis* stood out as the coral type whose weedy life history and branching sub-massive morphology most maximized coral lateral area capture and persistence. That colony size and fission/fusion dynamics significantly affect coral colony change and longevity supports a size-dependent and morphologically-focused approach to coral demography, which can more effectively inform the expectation of overall reef change.

2.2 Introduction

Coral populations are a complex mosaic of sexually and asexually produced colonies experiencing various growth, mortality and regrowth dynamics [Elahi and Edmunds, 2007, Tanner, 2001]. Because coral colonies are the principal reef building organisms in coral reef systems, quantifying coral colony change and the processes that influence that change are pivotal for understanding coral reef benthic dynamics and overall reef change [Pratchett et al., 2015, Spalding et al., 2001, Wells, 1957].

Coral colonies have been described as clonal, or modular, organisms that exhibit indeterminate, or unbounded, growth limited mainly by external factors [Bak, 1976, Buddemeier and Kinzie III, 1976, Jackson and Coates, 1986]. However, proportional change in colony area has been shown to be negatively related to initial colony size for various coral species irrespective of specific growth rate constants [Dornelas et al., 2017, Hughes and Jackson, 1985, Kayal et al., 2015, Osinga et al., 2011, Pratchett et al., 2015]. This suggests that intrinsic allometric constraints stemming from partitioning of life processes, like growth, reproduction, and maintenance, amongst modules, might slow the rate of colony expansion as size increases. For example, consider circular colonies with constant radial extension rates, geometric-based limitations on peripheral growth may be expected to emerge as the perimeter:area ratio decreases with increasing colony size (Fig. 2.6). Additionally, a balance between the rate of calcification to the rate of tissue production might be reached or constraints from differential access to resource acquisition by modules across the colony might also be limiting [Anthony et al.,

2002, Barnes, 1973, Kim and Lasker, 1998]. For example, Kim and Lasker [Kim and Lasker, 1998] showed how differential resource capture (e.g., of light, food, and freely circulating water) by modules (polyps) across a colony can limit colony size, since reduced access to resources by obstructed interior polyps has to be compensated for by redirecting available energy from growth and reproduction into overall maintenance of those polyps.

Another influence on coral colony areal change stems from life history strategies inherent to the biology of corals. Life history strategies are consistent, context-independent characteristics of organisms that maximize fitness by differentially allocating resources among life processes of growth, reproduction, and survival [Darling et al., 2012, Stearns, 1992]. Life history strategies in corals have been characterized as ranging over a continuum from fast-growing species ("r-selected") to slow-growing more morphologically-robust species ("K-selected") [Buddemeier and Kinzie III, 1976, MacArthur, R. H. & Wilson, 1967]. Darling et al. [Darling et al., 2012] define the prominent life history strategies in coral reefs as 1) competitive (competitive dominants exhibit efficient resource uptake; susceptible to environmental disturbance (fragmentation); fast-growing, "r-selected", e.g., *Acropora* spp) , 2) weedy (opportunistic colonizers; fast-growing; intermediate survival, e.g., *Madracis mirabilis*), 3) stress-tolerant (slow-growing; higher investment in larvae; stress-tolerant; long lifespans, "K-selected", e.g., *Orbicella* spp), and 4) generalists (combinations of other types; moderate growth rates, e.g., *Dichocoenia* spp). Based on these characterizations, we might expect that fast-growing weedy corals will exhibit higher and more variable rates of coral colony change, while, at the other end of the spectrum, the slow-growing stress-tolerant types might have slower rates and less variability in colony change over the same time periods. In terms of survivorship, or longevity, patterns, we would expect stress-tolerant types to exhibit greater longevity, since small colonies have a greater likelihood of complete mortality from disturbance events than larger colonies [Babcock, 1991, Hughes et al., 1992].

Coral colonies exhibit a wide-range of dynamics that add an additional layer of complexity to colony areal change. For example, disturbance processes

can result in whole colony mortality, partial mortality (shrinkage in size), temporary burial, or fission, where a larger colony divides into smaller independent patches of living tissue. When recovering from disturbances, colonies can regrow over exposed skeleton, re-emerge from holes, and, because of their clonal nature, fuse with other sub-colonies of the original parent colony [Bak, 1976, Furby et al., 2017, Hughes and Jackson, 1980, Tanner, 2000, Kayal et al., 2015]. Coral colony change can thus be expected to respond differently to this variation in fates. In this study, we explore the fate categories of fission, fusion, and simple isolated change within an individual colony, whether simple growth or shrinkage. Areal change arising from simple isolated change of an individual is expected to result in positive, negative, or no change as these could be the result of growth, shrinkage (partial mortality), or both balancing each other out. Because smaller colonies have a larger perimeter to area ratio, colony change after fission is expected to be positive with the resulting smaller colonies growing proportionally faster. Colony longevity after fission is expected to decrease because of well-documented decreases in survivorship for smaller colonies due to disturbance and overgrowth from other benthic organisms [Raymundo and Maypa, 2004, Vermeij and Sandin, 2008]. Alternatively, proportional colony change after fusion into larger colonies is expected to decrease as the perimeter to area ratio decreases, but longevity should increase because of increased survivorship (i.e. increased competitive dominance) as corals grow.

This study utilized a 4.5 year bi-annual photographic time series from Curacao to investigate the dependence of coral colony areal change and longevity on initial colony size, colony morphology, and fate. The four hard coral groups investigated, which differed in morphology and life history traits, included *Madracis mirabilis*, massives, *Agaricia agaricites*, and *Millepora* spp. Differences in coral colony areal change and longevity within and between groups and how these feed back to affect configuration and change of the emergent reefscape are discussed.

2.3 Methods

2.3.1 Study Site

Coral colonies were tracked for 4.5 years in a reef flat located shoreward from an Orbicella-dominated reef slope in Westpunt, Curacao (Fig. 2.1). This site is characterized by a high degree of rubble in the benthos with previous censuses for this region showing that the principal hard coral composition is comprised of: *Madracis* spp., *Agaricia* spp., *Orbicella* spp. and *Millepora* spp. [Bak, 1976, Van Duyl, 1985]. This site experiences episodic, short-lived storms that occasionally cause nutrient runoff from nearby resorts as well as re-suspension of sequestered nutrients from reef crevices [Vermeij, 2012]. This sudden nutrient input leads to ephemeral *Dictyota* spp. algal blooms that are then torn away by wind or other storm generated currents. This site is not very heavily populated by people compared to the urban center of Curacao, located about 40 km southeast, but it is heavily visited by tourists, particularly snorkelers and scuba divers. Throughout the study period, coral fractional cover remained relatively unchanged at a level of $0.040 +/- 0.007SD$ (one-way ANOVA, $F_{8,602} = 0.7$, $p = 0.69$).

2.3.2 Survey Protocols

A time series of permanent quadrat photographs was acquired from April 2009 to March 2013. Five 400 m2 circle plots marked with underwater buoys were established parallel to shore at depths between 6 to 8 meters. In each plot, a total of 40 permanent quadrats were located (20 randomly and 20 targeting coral colonies) throughout the plot and marked with two stainless steel eyebolts driven through numbered cattle tags. On average, photoquadrats were visited every six months at which point a 60 x 90 cm PVC frame was laid on top of the steel markers and a photograph taken using a Canon G12 camera. Given the length of the survey, steel eyebolts did occasionally erode which resulted in lost markers. Overall, approximately 200 photoquadrats ($0.54cm^2$ each) were surveyed 9 times over 4.5 years.

2.3.3 Focal Groups

Four main hard coral groups were tagged digitally and tracked through time in this study. These groups are largely based on taxonomy except for one group, the massives, which are unified by their dome-shaped morphology. The groups are: 1) the species *Madracis mirabilis*, 2) the massives, comprised of *Agaricia humilis*, *Orbicella* spp, *Siderastrea* spp, *Diploria* spp, and *Porites asteriodes*, 3) *Agaricia agaricites*, and 4) the hydrozoan *Millepora* spp. *M. mirabilis* colonies are highly heterotrophic branching corals that form densely packed hemispherical clumps of small pencil-sized branches physically connected by a common skeleton, but not always by tissue [Humann and Deloach, 2001]. They are found at various depths across the reef and are known to actively reproduce asexually through fragmentation making them a weedy species [Highsmith, 1982]. The consortium of species included in the massive category are characterized by their hemispherical growth form and are typically slower-growing, more fecund, and have longer generation times than other morphological types [Murdoch, 2007]. The foliaceous plating coral, *A. agaricites*, is an opportunistic (weedy) species characterized by high rates of recruitment, growth, and mortality [Hughes and Jackson, 1985]. A conspicuous coral on shallow reefs, *Millepora* spp are calcareous foliose hydrocorals functionally similar to hermatypic corals in that they contribute to reef construction and reproduce asexually through fragmentation [Edmunds, 1999]. Despite morphological similarities, *A. agaricites* and *Millepora* spp were treated separately in this study because of life history differences that are expected to influence their ecology, such as reproductive cycle (e.g., pelagic medusa in hydrocorals) and the presence of polymorphic polyps in hydrozoa. All hard-coral groups occurred regularly at this site and throughout the study period.

2.3.4 Image Analysis

Photoquads were analyzed using the free downloadable program, photoQuad, to manually trace, digitally tag, and export morphometric descriptors (e.g., area, percent cover etc.) for all individual colonies present in order to investigate their dynamics through time [Trygonis and Sini, 2012]. The program's layer-based

functionality, specifically the ability to label outlined species regions with a customized alpha-numeric naming scheme (refer to Fig. 2.7 for scheme), allowed for investigation of coral colony dynamics. The dynamics quantified included survivorship, and size-based changes stemming from growth, shrinkage and/or colony fission and fusion events. The unique naming scheme also allowed for subtracting holes, or areas within colony outlines where coral tissue was clearly dead or overgrown by other benthic organisms, from overall colony morphometrics. Exported morphometric data generated by photoQuad was analyzed using MATLAB 7.10.0 (2010a, The Mathworks, Inc.).

2.3.5 Data and Statistical Analyses

All coral colony analyses were based on two-dimensional projections of colony size in terms of area, which is the surface directly related to space and light capture (i.e., the main limiting resources). Coral colony change was defined as the log proportional difference in planar area at a given timepoint and at the timepoint immediately preceding it. Thus, log proportional change in area was always over sequential timepoint pairs without including pairs where an area estimate was absent (e.g., if a colony was not seen in the next timepoint). Because tracking fission and fusion events allowed for determining relatedness between colonies, change in planar area from one timepoint to the next was calculated by taking the difference between sum areas of all related colonies (i.e. the coral demographic unit) at each timepoint (Fig. 2.2). Using sum area allowed for tracking changes in coral units as well as in individually changing coral colonies, i.e., those that did not exhibit active fission/fusion dynamics (83.6 % of data). All coral colonies with area cut off by the frame or outside the image at a particular timepoint were not included in the analyses. Because rates of change did not exhibit significant temporal variations across the 4.5 years, all log proportional change data values were pooled together for each of the four hard coral groups (overall n = 4,385).

2.3.6 Proportional change

The relationship between log proportional areal change and log initial colony size was plotted to determine the general relationship in each of the four hard coral groups. The relationships were generally heteroscedastic and non-linear. As such, rather than employing linear analyses, a size-class based analysis was employed where colonies of each hard coral group were divided into three log base 10 initial size categories ($< 1cm^2$, $1cm^2$ to $10cm^2$, and $> 10cm^2$) to determine whether the average change per size class was above (positive) or below (negative) the no change zero line. Comparisons were also made across coral groups. The influence of dynamical fate on log proportional change within each size class, specifically stemming from isolated individual colony growth or shrinkage (iso), fission (fis), fusion (fus), or multi-fate (mul) processes, was also considered. We tested for significant differences ($\alpha = 0.05$) between the mean log proportional change in the isolated fate to each of the other fate types by using randomization techniques with 10,000 resampling iterations per size class in each coral group.

2.3.7 Longevity patterns

Longevity, or the number of timepoints a colony survived, was recorded for all coral colonies digitally tagged in the first photographic census (April 2009; 2,036 total colonies). Adapting the maximum likelihood approach of [Vermeij and Sandin, 2008], longevity patterns were analyzed as a function of colony size class for two condensed fate categories, iso and a combined fis/fus/mul category, within each of the four coral groups. Colony size classes were log base 2 bins with the geometric mean of the colony area being 0.06, 0.13, 0.25, ..., and $1024cm^2$. Statistical significance was determined using maximum likelihood estimates of log-linear relationships between mortality (the reciprocal of longevity) and size. Specifically, mortality was modeled with a Poisson distribution capturing the probability of a coral demographic unit dying at a given time interval, with rate parameter λ_c that described the mean time until mortality for a colony in size class c. For each hard coral group and fate category combination, the rate parameter of a Poisson mortality model was constructed in two functional forms: constant mor-

tality probability with size, $\lambda_c = m_0$, and log-linear mortality probability with size, $\lambda_c = m_0 + m_1 ln(c)$ with the constraint that $\lambda_c > 0$ for all c. The summed log likelihood of a particular model describing the observed data given values of parameters m_0 and m_1 was computed as follows:

$$L_x(m_o, m_1) = \sum_{i=1}^{n_x} \begin{cases} ln(\lambda_{ci,f})t_i + (-\lambda_{ci,f})t_i & \text{for } t_i < 9 \\ (-\lambda_{ci,f})t_i & \text{for } t_i = 9 \end{cases} \tag{2.1}$$

where $\lambda_{c_i,f}$ is the expected mortality probability based on function f (i.e., either constant or a linear function of colony size, c_i), n_x is the sample size of coral group $x = 1, 2, 3, or 4$, and t_i is the number of average 6-month time intervals until mortality for individual i. The equations in 2.1 correspond to the colony dying during the study or the colony surviving through the duration of the entire study. Maximum likelihood estimates were generated for each mortality model and the significance of the size-dependent term of the log-linear model was determined by a likelihood ratio test [Hilborn and Mangel, 1997].

2.4 Results

2.4.1 Proportional change as a function of initial colony size

Overall, change in the log proportional area of colonies was variable with a tendency towards positive change and higher variability among smaller size classes. At larger size classes, change was less variable and centered close to zero (i.e., no change in size) (Fig. 2.4). Linking colony areal change to dynamical fate (color coded data points) showed a similar trend for isolated, fission, and multi-fate categories, but not for the fusion category. Although variability still decreased with increasing initial colony size, for colonies with fusion fates (blue dots), proportional change was visibly aggregated above the zero no change line regardless of initial size in all four hard coral groups.

Distributions of log proportional change were divided into three log based size classes, which showed the location of means in relation to the zero (no change) line. For all hard-coral groups irrespective of fate, the mean proportional change

of small initial colonies less than $1cm^2$ was positive (Fig. 2.4a-d). The mean log proportional change for the intermediate and larger size classes, centered on the zero no change line with the large size classes also exhibiting left skewed distributions (Fig. 2.4i-l). Fission, fusion, and multi-fate dynamics were mostly present in all size classes of *M. mirabilis*, in the intermediate and larger size classes of *A. agaricites* and *Millepora* spp, and rarely occurred in the massive coral group. Particularly for *M. mirabilis*, the proportion of colonies experiencing fission, fusion, and multi-fate events increased from 9 % in small colonies to 20 % in intermediate colonies to 45 % in the larger colonies (Fig. 2.4 pie charts). A statistical comparison of the means between isolated fates and each of the other fates revealed that changes resulting from fusion were always positive with significant differences from the means of isolated fate distributions observed in intermediate and large size classes (Table 2.1). Fission and multi-fate processes tended to have a negative effect on log proportional change when compared to the means of isolated fate distributions.

2.4.2 Size-specific and fate-based longevity patterns

Longevity significantly increased ($p < 0.001$) with increasing size class for all hard coral groups in the isolated fate category (Fig. 2.5a-d). For each coral group, the size dependence of mortality is described by a log-linear function with colony size, c, as the following: *M. mirabilis*: $\lambda_c = 0.54 - 0.08ln(c)$, massives: $\lambda_c = 0.13 - 0.02ln(c)$, *A. agaricites*: $\lambda_c = 0.33 - 0.05ln(c)$, *Millepora* spp: $\lambda_c = 0.34 - 0.06ln(c)$. Larger colonies experienced decreased mortality probabilities, most prominently for massives in which 95 % of colonies larger than $64cm^2$ survived upwards of 1.5 years (Fig. 2.5b). In contrast, the size-based mortality effect disappeared for all groups in the combined fission, fusion, multi-fate category, except for *M. mirabilis* which retained a weak size dependent signal ($\lambda_c = 0.11 - 0.01ln(c)$) (Fig. 2.5e-h). Overall, mortality was quantitatively lower for fission, fusion, and multi-fate colonies relative to isolated fate colonies, as well as for the more robust stress-tolerant massives group compared to the other coral groups.

2.5 Discussion

The negative relationship observed between coral colony log proportional areal change and initial size is in line with the expectation of geometrically-constrained growth. Even though colonial organisms have been described to exhibit unbounded growth through the continual addition of polyps to their colonies, in practice there are geometric and structural constraints (Fig. 2.6). These arise as corals increasing in planar area from their periphery experience increasingly lower perimeter:area ratios that require a decrease in proportional growth rate with increasing size [Dornelas et al., 2017]. Notably, our results also showed differences in coral colony change stemming from other factors, including life history strategy, morphology, and fate.

Madracis mirabilis, the dominant coral at this site, strongly illustrates how a weedy life history strategist, with a branching sub-massive morphology prone to fragmentation, can maximize positive areal change by subdividing into smaller colonies that are geometrically capable of faster proportional growth and that appear to retain the lower mortality probability of larger corals once they are actively undergoing fission and fusion. The absence of size dependent survival in fragments of *M. mirabilis* corals has been observed before in Jamaica where fragment survivorship was found to instead be more sensitive to context (i.e. greater survivorship in forereef sites than in lagoon); although whole colonies were not considered in the 11 month study period [Bruno, 1998]. Notable as the taxon with the highest incidence of fission/fusion/multi-fate dynamics (26.5 %), the proportion of *M. mirabilis* colonies actively undergoing fission and fusion increased from 9 to 45 % as colonies became larger. This makes sense as we might expect larger colonies will have more branches susceptible to fragmentation, but it also indicates a potential significance of fission and fusion processes for this weedy, submassive branching taxon. In terms of longevity, *M. mirabilis* also stood out as the coral type whose colonies retained a weak size-dependent longevity effect regardless of fate. A decrease in the strength of size-dependent longevity due to active fission and fusion dynamics could potentially be another advantageous life history strategy in this species because it results in the increased longevity of smaller colonies overall.

In addition, *M. mirabilis* has also been shown to exhibit phenotypic morphological plasticity (e.g., in branch diameter and inter-branch distance), which allows it to become morphologically similar to resident conspecifics and therefore easily colonize and thrive in a variety of disturbed environments [Bruno and Edmunds, 1997].

Massive dome-shaped corals exhibit a stress-tolerant (k-selected) life history strategy that makes them hardy long-living corals [Murawski et al., 2007, van Woesik et al., 2012]. Our results support this demographic hypothesis, as the majority of massive colonies occurred in the intermediate and larger size classes. Longevity results also show that massives had the greatest proportion of colonies alive throughout the entire study period. Massives exhibited clear size dependent change, but had the lowest rates of log proportional change (data tightly concentrated around unity line in figure 2.3) and very minimal fission and fusion dynamics (4.6 %). In fact, fission and multi-fate dynamics had a significant negative effect on proportional change of the larger massive colonies. Other studies have reported comparable rates of fission and fusion in massive corals, $< 5\%$ and $< 3\%$ in the Gulf of Oman (Foster Foster, 2013) and 1 % and 6 % in Australia [Babcock, 1991]. These low rates might be related to the extent of tissue loss after fission as well as the distance between the resulting sub-colonies, which would also determine whether fusion in a subsequent year is possible given that massives have inherently slower growth rates that other coral types.

Both *A. agaricites* and *Millepora* spp. coral groups showed significant size dependent growth. This result indicates that size-dependent growth is prevalent across morphological types of both scleractinian and hydrozoan corals. Both coral types also exhibited strongly significant size dependent longevity patterns, which disappeared in colonies with active fission, fusion, and multi-fates. As in massives, this makes sense because fragmented colonies might retain their increased survivorship from when they were larger or because the positive effects on vital rates of fission/fusion, might be expressing themselves in longevity irrespective of size. The ecological similarities between *A. agaricities* and *Millepora* spp. on the reef were also captured by the closeness in parameter values of their log-linear size

dependent mortality functions. The parallels in vital rates between these two coral groups of the same morphological growth form support a morphologically-based approach to coral colony demography [Dornelas et al., 2017, Murdoch, 2007].

By combining quantitative size-dependent demographic patterns of coral colonies with knowledge of size structure and morphological composition, better approximations of coral cover change and the overall growth potential of a reef can be made. In this work, we emphasized the influence of fates on coral colony change, namely the negative effects of fission and the positive effects of fusion, which become important if the life histories of dominant corals on a reef are known to actively exhibit such dynamics. In our study, 16.4 % of colonies exhibited fission/fusion dynamics. Hughes and Jackson [Hughes and Jackson, 1980] showed an annual rate of 11.7 % for *A.agaricites* and *H.culcullata* colonies in Jamaica, while Elahi and Edmunds [Elahi and Edmunds, 2007] found that 42% of *S. siderea* colonies in a $200m^2$ area of reef had resulted from fission. Part of the reason for considering fission and fusion together is that they often occur in conjunction and/or in multiple sequential events within a demographic unit, especially in coral types like *M. mirabilis*, so that distinguishing between them becomes exponentially more complicated (hence, our multi-fate category). In general, these results suggest that by more systematically quantifying levels of fission/fusion, we might become better poised to characterize rates of occurrence by morphological types that can then be used to further improve estimates of coral cover change.

Overall, our results are in line with studies demonstrating size dependent demographic rates, including growth, reproduction, and survival [Alvarez-Noriega et al., 2016, Dornelas et al., 2017, Ferrari et al., 2012, Hughes, 1984, Kayal et al., 2015, Sebens, 1987, Zilberberg and Edmunds, 2001]. These findings are consistent with the importance of continuing to emphasize size-dependent and morphologically-focused demographic approaches. Because of the multi-scale dynamical nature of coral reefs, quantifying both individual coral colony areal change and dynamical fates that link to larger-scale coral cover patterns is vital for informing the mechanistic underpinnings and the expectation of the reef.

2.6 Acknowledgments

This work would have been impossible without the hard work and commitment of dedicated volunteers and interns: Esmeralda Alcantar, Naomi Tialavea, Zola Roper, Lennon Bruney, Ram Iyer, Andrew Moura, Liana Herberer, Cara Simonsen, Gabrielle Rossbach, Anne Freire de Carvalho, Kate Vasquez, and Alyssa Dubord. M. Brito-Millan supported by an NSF Graduate Fellowship and the Scripps Institution of Oceanography graduate department.

Chapter 2, in full, is material being prepared for submission to Marine Ecological Progress Series: Brito-Millan, M, MJA Vermeij, EA Alcantar, and SA Sandin. Aspects of coral colony size-dependent change and fission-fusion dynamics. The dissertation author was the primary investigator and author of this paper.

2.7 Figures

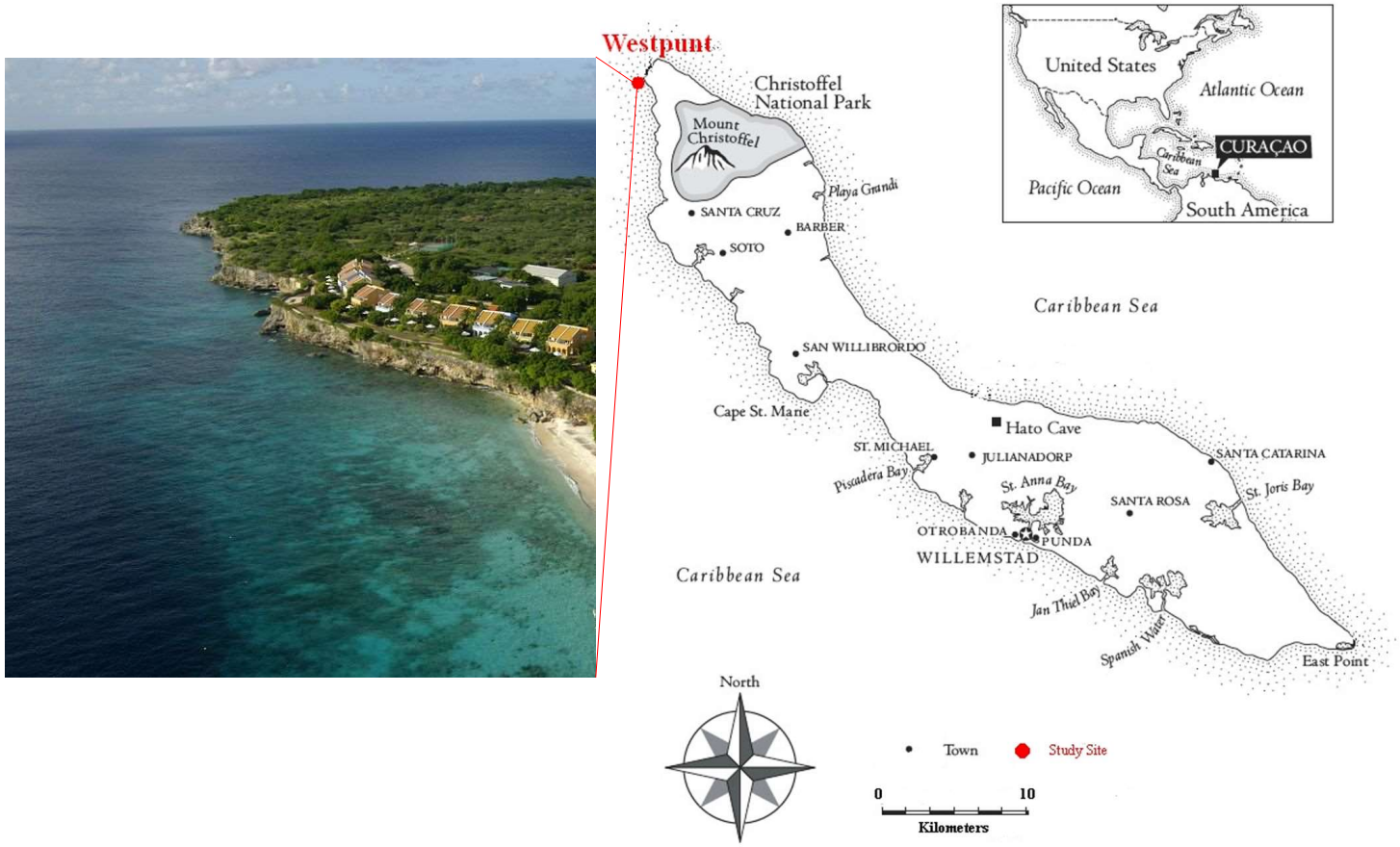

Figure 2.1: **Westpunt, Curacao study site.**
The Westpunt, Curacao study site is located on a *Madracis* dominated reef flat neighboring an *Orbicella* dominated reef slope of the southern Caribbean (map adapted from Tom Patterson).

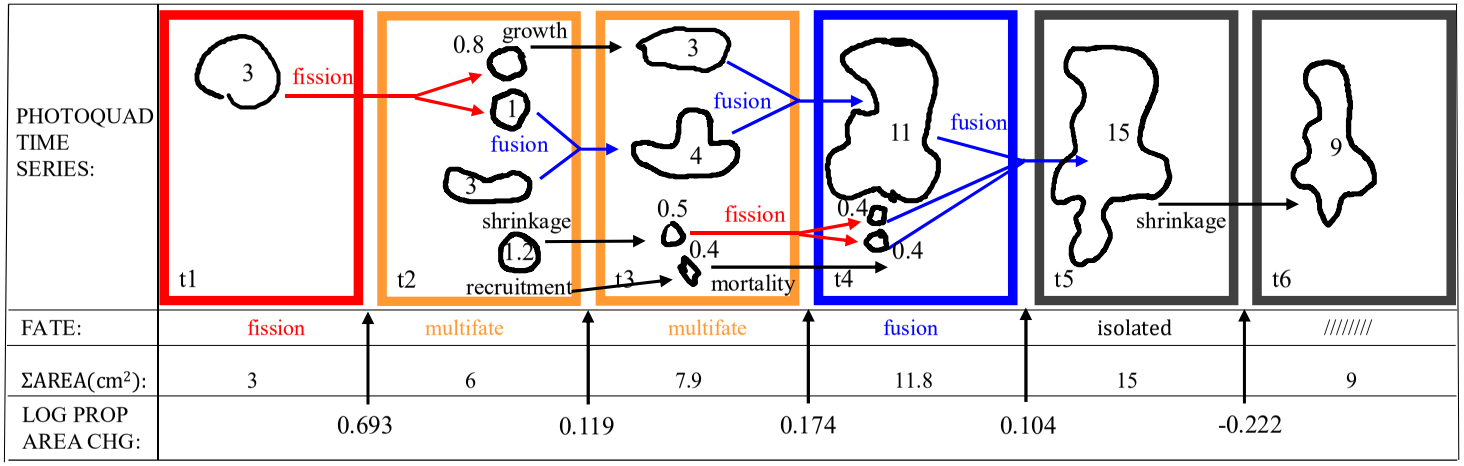

Figure 2.2: **Change in a hypothetical coral colony demographic unit.**
Hypothetical coral colony family area change through time and the resulting fate category assignments, where red = fission, orange = multi-fate, blue = fusion, and gray = isolated. Beneath each quad are shown the sum area of all colonies per timepoint and the log proportional change per timepoint pairs.

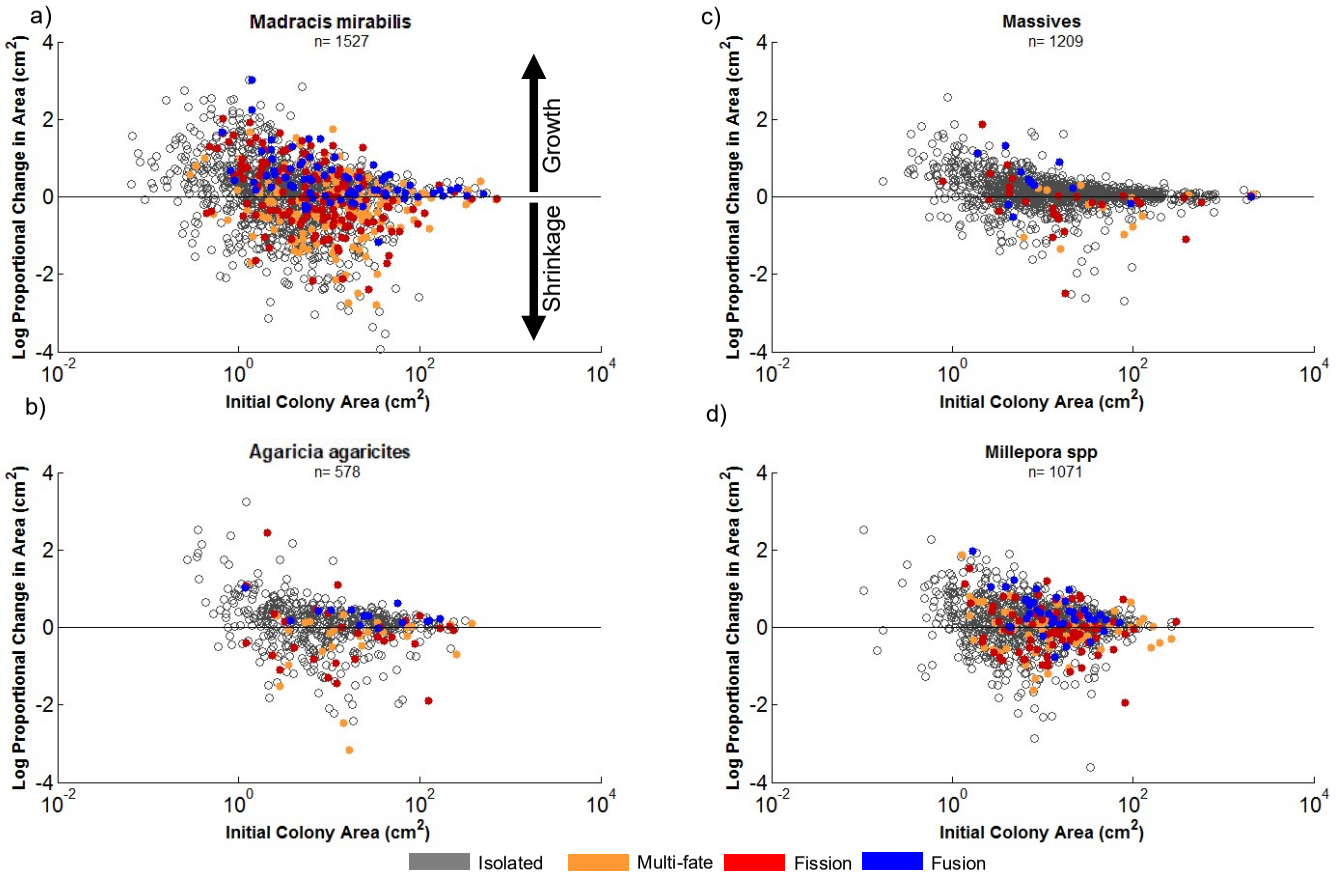

Figure 2.3: **Colony Log proportional areal change by coral group and fate.**
Log proportional change in area vs initial area for all timepoint pairs of the four coral types. Overall, the degree of areal change appears to decrease with increasing initial colony area, but fusion (blue) influenced changes show a net positive effect. Points color coded by fate (refer to legend). Black line is the zero change mark and n is total sample size.

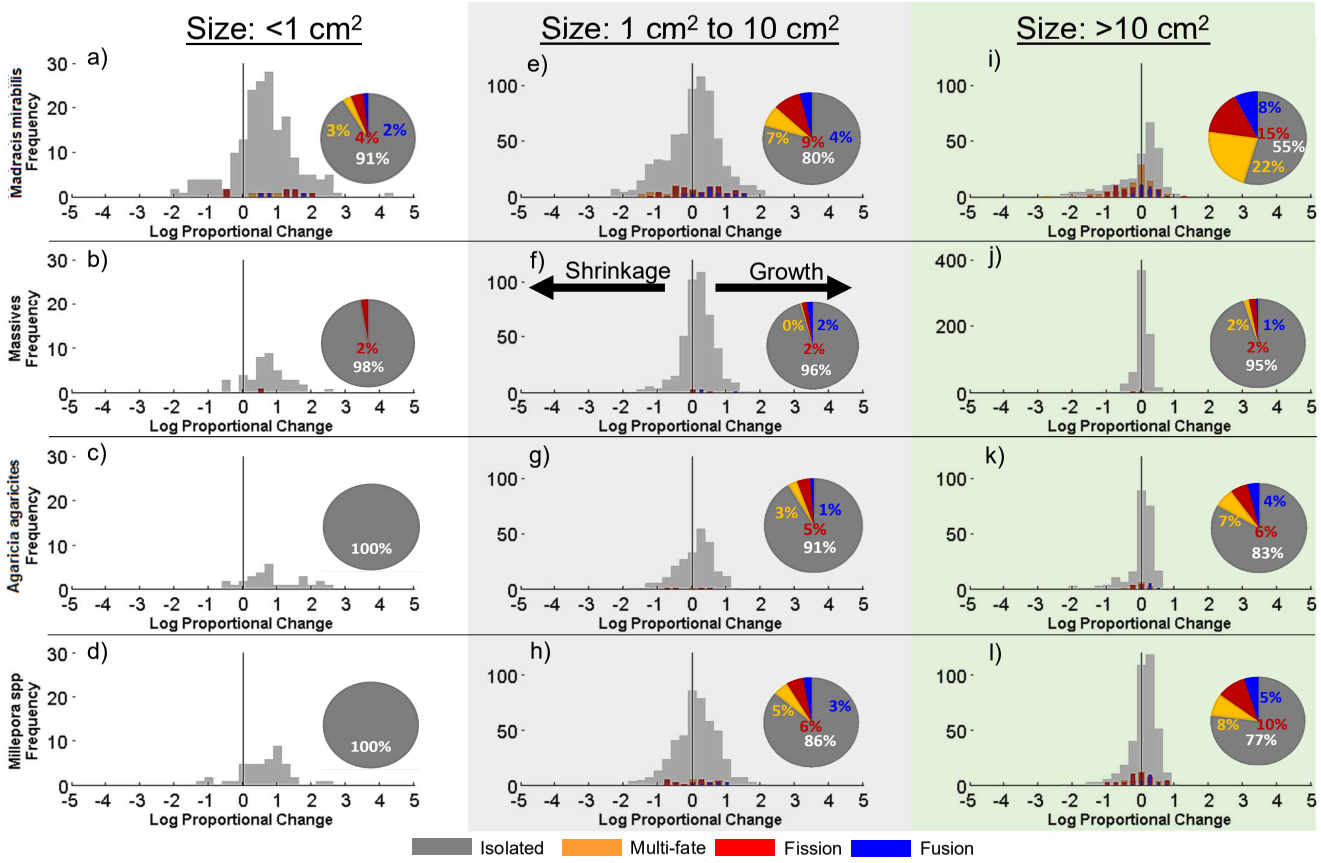

Figure 2.4: **Size-based distributions of log proportional colony area change.**
Size-based distributions of log proportional change for all timepoint pairs across 4.5 yrs. Shown are three log base 10 size classes for each of the four hard coral types. Small size classes dominated by positive growth, while intermediate sizes have both positive and negative change and the largest size classes are left skewed with more positive growth. Bars color-coded by fate (refer to legend). Black vertical line marks zero change point. Pie charts show proportion of data exhibiting a particular fate; increasing size classes of *M.mirabilis* show the most notable increase in fission/fusion/multi-fate dynamics.

Table 2.1: **Randomization results for effect of fate on colony log proportional areal change**
Summary statistics for the effect of fate on log proportional change corresponding to histograms in Figure 2.4. All statistically significant results are in bold using fate-based color legend in Figure 2.4. Change resulting from fusion has a significant positive effect in medium and large colonies. Change from fission and multi-fate processes are negative. p = p-value from randomization ($\alpha = 0.05$), diff = difference between mean of isolated influenced change in area and mean of either multi-fate, fission, or fusion influenced change in area, respectively. $\bar{x}$ = mean, sd = standard deviation, n.d = no data.

		<1cm^2				**1 to 10 cm^2**				**>10 cm^2**			
Coral Group	Stat	isolated	multifate	fission	fusion	isolated	multifate	fission	fusion	isolated	multifate	fission	fusion
M. mirabilis	*p*	//////////	0.349	0.211	0.537	//////////	0.166	0.101	**0.000**	//////////	0.400	0.452	**0.003**
	diff	//////////	-0.361	0.393	0.320	//////////	-0.154	0.165	**0.683**	//////////	-0.077	-0.080	**0.382**
	n	185	6	9	3	683	63	79	**34**	254	105	70	**36**
	$\bar{x}$	0.608	0.246	1.001	0.927	0.020	-0.134	0.185	**0.703**	-0.212	-0.289	-0.292	**0.170**
	sd	0.946	0.663	0.882	0.664	0.855	0.800	0.839	**0.699**	0.876	0.754	0.701	**0.367**
Massives	*p*	//////////	n.d	0.533	n.d	//////////	0.102	0.186	0.123	//////////	**0.028**	**0.000**	0.059
	diff	//////////	n.d	-0.308	n.d	//////////	-0.596	0.217	0.252	//////////	**-0.270**	**-0.452**	0.227
	n	41	0	1	0	438	2	9	9	674	**13**	**18**	4
	$\bar{x}$	0.717	n.d	0.409	n.d	0.179	-0.417	0.396	0.431	0.003	**-0.267**	**-0.449**	0.230
	sd	0.639	n.d	0.000	n.d	0.483	0.903	0.671	0.581	0.330	**0.493**	**0.625**	0.468
A. agaricites	*p*	//////////	n.d	n.d	n.d	//////////	**0.023**	0.561	0.211	//////////	**0.023**	0.106	**0.030**
	diff	//////////	n.d	n.d	n.d	//////////	**-0.526**	-0.111	0.429	//////////	**-0.342**	-0.248	**0.307**
	n	28	0	0	0	244	**8**	12	3	236	**19**	17	**11**
	$\bar{x}$	0.877	n.d	n.d	n.d	0.108	**-0.418**	-0.003	0.538	-0.047	**-0.389**	-0.295	**0.261**
	sd	0.834	n.d	n.d	n.d	0.623	**0.645**	1.051	0.432	0.517	**0.896**	0.682	**0.192**
Millepora spp	*p*	//////////	n.d	n.d	n.d	//////////	0.466	0.613	**0.002**	//////////	0.577	0.059	0.116
	diff	//////////	n.d	n.d	n.d	//////////	-0.097	0.066	**0.591**	//////////	-0.041	-0.141	0.145
	n	44	0	0	0	462	28	31	**15**	378	40	49	24
	$\bar{x}$	0.629	n.d	n.d	n.d	0.100	0.004	0.166	**0.691**	0.038	-0.002	-0.103	0.183
	sd	0.764	n.d	n.d	n.d	0.668	0.722	0.971	**0.514**	0.469	0.424	0.562	0.386

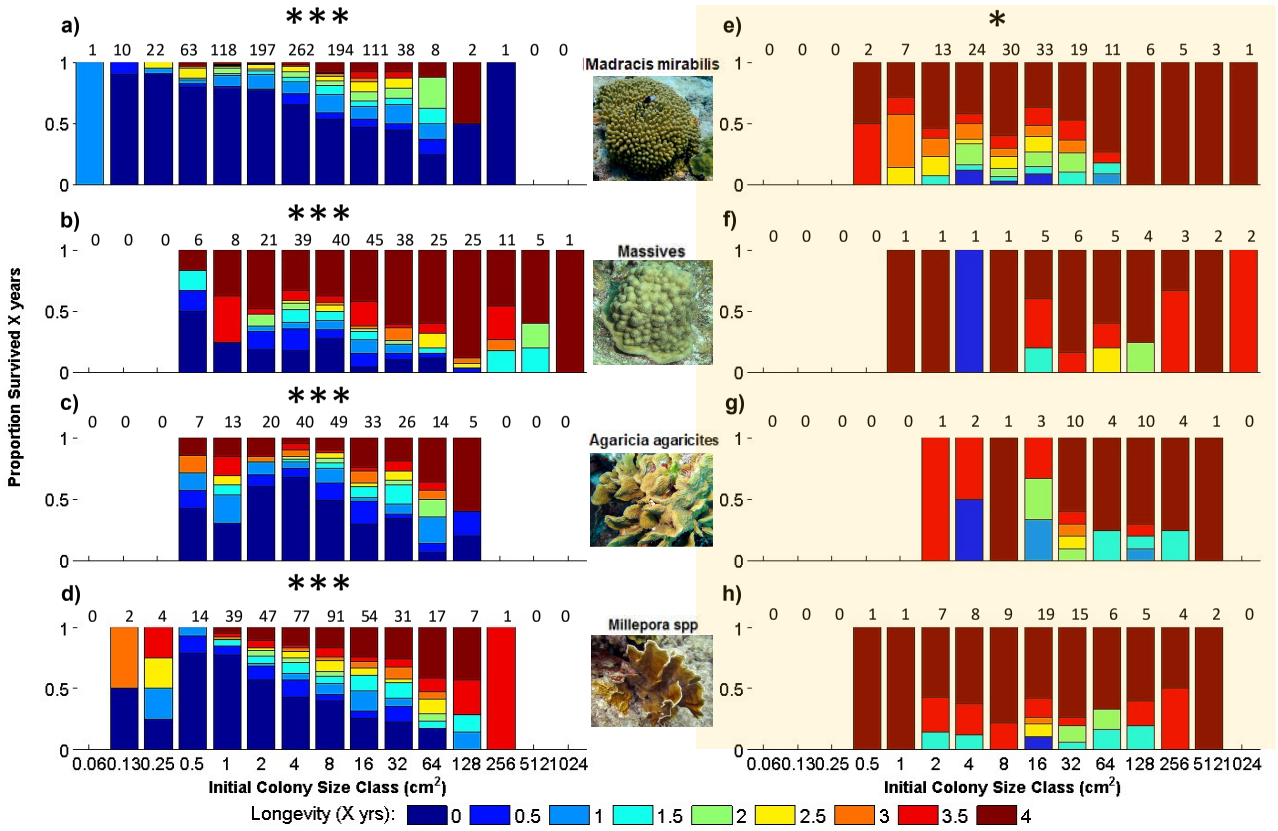

Figure 2.5: **Colony longevity as a function of size and fate.**
Proportion of colonies surviving for each longevity category (x yrs) as a function of initial size. For each hard coral group (represented by rows), data was divided into two general fate categories: isolated (left column) and fission/fusion/multi-fate (right column). Significant size dependent longevity occurs in isolated change colonies, which disappears in colonies with fission/fusion/multi-fate dynamics, which exhibit significantly increased longevity overall. Asterisks denote significant maximum likelihood-based log-linear relationships between longevity and size (* = $p < 0.05$; *** = $p < 0.001$). Values above bars are sample sizes. Note x-axis log base 2 scale.

2.8 Supporting Information

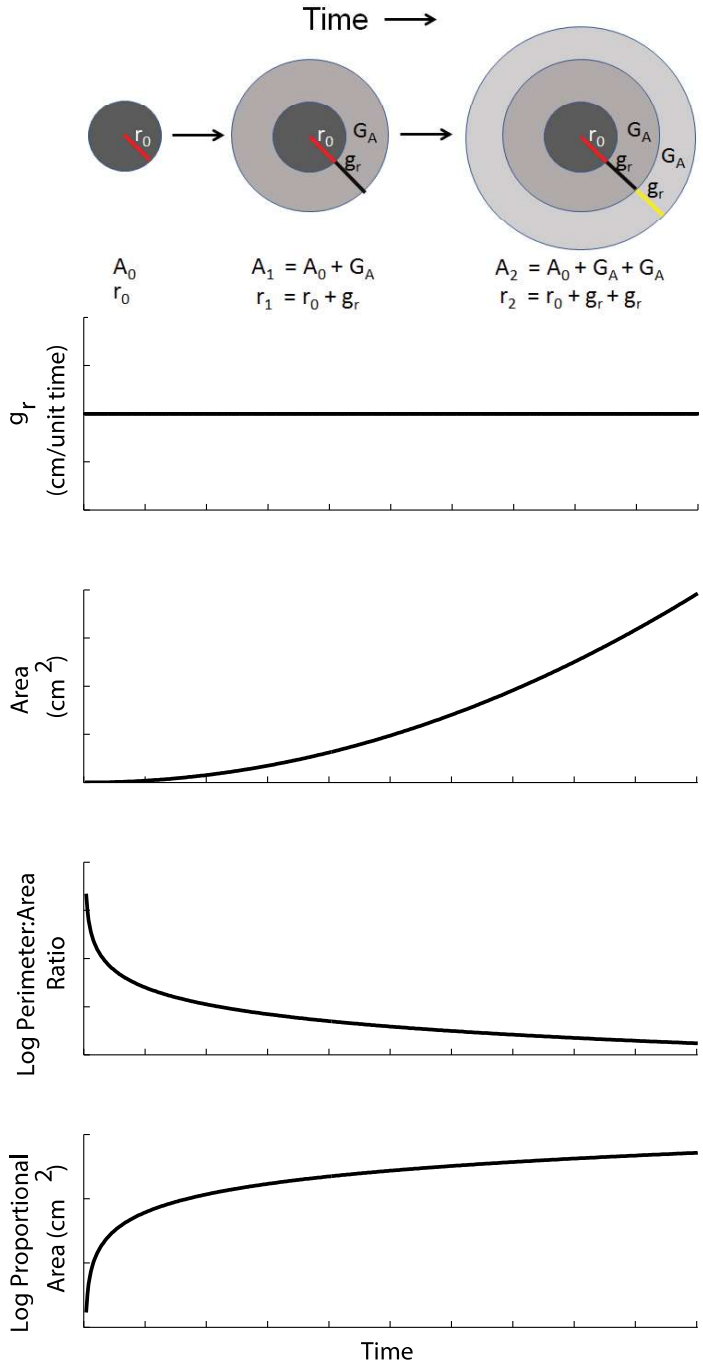

Figure 2.6: **Theoretical growth expectations based on geometric constraints.**
Theoretical geometric-based allometric constraints in growth expectations for circular colonies with constant radial extension. As colony size increases the perimeter:area ratio decreases and the change in log proportional area slows down. r is radius, g_r is growth rate, G_A is area resulting from growth interval.

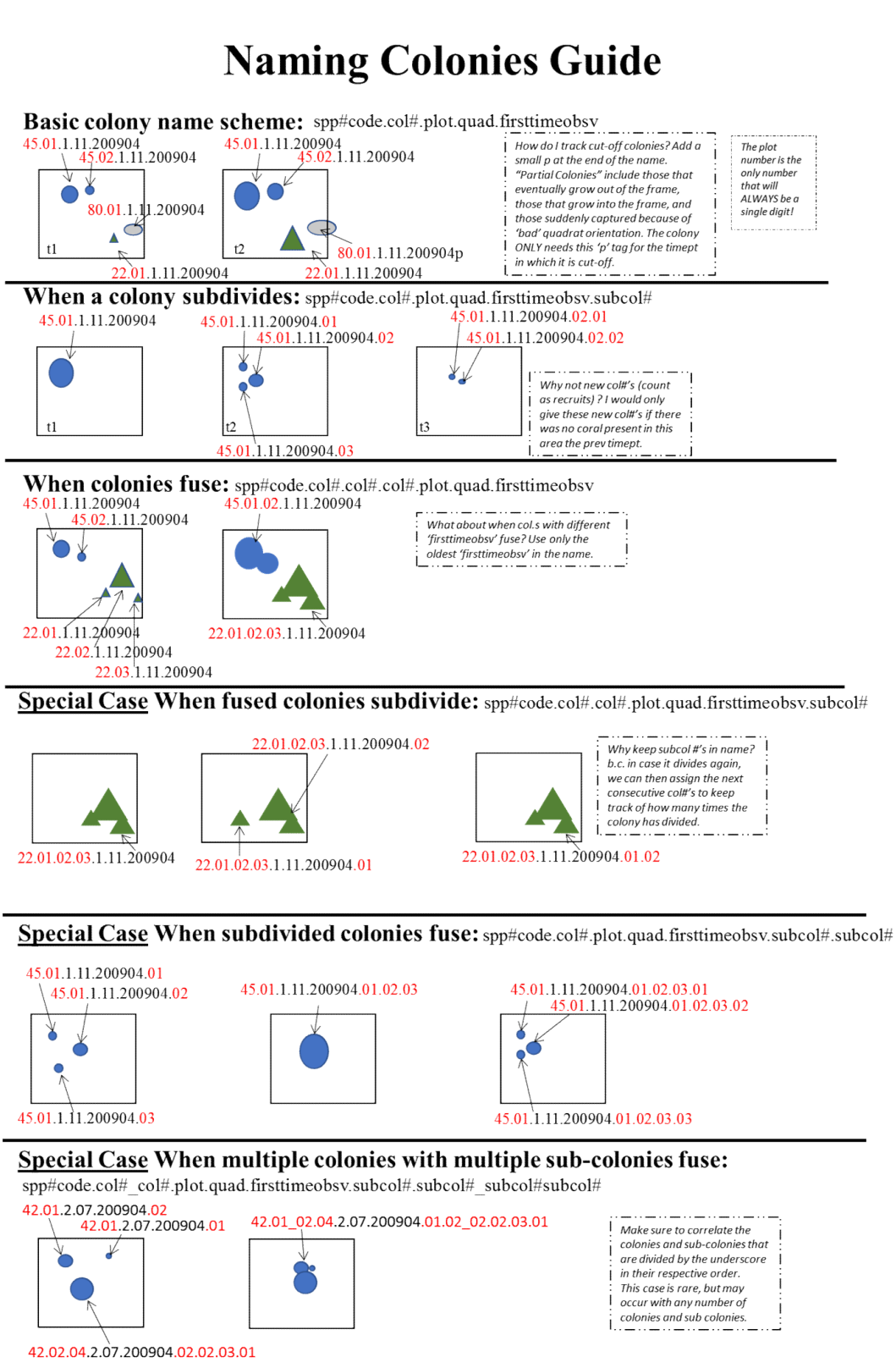

Figure 2.7: **Naming scheme for tracking colony change.**
The unique alpha-numeric naming scheme developed to track coral colony demographic unit change, including histories of fission and fusion.

Table 2.2: **Randomization results by timepoint for *M.mirabilis*.**
Randomization results by timepoint and size class for the effect of fate on log proportional change for *M.mirabilis*. All statistically significant results are in bold using fate-based color legend in Figure 2.4. Timepoints in *yearmo* format, p = p-value from randomization ($\alpha = 0.05$), diff = difference between mean of isolated fate change in area and mean of either multi-fate, fission, or fusion fate change in area, respectively, $\bar{x}$ = mean, sd = standard deviation, n.d = no data.

				<1cm^2				1 to 10 cm^2				>10 cm^2			
Coral Group	Timepoints		Stat	isolated	multifate	fission	fusion	isolated	multifate	fission	fusion	isolated	multifate	fission	fusion
M. mirabilis	200904	200908	*p*	//////////	n.d	n.d	n.d	//////////	0.851	**0.041**	**0.039**	//////////	0.051	0.124	0.069
			diff	//////////	n.d	n.d	n.d	//////////	-0.066	**0.572**	**0.863**	//////////	1.059	0.748	1.204
			n	13	0	0	0	78	2	**11**	**4**	16	4	6	2
			$\bar{x}$	0.595	n.d	n.d	n.d	-0.318	-0.383	**0.254**	**0.546**	-1.239	-0.180	-0.491	-0.035
			sd	0.786	n.d	n.d	n.d	0.907	1.283	**0.749**	**0.529**	1.047	0.932	1.027	0.295
	200908	201005	*p*	//////////	n.d	n.d	n.d	//////////	0.986	0.849	0.136	//////////	0.281	0.604	0.871
			diff	//////////	n.d	n.d	n.d	//////////	0.029	-0.093	0.595	//////////	-0.479	-0.242	0.072
			n	11	0	0	0	45	2	4	6	6	4	3	4
			$\bar{x}$	0.545	n.d	n.d	n.d	0.211	0.239	0.117	0.805	0.282	-0.197	0.040	0.354
			sd	0.863	n.d	n.d	n.d	0.869	1.554	1.544	0.931	0.538	0.830	1.102	0.419
	201005	201009	*p*	//////////	0.400	0.584	n.d	//////////	0.860	0.139	**0.015**	//////////	0.240	0.407	0.274
			diff	//////////	-0.825	0.421	n.d	//////////	-0.038	0.269	**0.706**	//////////	0.323	-0.214	0.439
			n	36	1	2	0	129	7	26	**8**	32	10	12	4
			$\bar{x}$	0.214	-0.610	0.636	n.d	-0.150	-0.188	0.119	**0.556**	-0.283	0.040	-0.497	0.156
			sd	1.013	0.000	1.433	n.d	0.817	0.945	0.940	**0.497**	0.743	0.827	0.828	0.263
	201009	201103	*p*	//////////	0.838	0.388	0.189	//////////	0.133	0.457	0.269	//////////	0.779	0.869	0.157
			diff	//////////	0.049	0.338	0.834	//////////	-0.371	-0.241	0.396	//////////	-0.077	0.142	0.521
			n	37	2	4	1	88	13	7	6	26	10	6	7
			$\bar{x}$	0.847	0.896	1.184	1.680	0.344	-0.028	0.103	0.739	-0.200	-0.277	-0.057	0.321
			sd	0.915	0.153	0.423	0.000	0.889	0.521	0.663	0.516	1.153	0.892	0.503	0.370
	201103	201109	*p*	//////////	0.540	0.291	n.d	//////////	0.325	0.470	**0.012**	//////////	0.386	0.061	0.524
			diff	//////////	-0.418	0.832	n.d	//////////	-0.227	-0.178	**0.848**	//////////	-0.158	-0.426	0.166
			n	21	1	1	0	116	11	10	**6**	48	18	13	8
			$\bar{x}$	0.581	0.163	1.413	n.d	0.062	-0.165	-0.116	**0.910**	0.046	-0.112	-0.380	0.212
			sd	1.011	0.000	0.000	n.d	0.700	0.722	0.744	**1.059**	0.680	0.642	0.617	0.238
	201109	201204	*p*	//////////	0.232	0.318	0.832	//////////	0.123	0.972	0.359	//////////	0.096	0.330	0.265
			diff	//////////	-1.161	1.297	-0.039	//////////	-0.359	0.013	0.523	//////////	-0.365	0.237	0.434
			n	20	1	1	1	89	14	4	2	46	18	14	4
			$\bar{x}$	0.715	-0.446	2.012	0.676	0.092	-0.267	0.105	0.614	-0.288	-0.653	-0.050	0.146
			sd	0.976	0.000	0.000	0.000	0.762	0.921	0.917	1.244	0.736	0.987	0.560	0.274
	201204	201208	*p*	//////////	n.d	0.231	n.d	//////////	0.990	**0.037**	n.d	//////////	0.470	0.538	0.930
			diff	//////////	n.d	-1.024	n.d	//////////	0.018	**0.551**	n.d	//////////	-0.137	-0.151	0.056
			n	17	0	1	0	70	4	**9**	0	46	22	11	5
			$\bar{x}$	0.599	n.d	-0.426	n.d	-0.344	-0.326	**0.206**	n.d	-0.231	-0.368	-0.382	-0.176
			sd	1.018	n.d	0.000	n.d	0.780	1.052	**0.591**	n.d	0.842	0.510	0.684	0.580
	201208	201303	*p*	//////////	0.935	n.d	0.805	//////////	0.223	0.212	0.658	//////////	0.346	0.255	0.738
			diff	//////////	-0.186	n.d	-0.339	//////////	-0.359	0.409	0.263	//////////	-0.208	-0.517	0.248
			n	30	1	0	1	68	10	8	2	34	20	4	2
			$\bar{x}$	0.765	0.579	n.d	0.426	0.397	0.039	0.807	0.661	0.007	-0.201	-0.510	0.255
			sd	0.830	0.000	n.d	0.000	0.911	0.826	0.634	0.324	0.862	0.667	0.471	0.315

Table 2.3: **Randomization results by timepoint for massives.**
Randomization results by timepoint and size class for the effect of fate on log proportional change for massives. All statistically significant results are in bold using fate-based color legend in Figure 2.4. Timepoints in *yearmo* format, p = p-value from randomization ($\alpha = 0.05$), diff = difference between mean of isolated fate change in area and mean of either multi-fate, fission, or fusion fate change in area, respectively, $\bar{x}$ = mean, sd = standard deviation, n.d = no data.

			<1cm²				1 to 10 cm²				>10 cm²			
Coral Group	Timepoints	Stat	isolated	multifate	fission	fusion	isolated	multifate	fission	fusion	isolated	multifate	fission	fusion
Massives	200904 200908	*p*	//////////	n.d	n.d	n.d	//////////	n.d	0.352	n.d	//////////	n.d	0.914	n.d
		diff	//////////	n.d	n.d	n.d	//////////	n.d	-0.323	n.d	//////////	n.d	0.070	n.d
		n	4	0	0	0	44	0	1	0	59	0	2	0
		$\bar{x}$	1.113	n.d	n.d	n.d	-0.047	n.d	-0.369	n.d	-0.134	n.d	-0.063	n.d
		sd	1.040	n.d	n.d	n.d	0.440	n.d	0.000	n.d	0.448	n.d	0.065	n.d
	200908 201005	*p*	//////////	n.d	n.d	n.d	//////////	n.d	n.d	0.932	//////////	0.494	0.136	n.d
		diff	//////////	n.d	n.d	n.d	//////////	n.d	n.d	0.172	//////////	-0.056	-0.286	n.d
		n	0	0	0	0	29	0	0	1	49	1	3	0
		$\bar{x}$	n.d	n.d	n.d	n.d	0.288	n.d	n.d	0.460	0.030	-0.026	-0.256	n.d
		sd	n.d	n.d	n.d	n.d	0.523	n.d	n.d	0.000	0.351	0.000	0.158	n.d
	201005 201009	*p*	//////////	n.d	n.d	n.d	//////////	n.d	0.778	n.d	//////////	0.530	**0.040**	0.374
		diff	//////////	n.d	n.d	n.d	//////////	n.d	-0.080	n.d	//////////	-0.090	**-0.556**	-0.172
		n	3	0	0	0	69	0	2	0	102	2	**1**	1
		$\bar{x}$	0.348	n.d	n.d	n.d	0.099	n.d	0.019	n.d	-0.006	-0.096	**-0.562**	-0.178
		sd	0.802	n.d	n.d	n.d	0.484	n.d	0.119	n.d	0.277	0.130	**0.000**	0.000
	201009 201103	*p*	//////////	n.d	n.d	n.d	//////////	n.d	0.837	0.121	//////////	0.329	0.165	**0.023**
		diff	//////////	n.d	n.d	n.d	//////////	n.d	0.098	-0.848	//////////	-0.191	-0.383	**0.417**
		n	3	0	0	0	57	0	2	1	92	2	4	**3**
		$\bar{x}$	0.324	n.d	n.d	n.d	0.317	n.d	0.415	-0.531	-0.051	-0.242	-0.434	**0.366**
		sd	0.751	n.d	n.d	n.d	0.603	n.d	0.251	0.000	0.448	0.748	0.492	**0.466**
	201103 201109	*p*	//////////	n.d	n.d	n.d	//////////	0.942	0.265	0.592	//////////	**0.003**	0.297	n.d
		diff	//////////	n.d	n.d	n.d	//////////	0.047	0.222	0.187	//////////	**-0.546**	-0.127	n.d
		n	9	0	0	0	63	1	3	1	90	**3**	3	0
		$\bar{x}$	0.918	n.d	n.d	n.d	0.175	0.221	0.397	0.361	0.074	**-0.472**	-0.052	n.d
		sd	0.548	n.d	n.d	n.d	0.346	0.000	0.479	0.000	0.192	**0.506**	0.119	n.d
	201109 201204	*p*	//////////	n.d	n.d	n.d	//////////	n.d	n.d	0.420	//////////	0.809	**0.010**	n.d
		diff	//////////	n.d	n.d	n.d	//////////	n.d	n.d	0.253	//////////	0.087	**-0.987**	n.d
		n	8	0	0	0	45	0	0	2	96	2	**2**	0
		$\bar{x}$	0.799	n.d	n.d	n.d	0.251	n.d	n.d	0.505	0.016	0.103	**-0.971**	n.d
		sd	0.654	n.d	n.d	n.d	0.460	n.d	n.d	0.193	0.300	0.093	**0.121**	n.d
	201204 201208	*p*	//////////	n.d	0.732	n.d	//////////	0.056	n.d	0.158	//////////	**0.012**	0.199	n.d
		diff	//////////	n.d	0.024	n.d	//////////	-1.145	n.d	0.392	//////////	**-0.564**	-0.191	n.d
		n	7	0	1	0	61	1	0	3	96	**3**	2	0
		$\bar{x}$	0.385	n.d	0.409	n.d	0.089	-1.055	n.d	0.481	0.043	**-0.521**	-0.148	n.d
		sd	0.534	n.d	0.000	n.d	0.428	0.000	n.d	0.780	0.230	**0.743**	0.221	n.d
	201208 201303	*p*	//////////	n.d	n.d	n.d	//////////	n.d	**0.002**	0.136	//////////	n.d	**0.017**	n.d
		diff	//////////	n.d	n.d	n.d	//////////	n.d	**1.602**	0.858	//////////	n.d	**-2.501**	n.d
		n	7	0	0	0	70	0	**1**	1	90	0	**1**	0
		$\bar{x}$	0.795	n.d	n.d	n.d	0.276	n.d	**1.878**	1.133	0.016	n.d	**-2.485**	n.d
		sd	0.376	n.d	n.d	n.d	0.490	n.d	**0.000**	0.000	0.350	n.d	**0.000**	n.d

Table 2.4: **Randomization results by timepoint for *A.agaricites*.**
Randomization results by timepoint and size class for the effect of fate on log proportional change for *A.agaricites*. All statistically significant results are in bold using fate-based color legend in Figure 2.4. Timepoints in *yearmo* format, p = p-value from randomization ($\alpha = 0.05$), diff = difference between mean of isolated fate change in area and mean of either multi-fate, fission, or fusion fate change in area, respectively, $\bar{x}$ = mean, sd = standard deviation, n.d = no data.

			<1cm²				1 to 10 cm²				>10 cm²			
Coral Group	Timepoints	Stat	isolated	multifate	fission	fusion	isolated	multifate	fission	fusion	isolated	multifate	fission	fusion
A. agaricites	200904 200908	*p*	//////////	n.d	n.d	n.d	//////////	n.d	0.253	n.d	//////////	0.679	0.751	0.086
		diff	//////////	n.d	n.d	n.d	//////////	n.d	-0.528	n.d	//////////	0.286	-0.050	0.600
		n	6	0	0	0	27	0	2	0	31	1	3	1
		$\bar{x}$	0.615	n.d	n.d	n.d	-0.034	n.d	-0.561	n.d	-0.293	-0.007	-0.343	0.306
		sd	0.410	n.d	n.d	n.d	0.649	n.d	0.240	n.d	0.527	0.000	0.077	0.000
	200908 201005	*p*	//////////	n.d	n.d	n.d	//////////	n.d	n.d	n.d	//////////	n.d	0.414	0.821
		diff	//////////	n.d	n.d	n.d	//////////	n.d	n.d	n.d	//////////	n.d	-0.372	0.041
		n	2	0	0	0	20	0	0	0	21	0	4	1
		$\bar{x}$	0.965	n.d	n.d	n.d	0.126	n.d	n.d	n.d	0.021	n.d	-0.351	0.062
		sd	1.989	n.d	n.d	n.d	0.673	n.d	n.d	n.d	0.735	n.d	1.312	0.000
	201005 201009	*p*	//////////	n.d	n.d	n.d	//////////	n.d	0.193	n.d	//////////	0.183	0.846	0.198
		diff	//////////	n.d	n.d	n.d	//////////	n.d	-0.479	n.d	//////////	-0.633	0.036	0.606
		n	3	0	0	0	43	0	3	0	30	4	3	1
		$\bar{x}$	0.412	n.d	n.d	n.d	0.120	n.d	-0.359	n.d	-0.297	-0.930	-0.262	0.308
		sd	1.184	n.d	n.d	n.d	0.575	n.d	1.251	n.d	0.750	1.512	0.512	0.000
	201009 201103	*p*	//////////	n.d	n.d	n.d	//////////	0.276	0.127	n.d	//////////	0.705	0.623	0.245
		diff	//////////	n.d	n.d	n.d	//////////	-0.326	0.601	n.d	//////////	0.035	-0.005	0.287
		n	5	0	0	0	35	4	2	0	28	2	1	2
		$\bar{x}$	1.357	n.d	n.d	n.d	-0.179	-0.505	0.422	n.d	-0.077	-0.041	-0.081	0.210
		sd	0.949	n.d	n.d	n.d	0.551	0.554	0.050	n.d	0.524	0.105	0.000	0.335
	201103 201109	*p*	//////////	n.d	n.d	n.d	//////////	n.d	**0.006**	0.294	n.d	0.569	**0.010**	0.878
		diff	//////////	n.d	n.d	n.d	//////////	n.d	**2.099**	0.379	n.d	-0.046	**-0.701**	0.018
		n	4	0	0	0	31	0	**1**	2	28	5	**3**	1
		$\bar{x}$	0.714	n.d	n.d	n.d	0.338	n.d	**2.438**	0.717	0.130	0.084	**-0.571**	0.149
		sd	0.762	n.d	n.d	n.d	0.531	n.d	**0.000**	0.426	0.204	0.152	**0.765**	0.000
	201109 201204	*p*	//////////	n.d	n.d	n.d	//////////	0.140	0.602	n.d	n.d	0.241	n.d	0.331
		diff	//////////	n.d	n.d	n.d	//////////	-0.895	-0.039	n.d	n.d	-0.159	n.d	0.111
		n	2	0	0	0	28	2	1	0	36	2	0	3
		$\bar{x}$	1.102	n.d	n.d	n.d	0.196	-0.699	0.157	n.d	0.157	-0.002	n.d	0.268
		sd	0.909	n.d	n.d	n.d	0.547	1.164	0.000	n.d	0.181	0.187	n.d	0.158
	201204 201208	*p*	//////////	n.d	n.d	n.d	//////////	0.856	0.410	0.894	n.d	0.237	0.767	n.d
		diff	//////////	n.d	n.d	n.d	//////////	0.125	-0.412	0.143	n.d	-0.412	0.072	n.d
		n	3	0	0	0	31	1	2	1	32	3	1	0
		$\bar{x}$	0.855	n.d	n.d	n.d	0.036	0.161	-0.376	0.179	-0.051	-0.463	0.021	n.d
		sd	0.831	n.d	n.d	n.d	0.615	0.000	1.030	0.000	0.519	0.231	0.000	n.d
	201208 201303	*p*	//////////	n.d	n.d	n.d	//////////	0.595	0.169	n.d	n.d	**0.027**	0.610	0.147
		diff	//////////	n.d	n.d	n.d	//////////	-0.389	-0.824	n.d	n.d	**-1.337**	-0.043	0.374
		n	3	0	0	0	29	1	1	0	30	**2**	2	2
		$\bar{x}$	1.096	n.d	n.d	n.d	0.302	-0.087	-0.522	n.d	0.036	**-1.301**	-0.007	0.410
		sd	0.726	n.d	n.d	n.d	0.758	0.000	0.000	n.d	0.318	**1.640**	0.015	0.316

Table 2.5: **Randomization results by timepoint for *Millepora* spp.**
Randomization results by timepoint and size class for the effect of fate on log proportional change for *Millepora* spp. All statistically significant results are in bold using fate-based color legend in Figure 2.4. Timepoints in *yearmo* format, p = p-value from randomization ($\alpha = 0.05$), diff = difference between mean of isolated fate change in area and mean of either multi-fate, fission, or fusion fate change in area, respectively, $\bar{x}$ = mean, sd = standard deviation, n.d = no data.

			<1cm²				1 to 10 cm²				>10 cm²			
Coral Group	Timepoints	Stat	isolated	multifate	fission	fusion	isolated	multifate	fission	fusion	isolated	multifate	fission	fusion
Millepora spp	200904 200908	*p*	//////////	n.d	n.d	n.d	//////////	**0.032**	0.436	n.d	n.d	0.259	0.537	0.476
		diff	//////////	n.d	n.d	n.d	//////////	**-1.584**	-0.425	n.d	n.d	-0.577	-0.235	0.441
		n	7	0	0	0	65	**1**	2	0	28	2	3	1
		$\bar{x}$	0.043	n.d	n.d	n.d	-0.038	**-1.622**	-0.462	n.d	-0.215	-0.792	-0.449	0.226
		sd	0.984	n.d	n.d	n.d	0.768	**0.000**	0.269	n.d	0.668	0.371	1.016	0.000
	200908 201005	*p*	//////////	n.d	n.d	n.d	//////////	0.393	0.424	**0.013**	n.d	0.226	0.995	**0.042**
		diff	//////////	n.d	n.d	n.d	//////////	-0.410	0.364	**1.443**	n.d	0.429	0.040	**0.551**
		n	3	0	0	0	34	4	5	**2**	17	2	2	**3**
		$\bar{x}$	1.044	n.d	n.d	n.d	0.156	-0.254	0.520	**1.599**	-0.104	0.325	-0.064	**0.447**
		sd	0.198	n.d	n.d	n.d	0.939	0.632	0.828	**0.535**	0.515	0.456	0.539	**0.200**
	201005 201009	*p*	//////////	n.d	n.d	n.d	//////////	0.707	0.614	**0.003**	n.d	0.422	0.087	0.671
		diff	//////////	n.d	n.d	n.d	//////////	0.134	-0.117	**0.790**	n.d	-0.206	-0.382	0.222
		n	7	0	0	0	79	4	9	**6**	44	3	8	1
		$\bar{x}$	0.680	n.d	n.d	n.d	-0.123	0.011	-0.240	**0.667**	-0.008	-0.214	-0.390	0.214
		sd	0.498	n.d	n.d	n.d	0.667	0.474	0.631	**0.336**	0.532	0.315	0.398	0.000
	201009 201103	*p*	//////////	n.d	n.d	n.d	//////////	0.098	0.364	n.d	n.d	0.316	0.674	0.190
		diff	//////////	n.d	n.d	n.d	//////////	0.425	0.222	n.d	n.d	-0.274	0.065	-0.320
		n	10	0	0	0	65	5	6	0	43	2	9	3
		$\bar{x}$	0.562	n.d	n.d	n.d	0.232	0.657	0.454	n.d	0.005	-0.269	0.071	-0.315
		sd	0.584	n.d	n.d	n.d	0.579	0.735	0.450	n.d	0.367	0.049	0.572	0.429
	201103 201109	*p*	//////////	n.d	n.d	n.d	//////////	0.368	0.784	0.513	n.d	0.612	0.929	**0.045**
		diff	//////////	n.d	n.d	n.d	//////////	-0.260	0.128	0.202	n.d	-0.051	-0.004	**0.238**
		n	10	0	0	0	70	5	3	5	54	9	3	**7**
		$\bar{x}$	0.812	n.d	n.d	n.d	0.146	-0.114	0.274	0.348	0.158	0.107	0.153	**0.396**
		sd	0.700	n.d	n.d	n.d	0.645	0.847	0.280	0.312	0.340	0.213	0.222	**0.275**
	201109 201204	*p*	//////////	n.d	n.d	n.d	//////////	0.247	0.299	n.d	n.d	0.889	0.080	0.327
		diff	//////////	n.d	n.d	n.d	//////////	0.402	-0.369	n.d	n.d	0.002	-0.297	-0.175
		n	3	0	0	0	56	3	3	0	67	7	9	5
		$\bar{x}$	0.006	n.d	n.d	n.d	0.070	0.472	-0.299	n.d	0.053	0.055	-0.244	-0.122
		sd	0.889	n.d	n.d	n.d	0.602	0.487	0.589	n.d	0.391	0.288	0.677	0.306
	201204 201208	*p*	//////////	n.d	n.d	n.d	//////////	0.318	0.247	0.074	n.d	0.444	**0.031**	0.988
		diff	//////////	n.d	n.d	n.d	//////////	-0.305	-0.692	0.876	n.d	-0.101	**-0.386**	0.061
		n	0	0	0	0	50	3	1	1	72	8	**5**	1
		$\bar{x}$	n.d	n.d	n.d	n.d	0.169	-0.136	-0.523	1.045	0.050	-0.051	**-0.336**	0.111
		sd	n.d	n.d	n.d	n.d	0.495	0.479	0.000	0.000	0.315	0.637	**0.333**	0.000
	201208 201303	*p*	//////////	n.d	n.d	n.d	//////////	0.053	0.074	0.980	n.d	0.939	0.662	0.252
		diff	//////////	n.d	n.d	n.d	//////////	-0.704	1.394	0.018	n.d	0.029	0.107	0.303
		n	4	0	0	0	43	3	2	1	53	7	10	3
		$\bar{x}$	1.429	n.d	n.d	n.d	0.362	-0.343	1.756	0.380	0.127	0.156	0.234	0.429
		sd	0.731	n.d	n.d	n.d	0.545	0.171	3.285	0.000	0.651	0.340	0.445	0.336

Chapter 3

Influence of Aggregation on Benthic Coral Reef Spatio-temporal Dynamics

3.1 Abstract

Spatial patterning of substrate-bound organisms constrains competition and short-term demographic rates, with dynamical implications propagating to much longer temporal scales. However, techniques for quantifying and analyzing the character of short- to intermediate- time-scale system behavior are lacking. A dynamical analysis of the time evolution of coral reef benthic systems, using results from numerical experiments obtained with a cellular model, shows that reefscape pathways can be divided into four stages: a repelling stage moving rapidly away from an unstable initial condition, a transient stage where spatial rearrangements bring key competitors into contact, an attracting stage during which the reef state decays to a steady-state attractor, and an attractor stage. The transient stage is dominated by nonlinear dynamics and the other three stages by linear dynamics. The relative durations of the stages are affected by the initial spatial configuration of corals and their competitors. Aggregation, a measure of spatial clumpiness, induces nonlinear dynamics in the transient stage in a manner similar to the effect of

finite-amplitude perturbations on reaction-diffusion systems. Reefscape states and dynamics are resolved using three dynamical variables: coral and macroalgae fractional cover and aggregation. Including diffusional processes in the model leads to pattern formation through increased clumping and scale separation between reefscape metrics (fractional cover and aggregation) and cell-level coral growth processes. The results suggest that spatial patterning of corals across a reefscape can influence rates of community change, with high aggregation patterns slowing loss in degraded systems and low aggregation configurations accelerating growth in healthy systems.

3.2 Significance

The spatial configuration of a coral reef can influence its decadal-scale time evolution, but the effects have not been investigated quantitatively. We apply the methods of complex systems to analyze the relationship between coral patterns and pathways tracking data-informed simulations initiated with varying levels of coral clumpiness, termed aggregation. Aggregation slows progression of a coral reef to its stable end-point and induces a transient stage that enhances coral-algae competitive interactions. These findings can be used to facilitate detection and analysis of reef pathways under climate change and human disturbance, and to inform management interventions of ways to speed recovery in healthy reefs and slow decay of degraded reefs.

3.3 Introduction

Coral reef ecosystems, one of the most biodiverse systems on the planet, are facing unprecedented degradation and system-wide losses stemming from warming waters, ocean acidification, sedimentation, pollution, overfishing, and other anthropogenic and environmental stressors [Nyström et al., 2000]. The predicted intensification of these stresses implies that models and other forms of research will be needed to infer the ways coral reefs are responding and will respond, with

the goal of facilitating possible interventions.

Most reefscape modeling and field studies focus on steady-state end-point or attractor perspectives, and not on the specific mechanisms operating along transient pathways connecting healthy reefs, dominated by coral, and degraded reefs, dominated by fleshy algae. The processes operating at these short- to intermediate-time scales are dependent on competitive interactions between coral and algae that are expected to be significantly affected by reefscape spatial patterns [Karlson et al., 2007]. Spatial location of individuals strongly influences outcomes of ecological interactions because these interactions occur over relatively short distances and are highly sensitive to the identity of neighbors [Lehman and Tilman, 1997, Dieckmann et al., 2000]. Therefore, the behavior of reefs is controlled, in part, by spatial arrangements that influence competition.

Spatial pattern formation in systems has been linked previously to the presence of nonlinearity. In ecology, nonlinearity arises from strong, tightly linked interactions of organisms, so that vital rates (e.g., mortality) are nonlinear functions of the densities of individuals [Dieckmann et al., 2000]. Pearson [Pearson, 1993] demonstrates that nonlinearity, excited by finite amplitude perturbations in reaction diffusion systems, can give rise to unexpected irregular spatio-temporal patterns that significantly affect how a system arranges itself to arrive at a particular configuration. As such, accounting for pre-existing aggregation patterns when initializing a system can result in time-evolution pathways that are markedly different from those that originate with either a homogenous or random configuration.

Aggregation is a measure of the degree to which individuals of the same type are spatially clumped [Murrell et al., 2001]. By changing the number of borders open to competitive interactions between different groups, higher levels of aggregation result in individuals interacting less with competitors in other groups and more with members from the same group than would be expected from overall abundance [Stoll and Prati, 2001]. Given that the range of fractional perimeter involved in algal interactions of Caribbean coral colonies has been empirically estimated between 0.61 and 0.80 [Barott et al., 2011], spatial aggregation of coral and algae is expected to play a central role in competitive outcomes and, ultimately,

the time-evolution of the reefscape [Crabbe, 2010]. For example, in coral and ascidian aggregation experiments, the rate with which strong competitors take over space is significantly reduced as their resources are redirected towards competing with each other, allowing weaker competitors to persist longer [Idjadi and Karlson, 2007, Hart and Marshall, 2009]. In reef restoration experiments, close spacing between outplants has been found to increase branching coral vertical growth rates, although overall fitness and long-term survival decreases [Raymundo, 2001]. Coral fragment experiments in numerical models also have found that growth is maximized in uniform, evenly spaced, gridded coral transplant arrangements, although competition with algae was not considered [Sleeman et al., 2005]. However, systematic numerical or experimental studies that quantify the relationship between aggregation and reef pathways have not been conducted.

Here we use a cellular model of interacting coral and algae organisms to investigate the evolution of benthic coral reefs with varying initial aggregation. Because coral reefs are complex systems, we employ the theoretical and analytical methods of complexity to explore reef dynamics in the model. The results are analyzed to determine the dynamical characteristics of reef pathways, the effect of aggregation on reef dynamics and implications for restoration management.

3.4 Results

Simulations were undertaken using a spatially explicit cellular model (100 cm^2 cells in a 200 x 200 cell lattice) parameterized for Caribbean reefs [Sandin and McNamara, 2011]. Coral reef benthic community dynamics are modeled for four spatially dominant, mutually exclusive functional groups: slowly evolving stony coral (CO), rapidly growing turf algae (TA) and macroalgae (MA), and crustose coralline algae (CCA), which acts as a type of substrate for growth of the other forms. Ecological processes determining the time evolution of the functional groups on the lattice include competition, growth, recruitment, algae succession, mortality, and herbivory of algae. Periodic boundary conditions are used and the model updates with time steps of 0.025 years (further details in Methods section).

The overall time-evolution of the reefscape is characterized using 1) fractional cover of CO, TA, MA and CCA, calculated as the area occupied by each type divided by the total area of the lattice, and 2) coral aggregation, calculated as the number of boundaries between adjacent CO cells divided by four times the number of CO cells. This metric for aggregation is zero when no two CO cells are neighbors and approaches one when all CO cells are arranged in a single clump.

To investigate the effect of aggregation on reefscape pathways, twelve initial configurations varying only in aggregation level from 0.66 to 0.99 with CO/TA/-MA/CCA initial fractional covers of 0.3/0.5/0.20/0.0 were constructed (Fig. 3.6) and simulated sixteen times, each set using a different random number generator seed. These configurations were created using gridded patterns of CO with varying distances between colonies (9 contiguous cells), plus one configuration with random placement of CO colonies (aggregation = 0.71).

The fractional cover pathways for all simulations can be empirically divided into a repelling stage, a transient stage (which might be absent), an attracting stage, and a CO-dominated attractor stage (Fig. 3.1). The repelling stage captures the initial response of the system to the initial aggregation condition. CO fractional cover pathways exhibit an initial decline attributed to limitations imposed on coral growth by the constrained number of CO borders open to growing into non-CO cells. The pathways during this stage exponentially move away from a repelling fractional cover value, as predicted by linearization around a repellor. The transient stage, dominated by the temporary but prolonged persistence of MA, is characterized by MA transitioning from TA cells, which recruit to the simulated reefscape at a faster rate than do MA or CO, and actively compete with CO. The transition to the attracting stage is marked by an increase beyond a threshold number of CO cell neighbors of MA, where MA becomes patchy or fragmented enough to expose sufficient borders for the dominant CO to overgrow it and for grazers to consume the remainder. The attracting stage is dominated by the steady recruitment and growth of CO onto CCA and TA cells. As predicted by a linear stability analysis, the pathways during this stage are consistent with an exponential decay to an attractor. In the attractor stage, the balance between

CO overgrowth of CCA/TA and CO mortality results in a simulated reefscape dominated by CO (0.586 +/- 0.002 SD fractional cover and 0.640 +/- 0.003 SD aggregation) and the passive CCA (see methods for definitions). In each of the four stages of the pathway, two-dimensional spatial power spectra of CO distribution were calculated on a detrended version of a binary CO cellular array. The power spectral density of this linear analysis is characterized by peaks associated with spacing of the initial aggregation (10m) in the repelling stage, which dissipate in the transient stage despite remnants of the initial pattern remaining visible (Fig. 3.7).

An analysis of the CO (Fig. 3.2a) and MA (Fig. 3.2b) pathways shows that increasing aggregation (blue to red) prolongs arrival to the attractor for both CO and MA. As initial aggregation increases, each CO fractional cover pathway exhibits an increasingly lower minimum as CO mortality outweighs CO growth more intensely when CO cells become more limited by CO cell neighbors that impede growth into surrounding space (Fig 3.2a). CO fractional cover pathways begin to recover from the decline only until enough CO cells undergo mortality, thus opening space (de-aggregating the pattern) for CO growth onto newly recruited CCA and TA. The CO repelling exponential time scale increases markedly as aggregation increases, with a doubling of the time scale between dispersed and clumped cases (Fig. 3.2c). This signifies that aggregation can constrain small-scale ecological processes of growth and competition that manifest in the pathways of fractional cover. The MA repelling time scale (Fig. 3.2d) exhibits a trend in the opposite direction, decreasing as aggregation increases in a manner that appears to be coupled to CO. MA competitive losses to the dominant CO cells are minimal and localized to the perimeter of the clumped CO, so that MA can more rapidly take over the inferior TA/CCA dominating the lattice, thereby reducing the MA time scale as aggregation increases.

Transient durations for both CO and MA (Fig. 3.2e, f) show a sharply increasing trend as aggregation increases, with the difference in transient duration between dispersed and clumped initial conditions exhibiting a ten-fold increase. This is consistent with the persistent influence of the initial condition found from

power spectrum analyses. The transient stage is mostly absent (duration between zero and five years) for initial aggregation less than 0.72, present in only some iterations for initial aggregation up to 0.75, and rises sharply to > 40 years thereafter, suggesting a threshold initial aggregation (Fig. 3.2e, f). Initial aggregation does not influence attracting time scales of either CO or MA (Fig. 3.2g, h) because of the dissolution of the initial pattern at this late stage (Fig. 3.1).

A partial state space constructed with CO and MA fractional covers (Fig. 3.3a) shows that a two-dimensional state space is inadequate for resolving the dynamics of the simulated reefscape because trajectories intersect themselves and other trajectories. Adding aggregation as an additional axis to the state space removes trajectory intersections (Fig. 3.3b). The system converges to a point attractor with CO fractional cover 0.586 +/- 0.002 SD, MA fractional cover <0.001 and aggregation 0.640 +/- 0.003 SD. That three dimensions is sufficient to resolve the dynamics of the system is supported by a false nearest neighbor (FNN) analysis [Kennel et al., 1992] applied to the CO fractional cover time series within the attractor, which illustrates that the fraction of FNNs decreases to near zero with three embedding dimensions (Fig. 3.8).

The observation that fractional cover pathways during the repelling and attracting stages appear to be exponential suggests the dominance of linear dynamics during these two stages. To test this hypothesis and to investigate dynamics during the transient and attractor stages, a spatio-temporal forecasting method was employed [Parlitz and Merkwirth, 2000, Grimes et al., 2015]. This method can be used to distinguish between linear and nonlinear dynamics by leveraging the much stronger dependence of forecast accuracy on position in state space for systems dominated by nonlinear dynamics. A spatial forecasting method was applied to sequences of reefscape snapshots of functional types on the lattice during the transient, attracting and attractor stages and forecasting skill was calculated as a function of the number of neighboring points in state space used to make the forecast. For linear dynamics, forecasting skill is expected to rise and remain at a constant value; for nonlinear dynamics, forecasting skill is expected to rise to a peak and then decrease. The results (Fig. 3.4) are consistent with dominance

of linear dynamics in the repellor, attracting and attractor stages, and nonlinear dynamics in the transient stage. Spatio-temporal forecasting results were similar for all pathways across aggregation levels, except for cases with short transient stages (< 5 years), for which the strength of nonlinearity is marginal (Fig. 3.9).

The simulations described so far were conducted with a moderate rate of algae herbivory (12 % of algae grazed per timestep), which gives coral a competitive advantage in occupying the reefscape. Coral reefs can become degraded when herbivore populations decline, as with overfishing. To test the effect of aggregation in degraded reefs, a second set of numerical experiments indicated that higher aggregation significantly increased the total time required to arrive at the attractor by a factor of about 1.5 for intact (high grazer) reefs and about 4.0 for degraded (low grazer) reefs (Fig. 3.5, 3.10). For the most clumped initial aggregation (0.99) alone, there was a ten-fold difference in arrival to the attractor between intact and degraded reefs.

3.5 Discussion

Aggregation sets the context for the processes of coral growth and coral-algae competition so that differences in aggregation can significantly influence annual to decadal scale predictions of fractional cover pathways. In the model, as initial aggregation increases, CO repelling time scale and duration of the transient stage increase because the processes of coral growth and competition are affected by the number of borders exposed to competitive interactions. In other words, outcomes of coral-algae competition are heavily influenced by the extent to which coral colony borders interact with neighboring algae, or the length of leading edges from which colonies grow and acquire space (intact reef) or shrink and lose space (degraded reef). Consequently, an intact (or degraded) reef starting with higher aggregation, all else being equal, requires more time to arrive at its attractor because coral cells must first be sufficiently dispersed to create space for coral growth (or shrinkage). That a low initial aggregation configuration (regular uniform arrangements) allows fractional cover to approach the attractor the fastest is also

in line with results from an agent-based model of coral fragments [Sleeman et al., 2005]. The observation that increasingly aggregated spatial patterns can lead to the emergence and persistence of transient dynamics in spatial systems expands understanding of the basis for transient behavior, which has been previously linked to increasing growth rates in density-dependent, spatially explicit population models [Hastings and Higgins, 1994, Hastings, 2004]. These results are also consistent with the argument that spatial distribution, as characterized by aggregation, is as important as competition coefficients, density, and the frequency of competitors in determining the nature of the pathway towards large-scale competitive dominance in spatially driven systems [Silvertown et al., 1992]. These results, following additional field and laboratory tests, have significant implications, as discussed below.

Previous studies of reefscape dynamics have used only coral and macroalgae fractional cover as the axes of state space (e.g., [Mumby et al., 2007, Sandin and McNamara, 2011]). However, trajectories in a two-dimensional state space of coral and macroalgae fractional cover intersect when varying initial aggregation, indicating that two variables (coral and macroalgae fractional cover) do not adequately represent the dynamics of the reefscape model. Adding aggregation as a third dimension of state space removes trajectory crossings and resolves trajectory pathways towards the attractor, suggesting that monitoring a metric of aggregation could be useful for analysis of coral reef dynamics and monitoring reef health.

A focus on the behavior of the system in short-to-intermediate scale pathways is not only essential for analyzing ecological system dynamics, but these scales also overlap with the durations of ecological research and management programs. Modeling decadal-scale futures have, by default, been based on random initial configurations that neglect the potential impact of reef aggregation patterns on dynamics, prediction outcomes and smaller-scale ecological behavior. Because aggregation provides the context for faster-scale organism-level change, measurements, monitoring, and modeling of organisms and comparisons between reefs should account for differences in aggregation.

Many aspects of spatial patterns close to an attractor or repellor can be

modeled accurately with linear dynamics, or a linearization of the underlying nonlinear dynamics [Nicolis, 1995]. Reefscape model results are consistent with linear dynamics at the beginning and end of the fractional cover pathway from initial configuration to attractor, with an intervening transient stage dominated by nonlinear dynamics. The finding that increasing initial aggregation leads to increasing transient stage duration and that a threshold aggregation might be required for the presence of a transient stage suggests that highly clumped coral acts as a finite amplitude perturbation (in comparison to a uniform or regularly dispersed base state) that excites nonlinear dynamics in the transient stage. A similar effect has been observed previously in numerical experiments using a reaction-diffusion chemical system, where irregular spatiotemporal patterns emerged in response to finite amplitude perturbations [Pearson, 1993]. The significance of a protracted transient stage dominated by nonlinear dynamics is that the interactions of organisms are more actively, or strongly, linked during this stage, meaning that competition could appear different during transient (recently disturbed) periods than during steady-state *pristine* conditions (long after a disturbance).

Scale separation, or the decoupling of dynamical interactions between different scales, is a required condition for pattern formation in systems through processes of self-organization and slaving [Werner, 1999, Rietkerk and van de Koppel, 2008]. Typically, scale separation occurs when the ratio between fast and slow time scales is at least two and often an order of magnitude apart. In the model, we found a plausible scale separation between macroalgae and coral (MA time scale about 5 years and CO time scale about 10 years), but not between the fractional cover/aggregation dynamics (about 8 years) and cell-level coral time scales (about 10 years). The dissipation that could cause cell-level coral dynamics to be damped over the longer time scales of coral patterns, thereby enabling scale separation, is absent in the model. To test whether the absence of self-organization can be attributed to a lack of dissipation, we added diffusion of CO, which is dissipative, to the model using a range of diffusion constants (Supplementary Information). The results (Fig. 3.11) indicate that diffusion enables self-organization and clumping in the model, but also acts to depress the steady-state CO fractional cover, which can

be explained by the effect of increased diffusion-driven aggregation on tipping the balance between coral mortality and growth. Further investigation is beyond the scope of this article, but these results suggest that dissipation, which might have a biological origin in coral colony fusion processes, is necessary for scale-separation and emergent pattern formation and should be considered in future research on coral reef models.

Rapid change in environmental conditions owing to global warming and other anthropogenic impacts can give rise to conditions in which coral reefs are repeatedly perturbed far from a steady state under the altered environment [Hughes et al., 2003]. Such changes could lead to more highly aggregated, or finite amplitude, conditions that might induce prolonged nonlinear dynamics as reefscapes follow pathways to new non-coral dominated attractors. Further studies of reefscapes recovering from recent perturbations or intact reefscapes on the path towards degradation could inform monitoring studies and interventions, because rates of benthic community change in these situations can be expected to be slower and more quantifiable. In comparing the impact of initial aggregation on subsequent reef development in different reef health scenarios, we found clumping was disadvantageous to inducing coral growth in both intact and degraded reefscapes, because exposed borders from which coral can grow and occupy non-coral space are severely limited by other coral neighbors. But in degraded reef scenarios initialized with small, competitively inferior coral colonies, clumping is advantageous for coral persistence (growth is still limited), because coral borders that would be exposed to negative competitive interactions are minimized (Supp. Info. and Fig. 3.13). Clumping also increases the persistence (transient duration) of macroalgae, which also exists in large patches when coral is clumped. For reef restoration initiatives that seek to maximize the growth of coral colony fragments cemented to artificial structures of various geometries and arrangements [Rinkevich, 1995], these results suggest that increasingly aggregated configurations of large, competitively dominant fragments can limit growth in both intact and degraded systems, but can increase persistence for small, competitively inferior fragments in degraded systems. This is particularly advantageous if fusion between genetically similar

fragments occurs and increases coral survival, given the improved ability of larger individuals to withstand assaults [Chornesky, 1991, Baums et al., 2006]. When considering the establishment of protected reef zones for restoration, complementing an evaluation of reefscape local health condition with level of coral colony aggregation might inform selections that target maximizing persistence and/or coral growth and dominance within a specified time frame.

The insight gained by combining numerical investigations of coral reefscape behavior with concepts and analysis techniques from studies of dynamics and complexity suggests that such a pairing could assist studies of coral reefs as well as studies of other pattern-forming ecological systems (e.g. alpine ribbon forests, arid, wetland, tundra, or savanna ecosystems). Analyzing the interactions between spatial patterning, temporal dynamics and ecological interactions can contribute to advances in modeling spatially driven systems [Hastings and Higgins, 1994, Kareiva and Wennergren, 1995, Dieckmann et al., 2000, Hastings, 2004, Hastings, 2010]. Specifically, expanding the focus beyond long-term outcomes to include short- to intermediate- scale pathways, and studying how competitive geometry related to aggregation patterns drives a significant quantitative effect on system spatio-temporal dynamics could have implications for ecological description, prediction, and questions of conservation significance.

3.6 Methods

In our implementation of a cellular reefscape model [Sandin and McNamara, 2011], the competitive hierarchy, in order of decreasing dominance, is CO belonging to large colonies above a colony size threshold ($C_{th} = 900cm^2$), MA, CO below the colony size threshold, TA, and CCA. CCA also includes open space, ignoring possible facilitating or competitive effects of certain CCA species [Harrington et al., 2004], which has been confirmed to not substantively affect model results [Eynaud et al., 2016]. All CO cells are set to represent branching coral types, which exhibit monotonic, potentially unlimited growth, although dynamics are qualitatively similar to massive coral [Sandin and McNamara, 2011].

Cell transition probabilities in the model are a function of the current state of a cell and that of its four nearest neighbor cells, with outcomes determined by the competitive dominance hierarchy. Growth of CO, TA, and MA on the reef occurs clonally (or vegetatively) by laterally expanding into neighboring space. The probability of an individual cell being overgrown by a neighboring cell is dependent on the growth rate of the neighboring functional type, G_x, where x denotes the functional type CO, TA, or MA, and the number of neighboring cells occupied by the functional type, n_x, which ranges from 0 to 4. Therefore, the probability of a cell being overgrown by functional type x is $1 - (1 - G_x)^{n_x}$.

Recruitment of benthic types occurs through the arrival and survival of mobile propagules into the juvenile population present on the reef. In the model, recruitment for each functional group is the composite probability of planktonic arrival in addition to survival into the juvenile class (i.e., growth to the size of a cell on the lattice). CO recruits to cells occupied by either CCA or TA with a probability of 0.01 per year; TA recruits to CCA cells at 0.80 per year. Because MA recruits from growing out of the TA assemblage, at each time step, a TA cell has a 0.33 per year probability of undergoing succession into MA. If a cell is slated to be overgrown by a neighboring cell as well as undergo recruitment, the outcome is determined by the competitive hierarchy.

Natural background mortality can affect all organisms. For algae, the tendency to exist as an assemblage of multiple individuals limits the likelihood of mortality for individuals in a particular area. For CO, cell mortality is simulated with the conversion of CO cells to CCA cells with a probability of 0.15 per year.

Herbivory of algae on reefs occurs from a suite of reef fishes and invertebrates. Because of their high mobility, herbivorous fish can explore wide areas of the benthic reefscape in their search for food. Grazing is simulated in a spatially random manner across the lattice, with TA and MA cell types having an equal likelihood of being consumed and converted to CCA. Algal food preference by grazers has been shown previously to have limited impact on model results [Eynaud et al., 2016]. Herbivory occurs at a specified grazing rate if enough algae cells are available and otherwise at a rate proportional to the total available

TA and MA cells. All initial configurations include coral colonies of size 30 cm x 30 cm, and results were found to be insensitive to increasing initial colony size. All simulations were conducted without disturbances (e.g., storm events) because numerical experiments conducted with stochastic disturbance events did not significantly impact the effect of aggregation on reefscape pathways (see Supporting Information).

Boundaries between the repelling, transient, attracting and attractor stages were determined using automated algorithms tailored for these simulated time series. For each random-seed-based set of aggregation levels, the boundary between repelling and transient stages was determined for the initial configuration that arrived at the attractor the fastest (i.e., the most regular initial aggregation pathway) and used for the remaining pathways in that set. The boundary was determined by following the pathway forward in time and flagging the time step where the slope of an exponential fit up to that point and the slope of an exponential fit over a window of three time steps differed by more than 1.5 times the standard deviation of the slope to that point. The boundary between transient and attracting stages was found as the inflection point between the concave-up (concave-down) transient curve and the concave-down (concave up) attracting curve for the CO (MA) pathway. The boundary between the attracting stage and the attractor stage was found by flagging the time step where the slope of the exponential fit from the beginning of the attracting stage and the slope of an exponential fit over a window of 10 time steps differed by less than 2 standard deviations of the slope to that point. Because the position of this point is sensitive to fluctuations, the pathways were pre-processed using an iterative diffusion smoothing method [Cai, 1988].

Temporal and spatial forecasting operate by reconstructing state space using lagged replicates of a portion of a series of points sampled in time [Sugihara and May, 1990] or space and time [Parlitz and Merkwirth, 2000]. Prediction skill from this reconstruction as a function of prediction distance, number of neighbors used to make a prediction, and other parameters, is evaluated and then used to assess properties of system dynamics, including linearity vs. nonlinearity. Spatio-temporal forecasting was implemented on a cube of cells with two directions being

spatial snapshots of the lattice and the third being time at intervals of one year [Grimes et al., 2015]. The state space was reconstructed using sequences of points from randomly chosen lines of cells in all three directions. Three cubes were considered: the first covering the time intervals of the transient stage, the second covering time intervals of the attracting stage and the third covering time intervals of the attractor stage. Forecast skill was calculated as a function of number of neighbors used in making the prediction for a total of 30,000 points using 5-fold cross validation. Linear dynamics is indicated by forecast skill that rises to a maximum value and stays constant as a function of number of neighbors used in making the prediction, and nonlinear dynamics is indicated by forecast skill that reaches a maximum value and then decreases as a function of number of neighbors used.

3.7 Acknowledgments

Insightful conversations with Y Eynaud and N Cortale are gratefully acknowledged. Supported by an NSF Graduate Fellowship to M Brito-Millan, the Department of Scripps Institution of Oceanography and The Gordon and Betty Moore Foundation. Author order ranked by contribution.

Chapter 3, in full, is material prepared for submission to Proceedings of the Royal Society B: Brito-Millan, M, BT Werner, SA Sandin, and D McNamara. Influence of Aggregation on Benthic Coral Reef Spatio-temporal Dynamics. The dissertation author was the primary investigator and author of this paper.

3.8 Figures

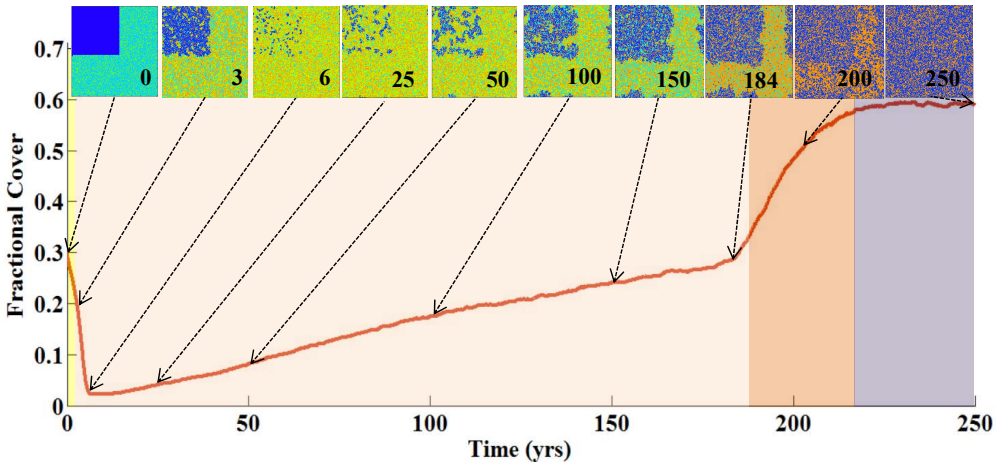

Figure 3.1: **Coral fractional cover pathway stages**
Coral fractional cover pathway vs. time illustrating four pathway stages: repelling (yellow), transient (peach), attracting (orange), and attractor (purple). Snapshots of the reefscape lattice at multiple points throughout the pathway show persistence of initial pattern into the attracting stage. Blue: CO; green: MA; bluish green: TA; orange: CCA.

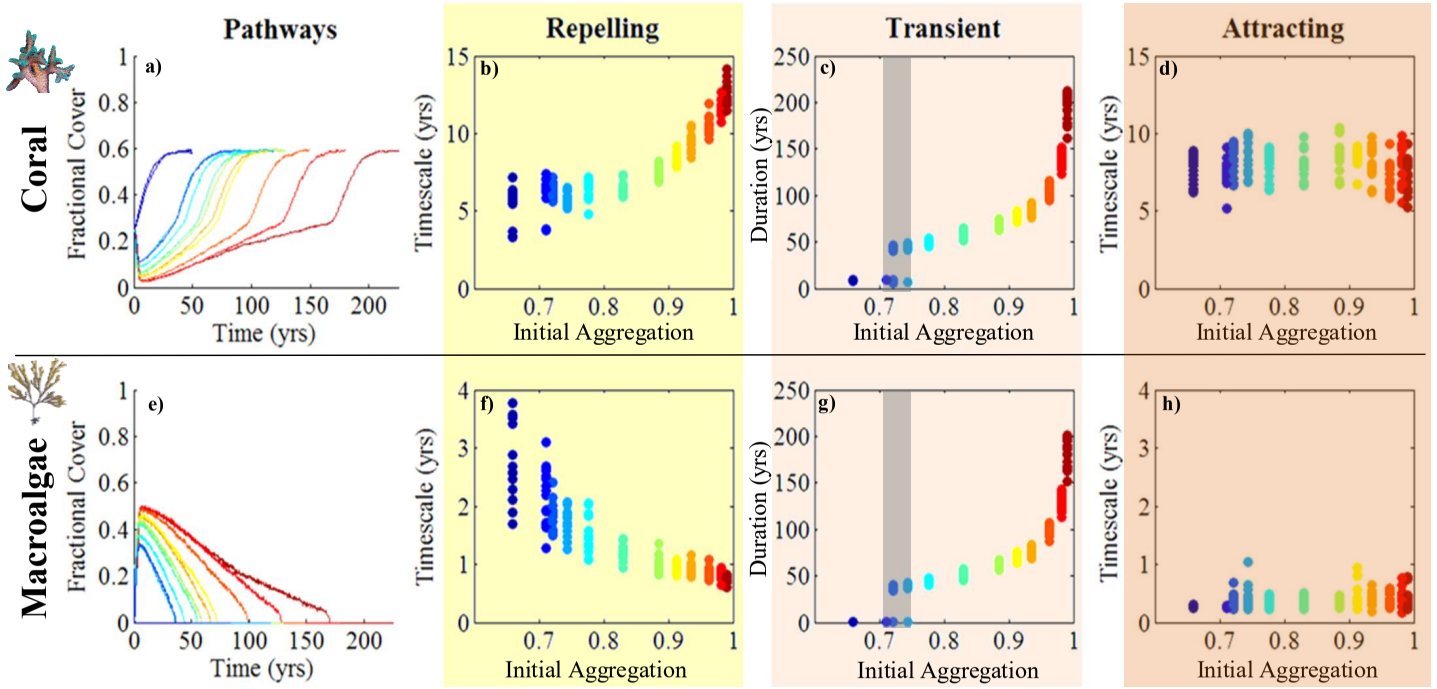

Figure 3.2: **Coral and macroalgae response to varying initial aggregation.**
Effect of increasing initial aggregation on CO and MA fractional cover pathways for twelve different initial aggregation configurations (n=16). Color gradient from blue to red in all panels represents increasing initial aggregation from the most regular (dark blue) to the most clumped (dark red). a) CO fractional cover pathways vs. time: increased delay in arrival at the attractor as initial aggregation increases; b) MA fractional cover pathways vs. time: increased delay in arrival at the attractor with increasing initial aggregation; c) CO repelling timescale doubles between two initial aggregation extremes; d) MA repelling timescale decreases as initial aggregation increases; e) CO transient duration increases as initial aggregation increases with threshold region (gray) showing durations with and without transient stage; f) MA transient duration increases as initial aggregation increases with threshold region (gray); g) CO attracting time scale appears independent of initial aggregation; h) MA attracting timescale appears independent of initial aggregation.

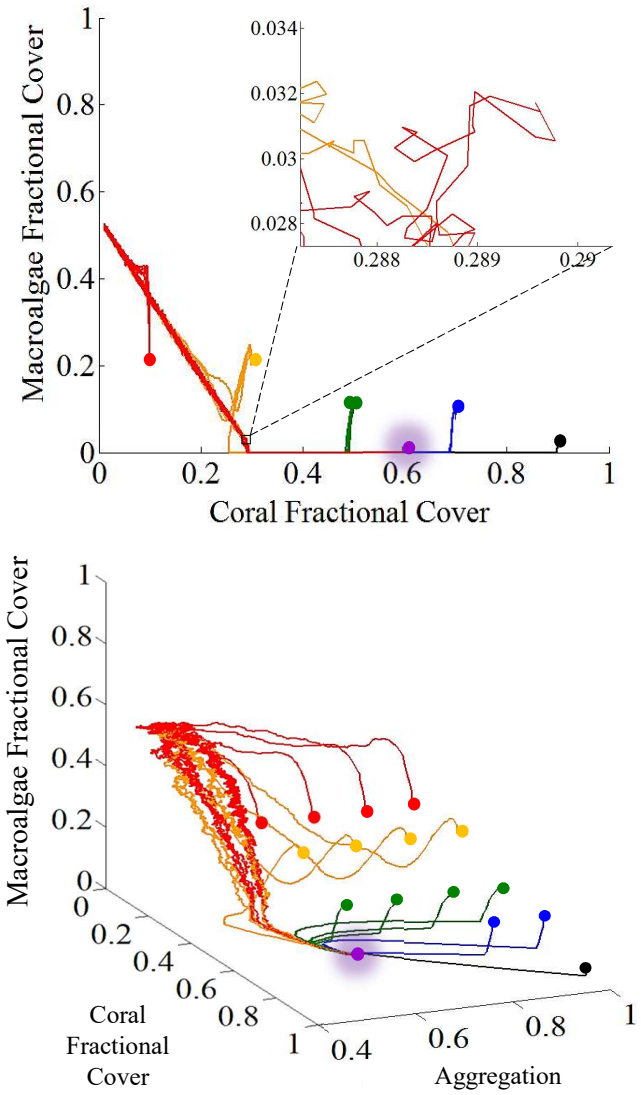

Figure 3.3: **Two-dimensional to three-dimensional phase space.** Simulated reefscape state space in two dimensions (a) and three dimensions (b), illustrates how addition of aggregation axis removes trajectory intersections and resolves dynamics. Trajectories color coded in groups of initial coral fractional cover, with dots indicating initial state and glowing purple dot the attractor for all trajectories. Initial CO fractional covers: 0.10 (red), 0.30 (gold), 0.50 (green), 0.70 (blue), and 0.90 (black); initial aggregation: 0.66, 0.77, 0.89, and 0.99.

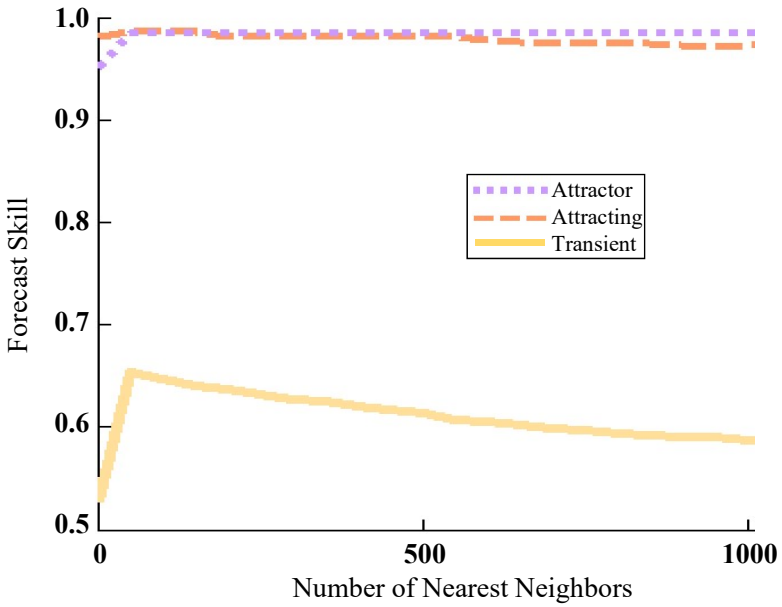

Figure 3.4: **Spatio-temporal forecasting of clumped initialization reveals nonlinear and linear stages.**
Nonlinear spatio-temporal forecasting of a clumped (0.96) initialization pathway tests for nonlinearity by stage. Forecast skill vs. number of nearest neighbors used to forecast the last three stages of the pathway. Nonlinear dynamics dominates transient stage and linear dynamics dominates attracting and attractor stages. The standard deviation for the attractor stage averaged 0.002 (range: 0.002 to 0.006), 0.002 (range: 0.001 to 0.004) for the attracting stage, and 0.030 (range: 0.010 to 0.027) for the transient stage.

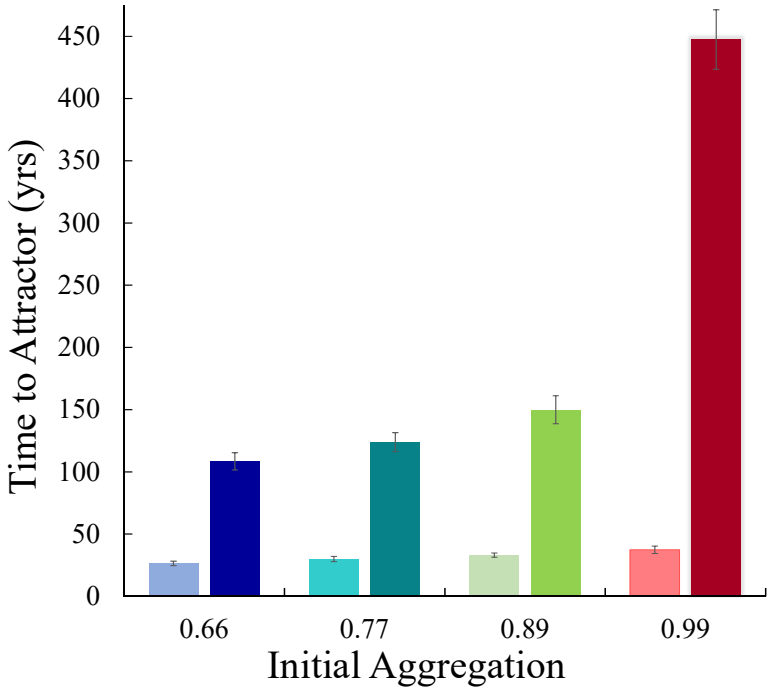

Figure 3.5: **Aggregation effect on time duration to attractor.**
Time duration to arrive at attractor vs. initial aggregation for intact (light) and degraded (dark) reefs. Degraded reefs amplify the effect of aggregation on the time duration to arrive at the attractor. Error bars are one standard deviation.

3.9 Supplementary Information

3.9.1 Effect of Stochastic Disturbance

The results shown in the article highlight the effect of aggregation on reefscape dynamics with competitively dominant coral colonies that exhibit increased coral survival and growth into space. The ability of large coral colonies to dominate reefscapes despite a degraded herbivore guild has been documented previously in Jamaica [Hughes, 1994], where a coral dominated reef with a depressed herbivory guild transitioned into an algae dominated reef only upon experiencing a large hurricane and subsequent urchin disease outbreak. Here, we explore how stochastic storm events affect the impact of aggregation on reefscape dynamics found in the main article (Fig. 3.12). The model was modified so that storms occur annually with probability 1/7. When a storm occurs, it kills 20 % of whole coral colonies on the reefscape. Simulations were run for an intact (24 % lattice grazed per time step) and degraded (4 % lattice grazed per time step) reef for initial aggregation levels of 0.66 (regular) and 0.99 (clumped). The effect of initial aggregation on coral fractional cover pathways remains significant, with regular initial aggregation configurations resulting in faster arrivals to the attractor (intact CO fractional cover attractor: 0.485 +/- 0.002 SD, degraded CO cover attractor: < 0.001). For intact reefs, clumped initial configuration delays arrival to the attractor by a decade. For degraded reefs, the regular initial configuration prolongs coral persistence on the reef by more than a century.

3.9.2 Effect of Small Colonies

The effect of initial aggregation on the more vulnerable, small, competitively inferior coral colonies was investigated because of its potential implications for management. Recruitment of small colonies into the adult population is necessary for the establishment of new coral in reefs [Hughes et al., 2000]. CO pathways initialized with regular and clumped aggregations of small coral colonies (4 contiguous cells) were simulated starting at fractional cover levels above (0.70) and below (0.30) the CO pathway attractors (intact: 0.586 +/- 0.002 SD; degraded:

$<$0.001). Starting fractional cover above and below the attractor for intact reefs allowed for exploring recovery pathways (from below) and pathways that might be considered degrading rather than stabilizing (from above). All small coral colony fractional cover pathways with clumped (red) initializations result in significant delays in arrival at the attractor in both intact and degraded scenarios (Fig. 3.13). In degraded reefs, clumping increases coral persistence by minimizing the number of coral borders that would be exposed to negative competitive interactions (Fig. 3.13a). In contrast, the apparent benefit of clumping becomes a disadvantage in intact reefs, where coral growth is constrained to the outer perimeter of the clump (until the clump is dissolved through mortality processes), thus producing a ten-year delay towards arrival at the steady-state attractor (Fig. 3.13b). Initializing coral pathways above and below the attractor confirmed that pathways eventually stabilize at the attractor determined by the parameters, including grazing level, independent of initial condition (basin of attraction is the entire state space). For intact reefs, starting coral fractional cover from above the attractor results in only a five-year delay towards steady-state for clumped initializations when compared to the initialization below the attractor, challenging the expectation that the coral pathway would have stabilized much sooner (traceable to the constraint on growth by clumping). Also, for intact reefs, the clumped coral fractional cover pathway from above the attractor crosses the attractor level early on (about year 3), which can be misinterpreted as an arrival at steady-state attractor if not viewed through a dynamics lens. Connecting significant declines in coral cover to high levels of aggregation can aid management responses in the face of unexpected declines.

3.9.3 Incorporating Coral Diffusion into the Model

In the model, the dynamics of coral (slow) and algae (fast) fractional cover are scale-separated, but coral fractional cover and aggregation only become scale separated from coral growth processes when diffusional processes are included. To test whether the absence of self-organization can be attributed to a lack of dissipation, we included CO diffusion, which is dissipative, in the model using a range of diffusion constants. A first order solution of the diffusion equation for

CO was implemented on a separate cellular lattice and transferred to the model lattice tracking the mutually exclusive occurrence of the four functional groups in each cell under the following two conditions. (1) If the value of CO in a cell in the diffusion lattice goes from less than 0.5 to greater than 0.5, the value of that cell in the diffusion lattice is set to 1 and the corresponding cell of the model lattice is set to CO. (2) If the value of CO in a cell in the diffusion lattice goes from greater than 0.5 to less than 0.5, the value of that cell in the diffusion lattice is set to 0 and the corresponding cell of the model lattice is set to MA, TA or CCA, randomly choosing the type amongst the neighboring cells. This process was constrained by the requirement that the net change in CO cells on the model lattice is 0. Coral growth rate was increased from 0.1m/y to 0.2m/y, which is within the measured range for branching coral types (Dullo 2005), because of the effect of diffusion on steady-state coral fractional cover (see below).

Diffusion leads to increased CO clumpiness, but only slight increases in CO aggregation, because aggregation increase is offset by decreases in coral fractional cover (Fig 3.11a, b). Steady-state coral fractional cover decreases as diffusion constant increases (Fig 3.11b). This is in line with the previously quantified effect of increased initial aggregation, where fewer coral borders open to competitive interactions results in mortality processes outweighing growth processes. CO diffusion continuously conserves some of that clumpiness, or growth limitation, which translates to a lower CO fractional cover at the attractor.

The time scale of decay to the attractor increases from 3.43 years to 18.80 years over a diffusion constant range of 0 to 0.16, suggesting that, with diffusion, CO clumps are self-organized and scale-separated from CO growth and mortality processes.

3.10 Supporting Information

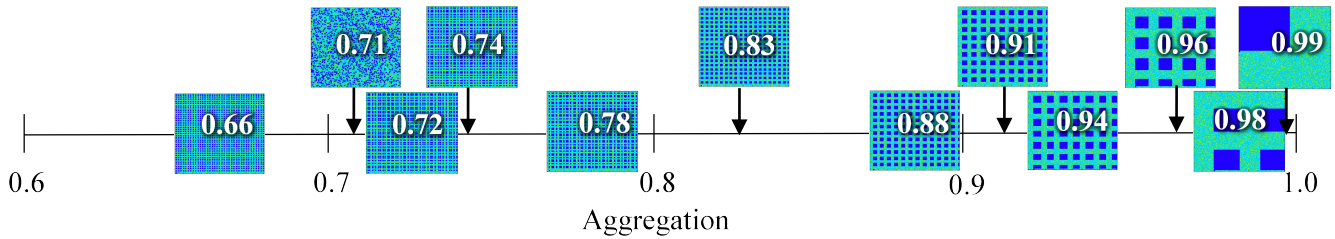

Figure 3.6: **Initial aggregation configurations**
The twelve initial aggregation configurations (all start at 0.30 fractional CO cover). Royal blue: CO; bluish-green: TA.

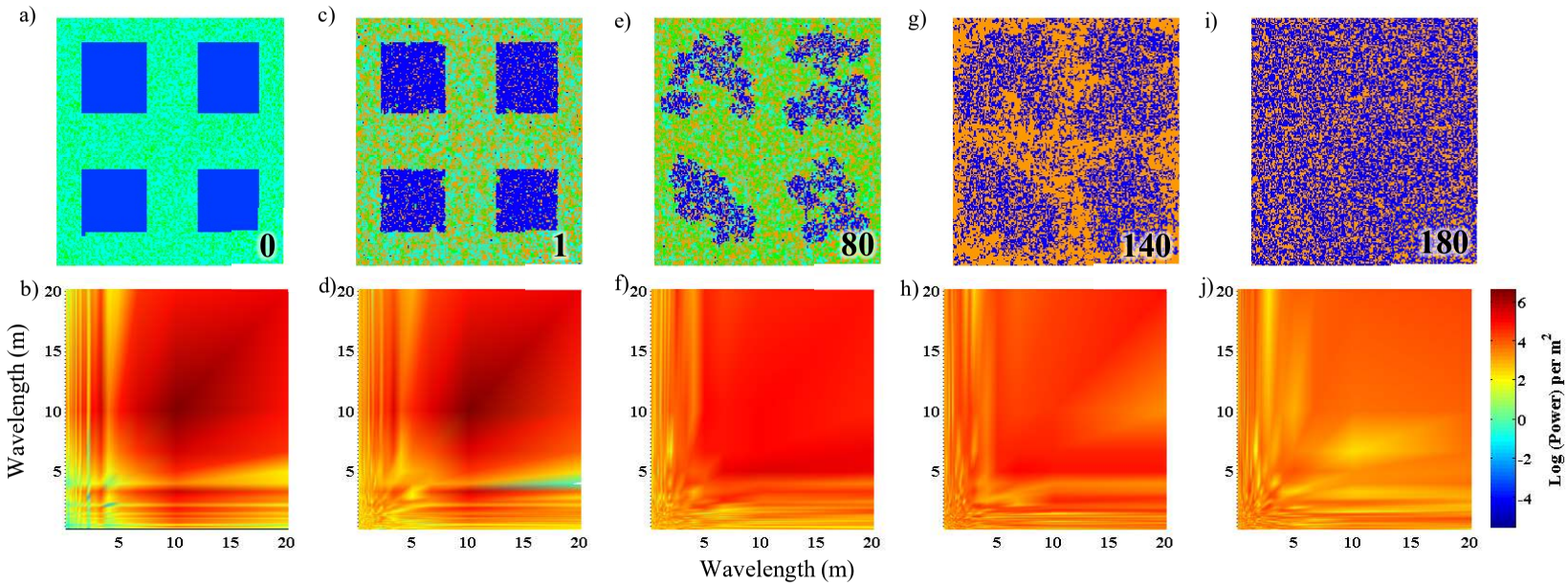

Figure 3.7: **Lattice and 2D Spectra.**
Snapshots of model lattice evolution (top row) and corresponding two-dimensional power spectra (bottom row) of detrended binary CO cellular arrays for an initial condition with four CO clumps at a) and b) initial state; year 0, c) and d) repelling stage; year 1, e) and f) transient stage; year 80, g) and h) attracting stage, year 140, i) and j) attractor stage, year 180. Spike (10 m) associated with spacing of initial aggregation pattern dissipates in transient stage.

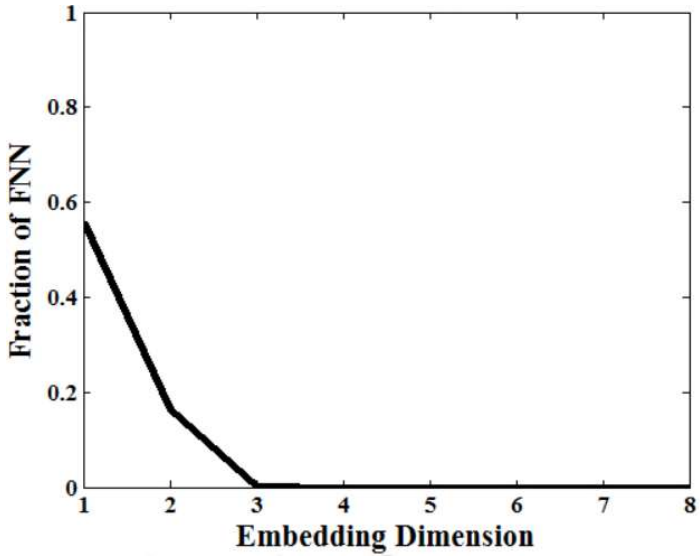

Figure 3.8: **Fraction of FNN minimized at three embedding dimensions.** Fraction of false nearest neighbors vs embedding dimension from phase space reconstruction of CO fractional cover 250-year time series in the attractor of the clumped initial condition (aggregation = 0.99; lag = 5 time steps) illustrates that three dimensions is sufficient to resolve system dynamics.

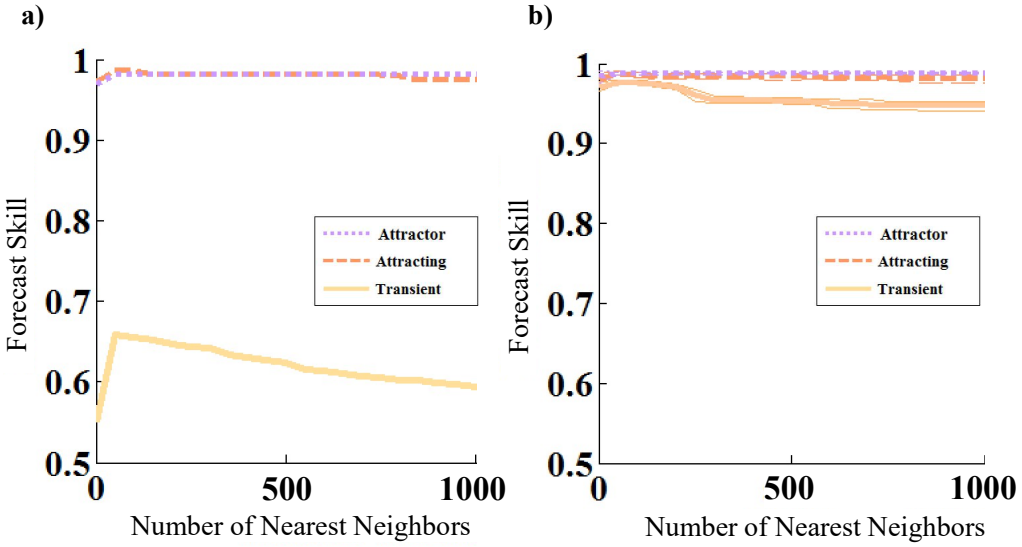

Figure 3.9: **Spatio-temporal forecasting of less clumped initializations reveals nonlinear and linear stages.**
Nonlinear spatio-temporal forecasting for pathways with initial aggregation (a) 0.88 and (b) 0.66. Nonlinear dynamics dominate transient stage for high values of initial aggregation, but nonlinearity is only marginally present in (b) because the transient stage in this pathway is short and interactions weak. For (a), the standard deviation for each stage averaged 0.002 (range: 0.001 to 0.004) for the attractor, 0.004 (range: 0.002 to 0.008) for the attracting stage, and 0.013 (range: 0.010 to 0.016) for the transient stage. For (b), the standard deviation for the attractor averaged 0.002 (range 0.001 to 0.008), 0.004 (range: 0.003 to 0.005) for the attracting stage, and 0.005 (range: 0.002 to 0.008) for the transient stage.

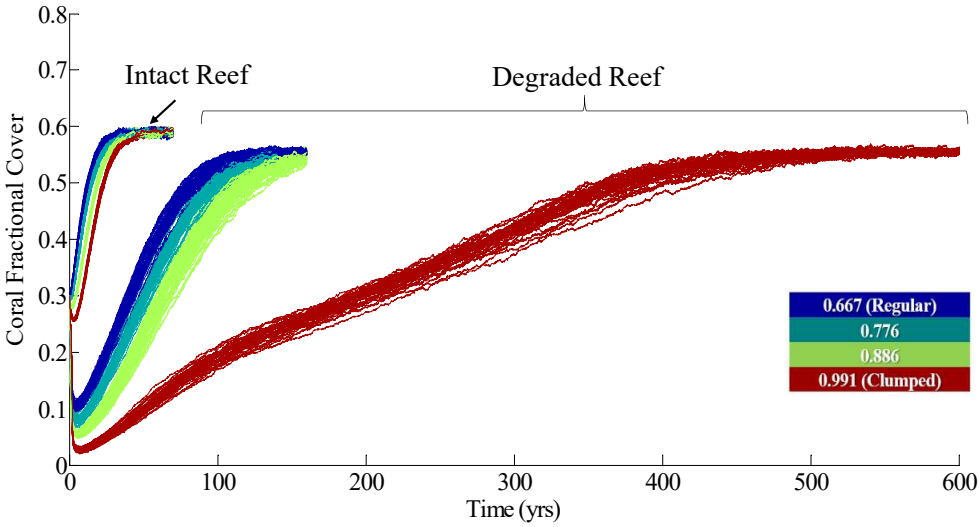

Figure 3.10: **Delay to attractor increases as aggregation and degradation increases.**
CO fractional cover vs. time for four values of initial aggregation (see colorbar) for an intact reef (24 % of lattice grazed per time step) and a degraded reef (4 % of lattice grazed per time step). n = 50.

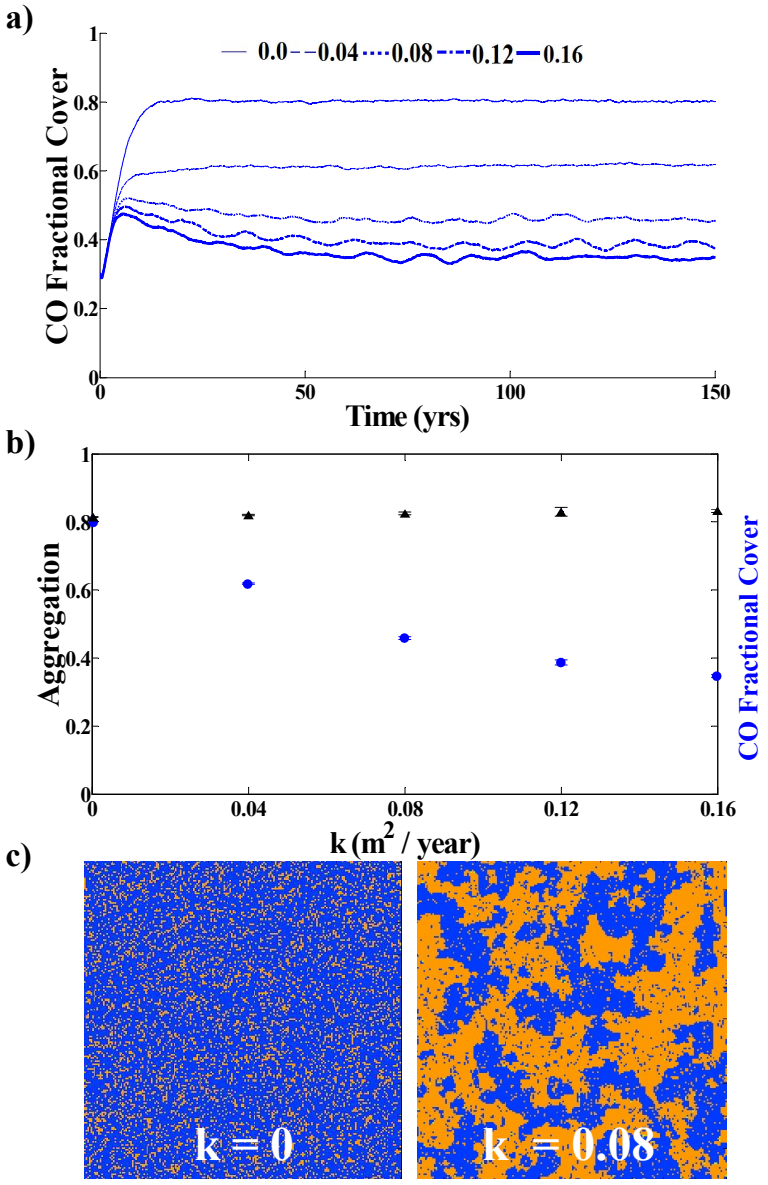

Figure 3.11: **Diffusion enables pattern formation.**
Incorporating CO diffusion into the model enables emergence of a long CO fractional cover time scale that leads to self-organization and clumping, but also depresses the steady-state CO fractional cover. (a) Coral fractional cover pathways for k = 0 m^2 /yr (thin) to k=0.016 m^2 /yr (thickest) shows increasing time scale to arrive at attractor. (b) Attractor values for CO fractional cover (blue circles) and aggregation (black triangles) as a function of coral diffusion, k. As diffusion increases, CO fractional cover decreases and aggregation increases slightly. Error bars are one standard deviation. (c) Snapshots of lattice at attractor (time = 140 yr) for k = 0 and 0.08 m^2/yr (Blue: CO; Orange: CCA).

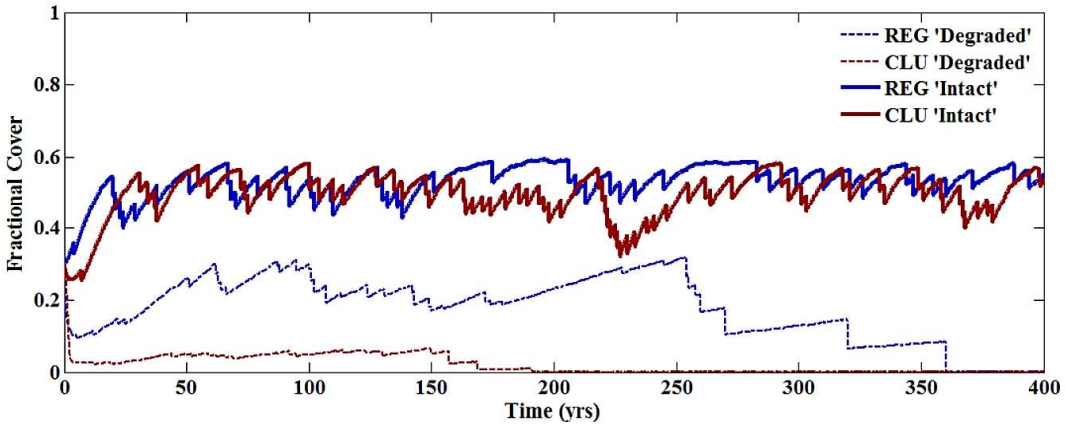

Figure 3.12: **Pathways for two aggregation levels with disturbance.** CO fractional cover vs. time for intact (heavy lines) and degraded (light lines) reefs starting from regular (0.71) and clumped (0.99) initial aggregations under a stochastic disturbance regime (storm every $\sim$7 years). As shown with non-disturbance pathways, higher initial aggregation significantly prolongs arrival at the attractor (intact CO fractional cover attractor: 0.485 +/- 0.002 SD, degraded CO cover attractor: < 0.001), despite storms.

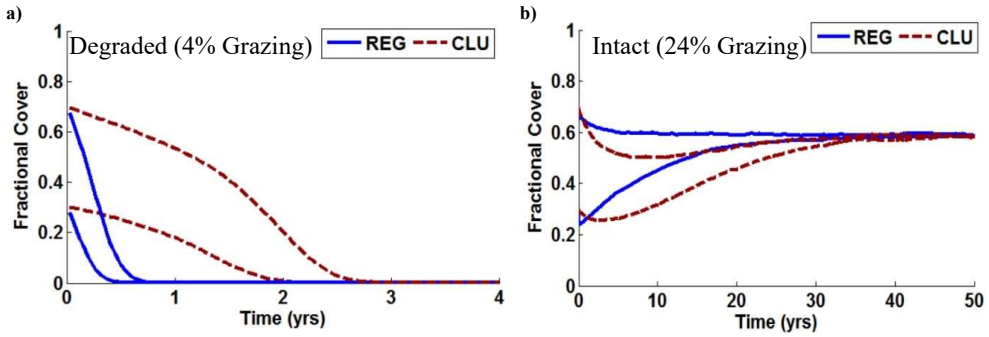

Figure 3.13: **Aggregation effects in degraded and intact reefs.**
CO fractional cover vs. time for (a) degraded and (b) intact reefs for both regular (blue) and clumped (red) initial aggregations of small coral colonies. Clumping prolongs CO persistence for 1.5 years for degraded reefs and delays arrival to the steady-state by 10 years for intact reefs.

Chapter 4

A continuum model for the dynamics of coral reefscapes

4.1 Abstract

Coral reefs are ecosystems comprised of a diverse array of spatially interacting organisms nonlinearly linked to a range of spatio-temporal processes and emergent patterns. Because of the complex and multi-scale nature of reefs, computer modeling has played a role in investigating reef change and its link to the interactions influencing foundational calcifying coral reef organisms. However, most models have failed to treat or properly characterize the impact of the intense competition for two-dimensional benthic space that is the foundational mechanism of coral reef formation and development. To address this gap and to develop the capability to model coral reef dynamics on the scale of islands and beyond, here I describe and explore a continuum model derived by averaging the processes operating in a cellular model of coral reef dynamics. Twelve fields that vary in space and time self-consistently characterize the reefscape; the fractional cover of four main functional groups on the reef (coral (CO), macroalgae (MA), turf algae (TA), and crustose coralline algae (CCA); length of interaction boundaries of the possible six inter-group combinations (CO-MA, CO-TA, CO-CCA,MA-TA,MA-CCA,TA-CCA); mean coral colony size; and fish biomass representing an herbivore popula-

tion coupled to the benthic community. Spatial averaging of reef processes results in twelve corresponding partial differential equations solved numerically using a finite difference predictor-corrector scheme. Comparisons between the continuum model and the cellular model show considerable correspondence in behavior but some differences in time scales and variable values in the attractors. These differences are attributable to differing treatment of the development of coral colony size, which affects CO-MA competition, and the effect of distributions of small-scale variables on nonlinear terms in the continuum model equations. An initial investigation of the spatial pattern forming capabilities of the continuum model yields the development of predator-prey-type cyclical attractors that form reaction-diffusion-type spatial patterns.

4.2 Introduction

Coral reefs are one of the most biodiverse complex ecosystems on Earth. The coral reef structural matrix itself is a living, growing foundation comprised of a milleu of interacting organisms that influence and are influenced by the larger- and longer- scale patterns of the reefscape. Because coral reef ecosystems can be characterized on multiple levels of description, studies have relied on computer modeling to elucidate the dynamics of foundational coral reef organisms and how they are linked to larger-scale patterns [Arias-González et al., 2011]. Dynamical representations have focused mainly on hard corals (the principal reef-builders) by emphasizing particular aspects of coral life histories or the interplay of functional groups occupying the reef. Functional groups are categorizations of reef organisms based on their function on the reef (e.g., reef builders, reef consolidators that cement the reef matrix, or bio-eroders). For benthic coral reef communities, models have investigated the effects of various factors known to shape the reef, including the effects of organism-level neighborhood composition on coral vital rates (e.g., growth, survival, mortality, longevity), influence of disturbance regimes, larval connectivity patterns, and the impacts of grazing on structuring the reef [Langmead and Sheppard, 2004, Melbourne-Thomas et al., 2011a, Sandin and McNamara,

2011, Eynaud et al., 2016, Mumby and Dytham, 2006]. These efforts have culminated in different end-member applications, including adaptive harvesting evaluation [Kramer, 2008], expansion of reef management tools [Melbourne-Thomas et al., 2011a], and advancement of theoretical explanations for the effect of spatially driven mechanisms (e.g. dispersed fish grazing vs locally constrained urchin grazing) on small-scale reef dynamics [Sandin and McNamara, 2011, Eynaud et al., 2016]. However, few models have attempted to explicitly connect organism-level dynamics to the scale of reefs surrounding islands.

Most models that have been developed for reefscapes are based on systems of ordinary differential equations that describe reef change as a function of time [Fung et al., 2011]. Coral reef benthic organisms fiercely compete to occupy space on the two-dimensional ocean bottom, marking space as a critical limiting resource. The regular patterns observed on reefs result, in large part, from the interplay of this competition to occupy space with processes connecting organisms to their environment [Mistr and Bercovici, 2003, Liu et al., 2014]. Studying the ecological dynamics of systems characterized by intense competition for space necessitates considering populations of organisms as functions of both time and space [Okubo and Levin, 2001].

Continuum models have been previously used to connect emergent, macroscopic behavior that varies smoothly in space and time with the behavior of smaller and faster scale microscopic behavior. For example, aspects of the macroscopic behavior of fluids can be represented using the Navier-Stokes equations, which enforce the constraints of mass and momentum conservation. These constraints can be linked to molecular-scale dynamics through calculation of macroscopic parameters such as viscosity, a coefficient of self-diffusion and velocity of sound via averaging of molecular scale processes [Rothman and Zaleski, 1997, Reif, 1965]. Because organism-level change is expected to be expressed differently at larger scales (e.g., fractional cover is a variable of the reefscape rather than benthic reef organisms), development of a continuum model can elucidate longer time scale variables and dynamics of the reefscape that both result from and constrain organism-level dynamics. Also, building a model based on the dynamics of the constituents and

relevant trophic interactions (e.g., grazing predators), allows for the inclusion of aggregating intra- and inter-group processes that lead to the formation of spatially concentrated patterns of organisms [Okubo and Levin, 2001]. In other complicated ecological systems, including mussel beds, savannas, and dryland vegetation ecosystems, continuum models have been used to model and investigate emergent pattern formation and scale dependent feedbacks [Liu et al., 2014, Klausmeier, 1999, Tarnita et al., 2017, Meron, 2016, Rietkerk and van de Koppel, 2008].

In this study, I derive a continuum-based macroscopic approximation for a cellular model of benthic coral reef dynamics. This is the first time that a continuum model representing the reef benthic community has been obtained by explicitly averaging the small-scale interactions represented in a cellular model that includes both demographic processes not influenced by benthic spatial arrangements and competition between neighboring organisms for space [Sandin and McNamara, 2011, Eynaud et al., 2016]. The result is a system of twelve nonlinear partial differential equations tracking, through time and space, the fractional cover of four main functional groups on the reef (coral (CO), macroalgae (MA), turf algae (TA), and crustose coralline algae (CCA)), the nondimensional interacting boundary lengths of the six possible inter-group combinations (CO-MA, CO-TA, CO-CCA,MA-TA,MA-CCA,TA-CCA), the mean coral colony size, and a fish population coupled to the reef. I compare the behavior of this model to the cellular model and describe an initial exploration of its pattern forming properties.

4.3 Methods

4.3.1 Cellular Model

The continuum model is based on a coral reef cellular model that simulates, on a two-dimensional grid of square cells (sized 0.01m^2), the shallow water reef habitat processes by which organisms for four major functional groups recruit, grow, compete, survive, and die on the reef [Sandin and McNamara, 2011]. These four functional groups, which represent dynamical function in the benthic community rather than particular species, are: stony coral (CO), turf algae (TA), fleshy

macroalgae (MA) and crustose coraline algae (CCA), a neutral substrate. The dynamics in the cellular model, which occur with time steps of 0.025y, are governed by cell-level processes at one- (vertical) and two- (planar) dimensions. First, recruitment, algae succession, mortality and grazing represent haphazard interactions of organisms with their environment in the vertical dimension. Secondly, growth and competition represent two-dimensional interactions of organisms with their immediate neighbors. Specifically, CO recruits onto CCA or TA, TA recruits onto CCA, MA grows from TA and CCA immediately recruits to empty cells. Simulating lateral growth and competition for space, the four groups expand to occupy a neighboring cell with a given probability and according to a competitive hierarchy. The competitive growth hierarchy has CO and MA dominating TA and CCA, TA dominating CCA, and CO dominating MA when it belongs to a colony above a threshold, and the reverse otherwise. CCA occupies empty cells with unit probability. Grazing, which is the removal of MA and TA by fish or other herbivores, is assumed to occur uniformly over the grid at a constant rate. Parameters characterizing these processes for the continuum model can be found in Table 4.2.

4.3.2 Continuum Model

Approach and scales

The continuum model is constructed by averaging cellular-level processes over a spatial patch consisting of a rectangle of $N * M$ cells. To enforce scale separation and ensure that averages are stable, the patch must consist of at least 10 x 10 cells (1 m x 1 m), but patches at least a factor of ten larger ensure well-defined emergent variables and smooth progression of reef dynamics.

General form of variables in continuum model

The variables of the continuum model reflect both the status of the four functional groups in their competition for space and the opportunities and constraints on these groups in competing for additional space on the reef. Four of these field variables represent the fraction of space occupied by each functional group

(CO, MA, TA, CCA). The relationship between fractional cover and functional groups occupying cells on the cellular model grid is:

$$f_{co} = \frac{\sum_{i=1}^{N}\sum_{j=1}^{M}(r_{co}(i,j))}{N*M} \tag{4.1a}$$

$$f_{ma} = \frac{\sum_{i=1}^{N}\sum_{j=1}^{M}(r_{ma}(i,j))}{N*M} \tag{4.1b}$$

$$f_{ta} = \frac{\sum_{i=1}^{N}\sum_{j=1}^{M}(r_{ta}(i,j))}{N*M} \tag{4.1c}$$

$$f_{cca} = \frac{\sum_{i=1}^{N}\sum_{j=1}^{M}(r_{cca}(i,j))}{N*M}, \tag{4.1d}$$

where f_b is the fractional cover of functional group b and $r_b(i,j)$ is 1 if the (i,j) cell is occupied by functional group b and 0 otherwise. The indices i and j range over a patch of size $N*M$ cells.

The level of aggregation within each of the functional types, or the level of spatial clumpiness within each group, characterizes the constant competition between four functional types. Aggregation, ag_b, is defined as the number of cell boundaries between cells of the same functional group $b = [co, ma, ta, cca]$ divided by the total number of cell boundaries of functional type b, calculated over the patch:

$$ag_{co} = \frac{\sum_{i=1}^{N}\sum_{j=1}^{M}(r_{co}(i,j)v_{co}(i,j))}{4N*Mf_{co}} \tag{4.2a}$$

$$ag_{ma} = \frac{\sum_{i=1}^{N}\sum_{j=1}^{M}(r_{ma}(i,j)v_{ma}(i,j))}{4N*Mf_{ma}} \tag{4.2b}$$

$$ag_{ta} = \frac{\sum_{i=1}^{N}\sum_{j=1}^{M}(r_{ta}(i,j)v_{ta}(i,j))}{4N*Mf_{ta}} \tag{4.2c}$$

$$ag_{cca} = \frac{\sum_{i=1}^{N}\sum_{j=1}^{M}(r_{cca}(i,j)v_{cca}(i,j))}{4N * Mf_{cca}}, \tag{4.2d}$$

where $v_b(i,j)$ is the number of neighbors of cell (i,j) that belong to functional group b.

Another set of related variables describe the opportunities for competition between different functional groups. Competition occurs along boundaries between cells containing different functional groups. The rate of competition between groups is proportional to the number of such boundaries, L_{b-c}, within the patch. Six nondimensional continuum variables, λ_{b-c}, can be constructed as the ratio of L_{b-c} to the total number of cell-cell boundaries within the patch, $4*N*M$:

$$\lambda_{b-c} = \frac{L_{b-c}}{4N * M}. \tag{4.3}$$

The relationship between variables in the cellular model and λ_{b-c} is given below:

$$\lambda_{co-ma} = \frac{\sum_{i=1}^{N}\sum_{j=1}^{M}(r_{co}(i,j)v_{ma}(i,j))}{4N * M} \tag{4.4a}$$

$$\lambda_{co-ta} = \frac{\sum_{i=1}^{N}\sum_{j=1}^{M}(r_{co}(i,j)v_{ta}(i,j))}{4N * M} \tag{4.4b}$$

$$\lambda_{co-cca} = \frac{\sum_{i=1}^{N}\sum_{j=1}^{M}(r_{co}(i,j)v_{cca}(i,j))}{4N * M} \tag{4.4c}$$

$$\lambda_{ma-ta} = \frac{\sum_{i=1}^{N}\sum_{j=1}^{M}(r_{ma}(i,j)v_{ta}(i,j))}{4N * M} \tag{4.4d}$$

$$\lambda_{ma-cca} = \frac{\sum_{i=1}^{N}\sum_{j=1}^{M}(r_{ma}(i,j)v_{cca}(i,j))}{4N * M} \tag{4.4e}$$

$$\lambda_{ta-cca} = \frac{\sum_{i=1}^{N}\sum_{j=1}^{M}(r_{ta}(i,j)v_{cca}(i,j))}{4N * M}. \tag{4.4f}$$

Similarly, aggregation, ag_b is two times the number of neighbors of type b for cells of functional group b, L_{b-b}, within the patch divided by the fractional

cover of b on the grid (the two is related to double counting of $b-b$ boundaries):

$$ag_b = \frac{2\lambda_{b-b}}{f_b}. \tag{4.5}$$

This relationship indicates that the previously defined aggregation variables (equation 4.2) are not independent from the λs. The sum of the L_{b-c} for each funtional group are constrained by the number of boundaries of the cells of type b in the patch:

$$4 * N * M f_b = 2L_{b-b} + \sum_{c'} L_{b-c'}, \tag{4.6}$$

where the sum is over the three other functional groups, or

$$f_b = 2\lambda_{b-b} + \sum_{c'} \lambda_{b-c'}. \tag{4.7}$$

Combining equation 4.7 with equation 4.5, aggregation, ag_b, is shown to be a function of λ_{b-c}. In summary, aggregation and nondimensional boundary lengths are related in the following manner:

$$ag_{co} = 1 - \frac{1}{f_{co}}\left(\lambda_{co-ma} + \lambda_{co-ta} + \lambda_{co-cca}\right) \tag{4.8a}$$

$$ag_{ma} = 1 - \frac{1}{f_{ma}}\left(\lambda_{co-ma} + \lambda_{ma-ta} + \lambda_{ma-cca}\right) \tag{4.8b}$$

$$ag_{ta} = 1 - \frac{1}{f_{ta}}\left(\lambda_{co-ta} + \lambda_{ma-ta} + \lambda_{ta-cca}\right) \tag{4.8c}$$

$$ag_{cca} = 1 - \frac{1}{f_{cca}}\left(\lambda_{co-cca} + \lambda_{ma-cca} + \lambda_{ta-cca}\right) \tag{4.8d}$$

Therefore, aggregation is not an independent dynamical variable in the continuum model. However, aggregation is used in some of the equations to simplify their expression.

The mean coral colony size, α, is a metric representing the coral colony size distribution, which determines the outcome of competitive interactions between coral and macroalgae. Departing from non-contiguous coral colonies in the cellular

model, α is calculated from the total number of CO cells in the patch, N_{co}, divided by the total number of coral colonies, N_{col}:

$$\alpha = \frac{N_{co}}{N_{col}} = \frac{f_{co} N * M}{\frac{f_{co} N * M}{\alpha}} \tag{4.9}$$

A final variable measures the population of fish, which is specified as the fish biomass per unit area, H_{pop}.

4.3.3 Dynamics

Derivation of the partial differential equations that describe the dynamics of the continuum model is divided into processes representing one-dimensional vertical interactions with the water column and processes representing competitive interactions with neighboring organisms.

One dimensional processes

The one-dimensional processes category includes recruitment, mortality, algae succession and grazing. Below I describe change per unit time for CO, while also tracking the corresponding changes in the other functional types.

Fractional cover. To find the rate of increase of f_{co} from recruitment, first consider the change in area of coral in the patch as:

$$\Delta area_{co} = \Delta t P_{cr} (f_{ta} + f_{cca}) N * M \Delta x^2, \tag{4.10}$$

with Δx as the size of a cell in the cellular model. Area is converted to fractional cover by dividing (4.8) by the area of the patch:

$$\Delta f_{co} = \frac{\Delta area_{co}}{N * M \Delta x^2}, \tag{4.11}$$

or

$$\frac{\partial f_{co}}{\partial t}_{recruitment} = P_{cr} (f_{ta} + f_{cca}). \tag{4.12}$$

The corresponding decreases in f_{ta} and f_{cca} are:

$$\frac{\partial f_{ta}}{\partial t}_{mortality} = -P_{cr} f_{ta}, \tag{4.13a}$$

$$\frac{\partial f_{cca}}{\partial t}_{mortality} = -P_{cr} f_{cca}. \tag{4.13b}$$

Similarly, coral mortality is proportional to a mortality rate, P_{cd}, and coral fractional cover:

$$\frac{\partial f_{co}}{\partial t}_{mortality} = -P_{cd} f_{co}, \tag{4.14}$$

with a corresponding increase in f_{cca}:

$$\frac{\partial f_{cca}}{\partial t}_{recruitment} = P_{cd} f_{co}. \tag{4.15}$$

Succession proceeds through the conversion of turf algae to macroalgae at rate P_{ma}:

$$\frac{\partial f_{ma}}{\partial t}_{succession} = P_{ma} f_{ta}, \tag{4.16}$$

with the corresponding decrease in f_{ta}:

$$\frac{\partial f_{ta}}{\partial t}_{succession} = -P_{ma} f_{ta}. \tag{4.17}$$

Finally, decreases owing to mortality of f_{ma} and f_{ta} occurs by herbivorous fish consumption of these algae types (same rate for both), which results in f_{cca} recruitment to the previous f_{ma} and f_{ta} cells. This process of grazing occurs at a rate, G_H, per fish biomass density, H_{pop}:

$$\frac{\partial f_{ma}}{\partial t}_{grazing} = -G_H H_{pop}\left(\frac{f_{ma}}{f_{ma} + f_{ta}}\right), \tag{4.18a}$$

$$\frac{\partial f_{ta}}{\partial t}_{grazing} = -G_H H_{pop}\left(\frac{f_{ta}}{f_{ma} + f_{ta}}\right). \tag{4.18b}$$

The corresponding change in f_{cca} simplifies to:

$$\frac{\partial f_{cca}}{\partial t}_{grazing} = G_H H_{pop}. \tag{4.19}$$

Generalizing these relationships to all functional groups results in the equations for change in fractional cover owing to one-dimensional processes:

$$\frac{\partial f_{co}}{\partial t} = P_{cr}(f_{ta} + f_{cca}) - P_{cd} f_{co}, \tag{4.20a}$$

$$\frac{\partial f_{ma}}{\partial t} = P_{ma} f_{ta} - G_H H_{pop}\left(\frac{f_{ma}}{f_{ma} + f_{ta}}\right), \tag{4.20b}$$

$$\frac{\partial f_{ta}}{\partial t} = P_{tr} f_{cca} - G_H H_{pop}\left(\frac{f_{ta}}{f_{ma} + f_{ta}}\right) - P_{cr} f_{ta} - P_{ma} f_{ta}, \tag{4.20c}$$

$$\frac{\partial f_{cca}}{\partial t} = P_{cd} f_{co} + G_H H_{pop} - (P_{cr} + P_{tr}) f_{cca}. \tag{4.20d}$$

Non-dimensional boundary lengths. The processes that impact cells in the cellular model through interactions with the water column described for fractional cover also result in changes in the nondimensional border lengths. For example, for λ_{co-ma}, these processes are CO recruitment and mortality, MA succession and grazing of MA. λ_{co-ma} is affected by CO recruitment because a prior MA-TA boundary converts to CO-MA upon CO recruiting onto a TA cell neighboring a MA cell. The rate of change in the number of CO-MA borders, L_{co-ma}, owing to CO recruiting to TA, is the rate at which CO recruits to TA, P_{cr}, times the mean number of MA neighbors of a single TA cell, $\frac{L_{ma-ta}}{f_{ta}N*M}$, times the number of TA cells in the patch, $f_{ta}N*M$, which simplifies to $P_{cr}L_{ma-ta}$ (Fig. 4.1). Additional processes that affect the rate of change of L_{co-ma} are calculated in a similar fashion, all in the form of a rate times the length of boundaries between CO or MA and the functional groups that replace or are replaced by these two. Converting to λs results in:

$$\frac{\partial \lambda_{co-ma}}{\partial t} = P_{cr}\lambda_{ma-ta} + P_{cr}\lambda_{ma-cca} - P_{cd}\lambda_{co-ma} + P_{ma}\lambda_{co-ta} - G_H H_{pop}\left(\frac{\lambda_{co-ma}}{f_{ma}+f_{ta}}\right). \tag{4.21}$$

Calculation of the rates of change of the five other λs proceeds in a similar fashion:

$$\frac{\partial \lambda_{co-ta}}{\partial t} = -P_{cr}\lambda_{co-ta} + P_{cr}f_{ta}ag_{ta} + P_{cr}\lambda_{ta-cca} - P_{cd}\lambda_{co-ta} - P_{ma}\lambda_{co-ta} + P_{tr}\lambda_{co-cca} - G_H H_{pop}\left(\frac{\lambda_{co-ta}}{f_{ma}+f_{ta}}\right) \tag{4.22a}$$

$$\frac{\partial \lambda_{co-cca}}{\partial t} = -P_{cr}\lambda_{co-cca} + P_{cr}f_{cca}ag_{cca} + P_{cr}\lambda_{ta-cca} + P_{cd}f_{co}ag_{co} + G_H H_{pop}\left(\frac{\lambda_{co-ma}}{f_{ma}+f_{ta}}\right) - P_{tr}\lambda_{co-cca} - P_{cd}\lambda_{co-cca} + G_H H_{pop}\left(\frac{\lambda_{co-ta}}{f_{ma}+f_{ta}}\right) \tag{4.22b}$$

$$\frac{\partial \lambda_{ma-ta}}{\partial t} = -P_{cr}\lambda_{ma-ta} - P_{ma}\lambda_{ma-ta} + P_{ma}f_{ta}ag_{ta} + P_{tr}\lambda_{ma-cca} - 2G_H H_{pop}\left(\frac{\lambda_{ma-ta}}{f_{ma}+f_{ta}}\right) \tag{4.22c}$$

$$\frac{\partial \lambda_{ma-cca}}{\partial t} = -P_{cr}\lambda_{ma-cca} + P_{cd}\lambda_{co-ma} + P_{ma}\lambda_{ta-cca} - G_H H_{pop}\left(\frac{\lambda_{ma-ca}}{f_{ma}+f_{ta}}\right) + G_H H_{pop}\left(\frac{f_{ma}ag_{ma}}{f_{ma}+f_{ta}}\right) - P_{tr}\lambda_{ma-cca} + G_H H_{pop}\left(\frac{\lambda_{ma-ta}}{f_{ma}+f_{ta}}\right) \quad (4.22d)$$

$$\frac{\partial \lambda_{ta-cca}}{\partial t} = -2P_{cr}\lambda_{ta-cca} + P_{cd}\lambda_{co-ta} - P_{ma}\lambda_{ta-cca} + G_H H_{pop}\left(\frac{\lambda_{ma-ta}}{f_{ma}+f_{ta}}\right) - P_{tr}\lambda_{ta-cca} + P_{tr}f_{cca}ag_{cca} - G_H H_{pop}\left(\frac{\lambda_{ta-cca}}{f_{ma}+f_{ta}}\right) + G_H H_{pop}\left(\frac{f_{ta}ag_{ta}}{f_{ma}+f_{ta}}\right). \quad (4.22e)$$

Note that equations 4.22 contain aggregation terms, which arise from $b-c$ boundaries changing to or from $b-b$ boundaries via processes that involve cells containing functional group b converting into functional group c or vice versa. For example, the aggregation term in the equation for λ_{co-ta} originates from the process of CO recruiting to TA, which converts $TA-TA$ boundaries, characterized by $\lambda_{ta-ta} = ag_{ta}f_{ta}/2$, represented as ag_{ta}, to $CO-TA$ boundaries.

Mean colony size. The corresponding changes to mean coral colony size, α, arise from a subset of these processes involving changes to or from CO cells, namely, CO recruitment to CCA, CO recruitment to TA, and CO mortality. The procedure for averaging the terms for the rate of change of α is to tabulate the effect in a patch of each process on the number of CO cells, N_{co}, and the number of colonies, N_{col}, given that each CO cell gain or lost is in one of three possible colony configurations (Fig. 4.2). The three possible colony configurations include a one-cell colony, a single cell that serves as a bridge between two parts of a colony, or a cell on the periphery or interior of a multi-cell colony. The probabilities of these three configurations were estimated as $P_1 = (1-\gamma)^4$, $P_2 = 6\gamma^2(1-\gamma^2)$ and $P_3 = 1-(1-\gamma)^4 - 6\gamma^2(1-\gamma)^2$, where $\gamma = \frac{\lambda_{co-b}}{f_b}$ is the probability that one of the neighbors of the cell of type b is CO. The change in α over a time Δt is calculated as:

$$\Delta\alpha_i = \left(\frac{N_{co}(t) + R_{co_i}P_i\Delta t}{N_{col}(t) + R_{col_i}P_i\Delta t} - \alpha\right), \quad (4.23)$$

where R_{co_i} and R_{col_i} are the rate of change of N_{co} and N_{col} for the specified process in the spatial configuration $i = [1, 2, 3]$.

To illustrate this procedure, consider the loss of CO cells from CO mortality events. From figure 4.2, the loss of a cell can occur within three possible configurations (Fig. 4.2 d, e, f). For configurations where the cells lost are located on the periphery of a colony (Fig. 4.2 f) and where only the numerator of α is affected, the change in α over time Δt is:

$$\Delta\alpha = \left(\frac{N_{co} - P_{cd} f_{co} N * M(1 - (1 - ag_{co})^4 - 6(1 - ag_{co})^2 ag_{co}^2)\Delta t}{N_{col}} - \alpha\right) \quad (4.24)$$

Expressing N_{co} and N_{col} in terms of f_{co} and α and simplifying, the rate of change in α from CO mortality on the periphery configuration is:

$$\frac{\partial\alpha}{\partial t}_{mortality(1)} = -P_{cd}\alpha(1 - (1 - ag_{co})^4 - 6(1 - ag_{co})^2 ag_{co}^2). \quad (4.25)$$

Similarly the corresponding rates for the other two possible configurations gives the total rate of change of α from CO mortality as:

$$\frac{\partial\alpha}{\partial t}_{mortality} = -P_{cd}\alpha\Big((1 - (1 - ag_{co})^4 - 6(1 - ag_{co})^2 ag_{co}^2) + (1 - \alpha)(1 - ag_{co})^4 + (1 + \alpha)6(1 - ag_{co})^2 ag_{co}^2\Big). \quad (4.26)$$

Repeating this process, for CO recruitment to TA and to CCA and combining with equation 4.23 results in:

$$\begin{aligned}\frac{\partial\alpha}{\partial t} = &-P_{cd}\alpha\Big((1 - (1 - ag_{co})^4 - 6(1 - ag_{co})^2 ag_{co}^2) + (1 - \alpha)(1 - ag_{co})^4 \\ &+ (1 + \alpha)6(1 - ag_{co})^2 ag_{co}^2\Big) \\ &+ P_{cr}\frac{f_{ta}}{f_{co}}\alpha\left[\left(1 - \left(1 - \frac{\lambda_{co-ta}}{f_{ta}}\right)^4 - 6\left(1 - \frac{\lambda_{co-ta}}{f_{ta}}\right)^2\left(\frac{\lambda_{co-ta}}{f_{ta}}\right)^2\right)\right. \\ &\left.+ (1 - \alpha)\left(1 - \frac{\lambda_{co-ta}}{f_{ta}}\right)^4 + 6(1 + \alpha)\left(1 - \frac{\lambda_{co-ta}}{f_{ta}}\right)^2\left(\frac{\lambda_{co-ta}}{f_{ta}}\right)^2\right] \\ &+ P_{cr}\frac{f_{cca}}{f_{co}}\alpha\left[\left(1 - \left(1 - \frac{\lambda_{co-cca}}{f_{cca}}\right)^4 - 6\left(1 - \frac{\lambda_{co-cca}}{f_{cca}}\right)^2\left(\frac{\lambda_{co-cca}}{f_{cca}}\right)^2\right)\right. \\ &\left.+ (1 - \alpha)\left(1 - \frac{\lambda_{co-cca}}{f_{cca}}\right)^4 + 6(1 + \alpha)\left(1 - \frac{\lambda_{co-cca}}{f_{cca}}\right)^2\left(\frac{\lambda_{co-cca}}{f_{cca}}\right)^2\right]. \quad (4.27)\end{aligned}$$

Two dimensional processes

The processes that give rise to changes in fractional cover and nondimensional boundary lengths operating on the two-dimensional benthic surface involve competitive overgrowth of one functional group by another. The three considerations that determine the rates of change are 1) the nondimensional boundary lengths connecting two functional groups b and c, 2) the functional group that is dominating, and 3) the rate at which the dominant functional group overgrows the other. The competition hierarchy is fixed, except for CO and MA, which depends on coral colony size relative to a threshold size, α_{th}. The hierarchy is 1) CO overgrows MA, TA, and CCA, 2) MA overgrows CO, TA and CCA, and 3) TA overgrows CCA.

In the cellular model, the colony size is tracked via a colony ID that spreads via overgrowth by CO. In the continuum model, colonies are geometrically contiguous sets of CO cells. The probability that a CO cell belongs to a colony below the competitive size threshold, η, is determined by assuming that CO colony size is Poisson distributed, and by summing the number of CO cells in colonies with size below α_{th}:

$$\eta = \frac{\left(\int_0^{\alpha_{th}} P(\alpha', \alpha) d\alpha \left(\frac{N*Mf_{co}}{\alpha} \right) \alpha' \right) \frac{N*Mf_{co}}{\alpha}}{N * Mf_{co}}, \tag{4.28}$$

where $P(\alpha', \alpha)$ is the Poisson distribution with mean α. The fraction of CO cells above the threshold, α_{th}, in the patch is then $1 - \eta$. The assumption of Poisson distributed colonies is computationally convenient and has some support for some stages of reef development (Fig. 4.13), but alternative distributions can be substituted.

Fractional cover. Changes in fractional cover are calculated by assuming that the growth of functional group b over functional group c occurs within the patch along a front of length L_{b-c} (Fig. 4.3). The change in area within the patch during time step Δt is then $G_b L_{b-c} \Delta t \Delta x^2$. The corresponding change in fractional cover of b (dividing by $N * M * \Delta x^2$) is: $4 G_b \lambda_{b-c} \Delta t$. For CO overgrowing MA, this term is multiplied by $(1 - \eta)$ and multiplied by η for MA overgrowing CO. Tabulating

all overgrowth processes and collecting the terms gives:

$$\frac{\partial f_{co}}{\partial t} = 4[G_{co}(\lambda_{co-ta} + \lambda_{co-cca}) + G_{co}\lambda_{co-ma}(1-\eta) - G_{ma}\lambda_{co-ma}\eta] \quad (4.29a)$$

$$\frac{\partial f_{ma}}{\partial t} = 4[G_{ma}(\lambda_{ma-ta} + \lambda_{ma-cca}) + G_{ma}\lambda_{co-ma}\eta - G_{co}\lambda_{co-ma}(1-\eta)] \quad (4.29b)$$

$$\frac{\partial f_{ta}}{\partial t} = 4[G_{ta}\lambda_{ta-cca} - G_{co}\lambda_{co-ta} - G_{ma}\lambda_{ma-ta}] \quad (4.29c)$$

$$\frac{\partial f_{cca}}{\partial t} = 4[-G_{co}\lambda_{co-cca} - G_{ma}\lambda_{ma-ca} - G_{ta}\lambda_{ta-cca}], \quad (4.29d)$$

Non-dimensional boundary lengths. The rate of change of nondimensional boundary length, λ_{b-c}, from overgrowth processes is calculated by considering processes that result in changes involving cells of functional groups b and/or c (Fig. 4.4). For example, the rate of decrease of λ_{co-c} is influenced by the following processes: CO overgrows MA, MA overgrows CO, CO overgrows TA and CO overgrows CCA. Therefore, it is calculated as the sum of the rates at which CO cells are added by overgrowth along a front, $G_{co}\lambda_{co-c}$, times the mean number of CO neighbors of functional type, c, that are being overgrown, $\frac{4\lambda_{co-c}}{f_c}$. For example, if c= ma and MA is dominant, the rate of decrease of λ_{co-ma} is the rate at which CO cells are being overgrown, $G_{ma}\lambda_{co-ma}$, times the mean number of CO neighbors of CO, ag_{co}. The rates for CO overgrowing MA are reduced by the factor $(1-\eta)$, and by the factor η for MA overgrowing CO. Collecting the terms results in:

$$\frac{\partial \lambda_{co-ma}}{\partial t} = 4\left[G_{co}\lambda_{co-ma}(1-\eta)\left(ag_{ma} - \frac{\lambda_{co-ma}}{f_{ma}}\right) + G_{ma}\lambda_{co-ma}\eta \right.$$
$$\left(ag_{co} - \frac{\lambda_{co-ma}}{f_{co}}\right) + G_{co}\lambda_{co-ta}\frac{\lambda_{ma-ta}}{f_{ta}} + G_{co}\lambda_{co-cca}\frac{\lambda_{ma-cca}}{f_{cca}} + G_{ma}\lambda_{ma-ta}\frac{\lambda_{co-ta}}{f_{ta}}$$
$$\left. + G_{ma}\lambda_{ma-cca}\frac{\lambda_{co-cca}}{f_{cca}}\right]. \quad (4.30)$$

In general, λ_{b-c} changes at a rate calculated as the rate of change at which b cells grow along a front, $G_b\lambda_{b-c}$, times the mean number of b neighbors of c, $\frac{4\lambda_{b-c}}{f_c}$. The

remaining equations for the rates of change of λ_{b-c} are:

$$\frac{\partial \lambda_{co-ta}}{\partial t} = 4\left[G_{co}\lambda_{co-ta}\left(ag_{ta} - \frac{\lambda_{co-ta}}{f_{ta}}\right) + G_{co}\lambda_{co-ma}(1-\eta)\frac{\lambda_{ma-ta}}{f_{ma}} + G_{co}\lambda_{co-cca}\frac{\lambda_{ta-cca}}{f_{cca}} + G_{ta}\lambda_{ta-cca}\frac{\lambda_{co-cca}}{f_{cca}} - G_{ma}\lambda_{co-ma}\eta\frac{\lambda_{co-ta}}{f_{co}} - G_{ma}\lambda_{ma-ta}\frac{\lambda_{co-ta}}{f_{ta}}\right] \quad (4.31a)$$

$$\frac{\partial \lambda_{co-cca}}{\partial t} = 4\left[G_{co}\lambda_{co-cca}\left(ag_{cca} - \frac{\lambda_{co-cca}}{f_{cca}}\right) + G_{co}\lambda_{co-ma}(1-\eta)\frac{\lambda_{ma-cca}}{f_{ma}} + G_{co}\lambda_{co-ta}\frac{\lambda_{ta-cca}}{f_{ta}} - G_{ma}\lambda_{co-ma}\eta\frac{\lambda_{co-cca}}{f_{cca}} - G_{ma}\lambda_{ma-cca}\frac{\lambda_{co-cca}}{f_{cca}} - G_{ta}\lambda_{ta-cca}\frac{\lambda_{co-cca}}{f_{cca}}\right] \quad (4.31b)$$

$$\frac{\partial \lambda_{ma-ta}}{\partial t} = 4\left[G_{ma}\lambda_{ma-ta}\left(ag_{ta} - \frac{\lambda_{ma-ta}}{f_{ta}}\right) + G_{ma}\lambda_{co-ma}\eta\frac{\lambda_{co-ta}}{f_{co}} + G_{ma}\lambda_{ma-cca}\frac{\lambda_{ta-cca}}{f_{cca}} + G_{ta}\lambda_{ta-cca}\frac{\lambda_{ma-cca}}{f_{cca}} - G_{co}\lambda_{co-ma}(1-\eta)\frac{\lambda_{ma-ta}}{f_{ma}} - G_{co}\lambda_{co-ta}\frac{\lambda_{ma-ta}}{f_{ta}}\right] \quad (4.31c)$$

$$\frac{\partial \lambda_{ma-cca}}{\partial t} = 4\left[G_{ma}\lambda_{ma-cca}\left(ag_{cca} - \frac{\lambda_{ma-cca}}{f_{cca}}\right) + G_{ma}\lambda_{co-ma}\eta\frac{\lambda_{co-cca}}{f_{co}} + G_{ma}\lambda_{ma-ta}\frac{\lambda_{ta-cca}}{f_{ta}} - G_{co}\lambda_{co-ma}(1-\eta)\frac{\lambda_{ma-cca}}{f_{ma}} - G_{co}\lambda_{co-cca}\frac{\lambda_{ma-cca}}{f_{cca}} - G_{ta}\lambda_{ta-cca}\frac{\lambda_{ma-cca}}{f_{cca}}\right] \quad (4.31d)$$

$$\frac{\partial \lambda_{ta-cca}}{\partial t} = 4\left[G_{ta}\lambda_{ta-cca}\left(ag_{cca} - \frac{\lambda_{ta-cca}}{f_{cca}}\right) - G_{co}\lambda_{co-ta}\frac{\lambda_{ta-cca}}{f_{ta}} - G_{co}\lambda_{co-cca}\frac{\lambda_{ta-cca}}{f_{cca}} \quad (4.31e)$$

$$- G_{ma}\lambda_{ma-ta}\frac{\lambda_{ta-cca}}{f_{ta}} - G_{ma}\lambda_{ma-cca}\frac{\lambda_{ta-cca}}{f_{cca}}\right] \quad (4.31f)$$

Mean colony size The effect of overgrowth processes on mean colony size, α, were determined using the same logic as for processes involving interactions with the water column, except for accounting for different rates and the fraction of CO cells below the threshold, η, for CO-MA overgrowth:

$$\frac{\partial\alpha}{\partial t} = 4\Bigg[G_{co}\frac{\lambda_{co-ma}}{f_{co}}(1-\eta)\alpha(1+\alpha)6\left(\frac{\lambda_{co-ma}}{f_{ma}}\right)^2\left(1-\frac{\lambda_{co-ma}}{f_{ma}}\right)^2 + G_{co}\frac{\lambda_{co-ma}}{f_{co}}$$
$$(1-\eta)\alpha\left(1-6\left(\frac{\lambda_{co-ma}}{f_{ma}}\right)^2\left(1-\frac{\lambda_{co-ma}}{f_{ma}}\right)^2\right) - G_{ma}\frac{\lambda_{co-ma}}{f_{co}}\eta\alpha(1-\alpha)(1-ag_{co})^4$$
$$- G_{ma}\frac{\lambda_{co-ma}}{f_{co}}\eta\alpha(1+\alpha)6(1-ag_{co})^2ag_{co}^2 - G_{ma}\frac{\lambda_{co-ma}}{f_{co}}\eta\alpha(1-(1-ag_{co})^4$$
$$- 6(1-ag_{co})^2ag_{co}^2) + G_{co}\frac{\lambda_{co-ta}}{f_{co}}\alpha(1+\alpha)6\left(\frac{\lambda_{co-ta}}{f_{ta}}\right)^2\left(1-\frac{\lambda_{co-ta}}{f_{ta}}\right)^2$$
$$+ G_{co}\frac{\lambda_{co-ta}}{f_{co}}\alpha\left(1-6\left(\frac{\lambda_{co-ta}}{f_{ta}}\right)^2\left(1-\frac{\lambda_{co-ta}}{f_{ta}}\right)^2\right) + G_{co}\frac{\lambda_{co-cca}}{f_{co}}\alpha(1+\alpha)6\left(\frac{\lambda_{co-cca}}{f_{cca}}\right)^2$$
$$\left(1-\frac{\lambda_{co-cca}}{f_{cca}}\right)^2 + G_{co}\frac{\lambda_{co-cca}}{f_{co}}\alpha\left(1-6\left(\frac{\lambda_{co-cca}}{f_{cca}}\right)^2\left(1-\frac{\lambda_{co-cca}}{f_{cca}}\right)^2\right)\Bigg] \quad (4.32)$$

Diffusion

Stochastic birth, death and overgrowth at the level of individual cells leads to diffusive behavior at the patch scale. The magnitude and form of diffusion is approximated by a calculation paralleling the calculation of the self-diffusion coefficient in the kinetic theory of gases [Reif, 1965], applied to the movement of interfaces between two functional groups b and c. These interfaces are assumed to engage in a random walk, with step size given by the mean distance between interfaces connecting two different functional types. The flux of such interfaces crossing a boundary in the y direction, J_{b-c}, is

$$J_{b-c} = -D_{b-c}\frac{\partial n_{b-c}}{\partial x}, \quad (4.33)$$

with n_{b-c} the number of $b-c$ interfaces per unit area, $D_{b-c} = \frac{1}{2}G_{b-c}l_*\Delta x$, where G_{b-c} is the rate at which the dominant organism b overgrows the other organism c (e.g., G_{co} if CO overgrows MA) and l_* the mean free path of a $b-c$ boundary,

which is approximated as the mean distance between interfaces connecting two different functional groups:

$$l_* = \frac{\Delta x}{\lambda_{co-ma} + \lambda_{co-ta} + \lambda_{co-cca} + \lambda_{ma-ta} + \lambda_{ma-cca} + \lambda_{ta-cca}}. \tag{4.34}$$

Replicating this calculation in the y direction and calculating the change in n_{b-c} within a path yields a diffusion equation for n_{b-c}:

$$\frac{\partial n_{b-c}}{\partial t} = D_{b-c}\nabla^2 n_{b-c}. \tag{4.35}$$

The relationship between n_{b-c} and λ_{b-c} is $n_{b-c} = \frac{\lambda_{b-c}}{\Delta x}$, leading to

$$\frac{\partial \lambda_{b-c}}{\partial t} = D_{b-c}\nabla^2 \lambda_{b-c}. \tag{4.36}$$

To find the diffusion term for fractional cover of functional group b, first consider the differential effect on fractional cover of $b-c$ interfaces moving into and out of a patch:

$$\Delta f_b = l_* J_{b-c}(x,y)\Delta t - l_* J_{b-c}(x+N\Delta x, y)\Delta t + l_* J_{b-c}(x,y)\Delta t - l_* J_{b-c}(x, y+M\Delta x)\Delta t \tag{4.37}$$

or

$$\frac{\partial f_b}{\partial t}_{diff} = 4 l_{**} \sum D_{b-c}\nabla^2 \lambda_{b-c}, \tag{4.38}$$

where l_{**} is $\frac{l*}{\Delta x}$ and the sum is over c representing all functional groups except b.

Unlike the case with gases, when the velocity of particles engaging in the random walk is large, the effective velocities of the interfaces, $G_{b-c}\Delta x$, are order $1m/yr$ or less, meaning that self-diffusion from cell-level randomness is at most $0.1m^2/yr$. Additional self-diffusion terms were also included for all dynamical variables to account for organism-level and larger scale diffusive processes not related to randomness, such as coral colony fusion.

Fish Population

A single density-dependent herbivore fish population is coupled to the coral reef benthic model, measured as fish biomass per unit area, H_{pop}. The fish population varies over the reef domain and changes according to the availability of

its food source, TA and MA, and is subject to mortality at a rate a_{HH} [Kramer, 2008], which is reduced in regions of high coral fractional cover [Bell and Galzin, 1984, Friedlander and Parrish, 1998, Hixon, 1991]. Fish harvesting by fishers is not included. Therefore the rate of change of H_{pop} can be written as:

$$\frac{\partial H_{pop}}{\partial t} = a_{HA} H_{pop}(f_{ma} + f_{ta}) - (a_{HH} - \epsilon(1 - f_{co}))H_{pop} + d_{hpop}\nabla^2 H_{pop}, \quad (4.39)$$

where a_{HA} is the herbivore-algae interaction coefficient, ϵ is a coefficient that measures the reduction in mortality rate owing to taking refuge in coral, and ∂H_{pop} is a self-diffusion coefficient for fish.

Numerical solution

The system of equations is solved using a finite difference predictor corrector time stepping scheme with variable time step [Acton, 1970].

Expected Differences

Although most dynamics of the cellular model transformed in a reasonably straightforward manner to the continuum model, there are two notable differences that are expected to affect the results. First, treatment of coral colony size in the continuum model differs substantially from the treatment in the cellular model, both by assumption of a Poisson distribution and by defining colonies as contiguous cells, rather than families that spread via overgrowth. The differences are expected to be most pronounced where coral fractional cover is reduced in response to unfavorable initial conditions. Second, the squared terms (of the form λ^2_{b-c}) that occur in equations for nondimensional boundary lengths were calculated without accounting for differences between the mean of a product and the product of the means for variables with broad distributions (see Fig.s 4.14, 4.15). These differences are expected to introduce biases in the trends of some of the variables, which potentially could be compensated for partially through modest adjustments in parameters or coefficients of the affected terms.

4.4 Example numerical solutions

4.4.1 Comparisons with cellular model

The behavior of the cellular model has been previously described in terms of metrics of fractional cover averaged over the spatial extent of simulations and shown to arrive at steady states characteristic of coral reefs: either a coral-dominated attractor or an algae dominated attractor ([Sandin and McNamara, 2011], Chapter 3). It also has been shown to exhibit transient dynamics triggered by clumped initial conditions with high coral aggregation. The general time evolution of the cellular model is characterized by a repelling stage, with rapid evolution away from the initial condition, a transient stage with complicated dynamics, an attracting stage decaying exponentially to a stable attractor stage. The initial conditions for the cellular model results for three cases (CO dominated attractor, MA dominated attractor, and CO dominated attractor with a long transient) were used in the continuum model to compare the corresponding continuum-based model results (with the same parameters as in the cellular model (base) or adjusted parameters) (Tables 4.1, 4.2, 4.3). The fish population was fixed in the continuum model and calculations were carried out at a single spatial position.

First, for the MA-dominated case with base parameters, the functional form towards arriving at the attractor (i.e., $\sim$ linear for cellular model and $\sim$ exponential for continuum model) and the attractor value were different between the two models. Yet, the overall pathway between initial condition and attractor matched (Fig. 4.16). Moderate adjustment of the level of fish grazing (Table 4.3) in the continuum model yielded nearly identical pathways towards the MA dominated attractor, although the decay of f_{ma} to the attractor was more linear in the cellular model and more exponential in the continuum model (Fig. 4.5). The fractional cover attractor values for the adjusted parameters were approximately the same in the two models. The underlying changes in the nondimensional interaction boundaries showed discrepancies between the cellular and continuum models, namely for λ_{ma-ta} and λ_{ma-cca} (Fig.4.6).

A comparison of the pathways towards a CO-dominated attractor between

the two models shows that the general behavior was different using the base parameters: the cellular model showed a simple exponential rise to CO dominated attractor and the continuum model showed a CO dominated attractor with a twelve year transient (4.17). After making small adjustments in the grazing and mean colony size threshold parameters of the continuum model, the pathways became more similar, with fast initial decline in the fractional cover of macroalgae and turf algae, and an initial dip in CO fractional cover (although more pronounced in the continuum model pathway) (Fig.4.7). The attractor values for both CO and CCA fractional cover were also about 5 % higher and 5 % lower in the continuum model, respectively. The reason for this difference is rooted in the differential values of the lambdas between the two models, particularly in λ_{co-cca} (Fig. 4.8). Given that λ_{co-cca} is elevated by 0.012 in the continuum model, the impact it has on the value of f_{co} in the attractor can be deduced. Focusing on the terms with CO and CCA from the fractional coral cover, f_{co}, equation:

$$\frac{\partial f_{co}}{\partial t} = -P_{cd} f_{co} + P_{cr}(1 - f_{co}) + 4G_{co}\lambda_{co-cca}. \tag{4.40}$$

The difference between the $\lambda_{co-cca}s$ of the ceulluar and continuum models is 0.02. By setting the derivative to zero (attractor) and propagating this difference through equation 4.40 , the expected difference in f_{co} between the models is 0.05, matching the observed differences.

Finally, the CO dominated attractor with a long transient occurs when the cellular model is initialized with high coral aggregation. Using the base initial conditions, the continuum model reproduces the same behavior as the cellular model (Fig. 4.18), except that the duration of the transient is about 45 years shorter. Additionally, the time scale of CO decay to the attractor is smaller for the continuum model than for the cellular model. With modest adjustments to the parameters, the transient duration increases and thus decreases the time scale mismatch between the two models (Fig. 4.9). The duration of the transient (i.e. turf and macroalgae fractional cover goes to zero) differs by about 35 years in the two models, reflecting the persistent time scale mismatch.

4.4.2 Pattern formation

The spatial pattern formation properties of the continuum model were investigated using a version incorporating the fish population model, with the effect of coral fractional cover on fish mortality excluded ($\epsilon = 0$) and the self-diffusion coefficient of fish set to a moderate level ($32m^2/yr$) on a $200x40$ grid. Neumann boundary conditions (with zero gradient) are enforced at the onshore and offshore boundaries, and periodic boundary conditions at the alongshore boundaries. The model was initialized with the same initial conditions as used for the CO dominated attractor with long transient case, with random variations at the 1% level in the fractional covers and fish biomass. This case results in the emergence of predator prey oscillations distinguished by cycles of compressed transients between algae and fish population maxima (Fig. 4.10). A corresponding phase portrait of the system reveals a cyclical attractor, suggesting that sufficient dissipation exists in the system to result in a well-defined basin of attraction (Fig. 4.11).

Accompanying these cycles is the development of a stable reaction-diffusion type pattern of cross-shore stripes where algae and fish growth are focused (Fig.s 4.12). Coral largely disappears when algae is dominant (Fig.s 4.10, 4.12 b) and remains at a modest fractional cover even when fish have grazed the algae (Fig. 4.12 c). Alternative parameters and initial conditions allow for a mixed coral and macroalgae attractor: for example, with large fish diffusion constants or initializing with the coral attractor except for an algae patch.

4.5 Discussion

Building off of the dynamical analysis of Chapter 3, here I presented the derivation of equations for the emergent behavior of a coral reefscape, based on the dynamics of a cellular model of coral reef benthic community dynamics. This approximate representation of the emergent behavior of the cellular model requires twelve field variables that vary in time and two-dimensional benthic space: fractional cover of four functional groups, six nondimensional boundary lengths of contact between the functional groups that represent sites for competition, a mean

coral colony size and fish biomass density. The twelve corresponding partial differential equations include terms representing reef interactions with the water column and terms that represent competitive overgrowth. The equations for nondimensional boundary lengths include nonlinear terms that contain the seeds of complex behavior.

The continuum model reproduces much of the dynamical behavior observed in the cellular model, albeit with some differences in time scales, parameter values and variable values in the fixed point attractors. These differences probably arise from two sources: the differences in the way the two models determine the fraction of coral above and below the competitive threshold colony size, and the effect of small-scale variations of nondimensional boundary lengths on nonlinear terms in the equations. The first source of difference can be addressed by developing a more robust model for quantifying the amount of coral above the threshold by explicitly tracking this quantity, rather than inferring it from colony size. The second source of difference could be addressed by assuming that the number of neighbors of functional group c of a cell from functional group b is Poisson distributed, and explicitly calculating the corrections to the means at the patch scale.

A significant advantage to deriving and employing a continuum model of coral reefscapes versus inferring the emergent properties of the reefscape from averages calculated from a cellular model is that the dynamics at the emergent scale is much more transparent. For example, dynamical time scales, variable values in the attractors and the stability of attractors can be calculated explicitly (although such calculation is not trivial: e.g., determination of the variable values in the attractors involves solving a system of twelve nonlinear equations). Additionally, the contribution of different terms in the equations can be easily tracked. Further research along these lines could potentially illuminate the origin of common reefscape behaviors. For example, the processes underlying the nonlinear dynamics of the transient stage, first detected in Chapter 3, could be traced to specific processes.

The initial examples explored here provide strong evidence that the continuum model possesses rich pattern-forming potential, including the well-studied

predator-prey reaction-diffusion dynamics [Garvie, 2007, Upadhyay et al., 2008, Guin et al., 2015]. Regular patterns in coral reefs across multiple scales [Rietkerk and van de Koppel, 2008, Dizon and Yap, 2006, Pandolfi, 2002, Edwards et al., 2017], patterns of coral and algae in degraded reef systems, and patterns of bleaching could be modeled and analyzed using the continuum model and extensions of it.

From a management standpoint, the continuum model can be used for evaluating the response of a reef to different climatic, chemical and nutrient scenarios, including climate change effects, variations in water chemistry, nutrient and sediment inputs, storms and competitive invasions, and for exploring the potential impacts of management and policy initiatives. In terms of continuing to expand on investigations characterizing the dynamics of the coral reef complex system, a promising and exciting line of research is that through coupling the coral reef system continuum model and traditional subsistence-based human societies it might be possible to expand knowledge of co-adapted systems and multi-scale dynamics that have led to their success and degradation.

4.6 Acknowledgments

We are thankful to D. McNamara for useful comments on this manuscript. Funding for M.Brito-Millan came from NSF Graduate Fellowship, University of California, San Diego and the Scripps Institution of Oceanography department.

Chapter 4, in full, is a manuscript prepared for submission to Physical Review E as: Brito-Millan, Marlene and BT Werner. A continuum model for the dynamics of coral reefscapes. The dissertation author was the primary investigator and author of this paper.

4.7 Appendix

The combined derivations of all processes for all twelve dynamical variables results in:

$$\begin{aligned}\frac{\partial f_{co}}{\partial t} &= P_{cr} f_{ta} + P_{cr} f_{cca} - P_{cd} f_{co} \\ &\quad + 4[G_{co}(\lambda_{co-ta} + \lambda_{co-cca}) + G_{co}\lambda_{co-ma}(1-\eta) - G_{ma}\lambda_{co-ma}\eta] \\ &\quad + 4l_{**}\left[D_{CO-ma}(1-\eta)\nabla^2\lambda_{co-ma} + D_{co-MA}\eta\nabla^2\lambda_{co-ma}\right. \\ &\quad \left. + D_{co-ta}\nabla^2\lambda_{co-ta} + D_{co-cca}\nabla^2\lambda_{co-cca}\right] \quad (4.41a)\end{aligned}$$

$$\begin{aligned}\frac{\partial f_{ma}}{\partial t} &= P_{ma} f_{ta} - G_H H_{pop}\left(\frac{f_{ma}}{f_{ma} + f_{ta}}\right) \\ &\quad + 4[G_{ma}(\lambda_{ma-ta} + \lambda_{ma-cca}) + G_{ma}\lambda_{co-ma}\eta - G_{co}\lambda_{co-ma}(1-\eta) \\ &\quad + 4l_{**}\left[D_{CO-ma}(1-\eta)\nabla^2\lambda_{co-ma} + D_{co-MA}\eta\nabla^2\lambda_{co-ma}\right. \\ &\quad \left. + D_{ma-ta}\nabla^2\lambda_{ma-ta} + D_{ma-cca}\nabla^2\lambda_{ma-cca}\right] \quad (4.41b)\end{aligned}$$

$$\begin{aligned}\frac{\partial f_{ta}}{\partial t} &= P_{tr} f_{cca} - G_H H_{pop}\left(\frac{f_{ta}}{f_{ma} + f_{ta}}\right) - P_{cr} f_{ta} - P_{ma} f_{ta} \\ &\quad + 4[G_{ta}\lambda_{ta-cca} - G_{co}\lambda_{co-ta} - G_{ma}\lambda_{ma-ta}] \\ &\quad + 4l_{**}\left[D_{co-ta}\nabla^2\lambda_{co-ta} + D_{ma-ta}\nabla^2\lambda_{ma-ta} + D_{ta-cca}\nabla^2\lambda_{ta-cca}\right] \quad (4.41c)\end{aligned}$$

$$\begin{aligned}\frac{\partial f_{cca}}{\partial t} &= P_{cd} f_{co} + G_H H_{pop} - (P_{cr} + P_{tr}) f_{cca} \\ &\quad + 4[-G_{co}\lambda_{co-cca} - G_{ma}\lambda_{ma-ca} - G_{ta}\lambda_{ta-cca}] \\ &\quad + 4l_{**}\left[D_{co-cca}\nabla^2\lambda_{co-cca} + D_{ma-cca}\nabla^2\lambda_{ma-cca} + D_{ta-cca}\nabla^2\lambda_{ta-cca}\right] \quad (4.41d)\end{aligned}$$

$$\frac{\partial \alpha}{\partial t} = -P_{cd}\alpha\Bigg((1-(1-ag_{co})^4 - 6(1-ag_{co})^2 ag_{co}^2) + (1-\alpha)(1-ag_{co})^4 + (1+\alpha)6(1-ag_{co})^2 ag_{co}^2\Bigg) + P_{cr}\frac{f_{ta}}{f_{co}}\alpha\Bigg[\Bigg(1-\Bigg(1-\frac{\lambda_{co-ta}}{f_{ta}}\Bigg)^4 - 6\Bigg(1-\frac{\lambda_{co-ta}}{f_{ta}}\Bigg)^2\Bigg(\frac{\lambda_{co-ta}}{f_{ta}}\Bigg)^2\Bigg) + (1-\alpha)\Bigg(1-\frac{\lambda_{co-ta}}{f_{ta}}\Bigg)^4 + 6(1+\alpha)\Bigg(1-\frac{\lambda_{co-ta}}{f_{ta}}\Bigg)^2\Bigg(\frac{\lambda_{co-ta}}{f_{ta}}\Bigg)^2\Bigg] + P_{cr}\frac{f_{cca}}{f_{co}}\alpha\Bigg[\Bigg(1-\Bigg(1-\frac{\lambda_{co-cca}}{f_{cca}}\Bigg)^4 - 6\Bigg(1-\frac{\lambda_{co-cca}}{f_{cca}}\Bigg)^2\Bigg(\frac{\lambda_{co-cca}}{f_{cca}}\Bigg)^2\Bigg) + (1-\alpha)\Bigg(1-\frac{\lambda_{co-cca}}{f_{cca}}\Bigg)^4 + 6(1+\alpha)\Bigg(1-\frac{\lambda_{co-cca}}{f_{cca}}\Bigg)^2\Bigg(\frac{\lambda_{co-cca}}{f_{cca}}\Bigg)^2\Bigg] + 4\Bigg[G_{co}\frac{\lambda_{co-ma}}{f_{co}}(1-\eta)\alpha(1+\alpha)6\Bigg(\frac{\lambda_{co-ma}}{f_{ma}}\Bigg)^2\Bigg(1-\frac{\lambda_{co-ma}}{f_{ma}}\Bigg)^2 + G_{co}\frac{\lambda_{co-ma}}{f_{co}}(1-\eta)\alpha\Bigg(1-6\Bigg(\frac{\lambda_{co-ma}}{f_{ma}}\Bigg)^2\Bigg(1-\frac{\lambda_{co-ma}}{f_{ma}}\Bigg)^2\Bigg) - G_{ma}\frac{\lambda_{co-ma}}{f_{co}}\eta\alpha(1-\alpha)(1-ag_{co})^4 - G_{ma}\frac{\lambda_{co-ma}}{f_{co}}\eta\alpha(1+\alpha)6(1-ag_{co})^2 ag_{co}^2 - G_{ma}\frac{\lambda_{co-ma}}{f_{co}}\eta\alpha(1-(1-ag_{co})^4 - 6(1-ag_{co})^2 ag_{co}^2) + G_{co}\frac{\lambda_{co-ta}}{f_{co}}\alpha(1+\alpha)6\Bigg(\frac{\lambda_{co-ta}}{f_{ta}}\Bigg)^2\Bigg(1-\frac{\lambda_{co-ta}}{f_{ta}}\Bigg)^2 + G_{co}\frac{\lambda_{co-ta}}{f_{co}}\alpha\Bigg(1-6\Bigg(\frac{\lambda_{co-ta}}{f_{ta}}\Bigg)^2\Bigg(1-\frac{\lambda_{co-ta}}{f_{ta}}\Bigg)^2\Bigg) + G_{co}\frac{\lambda_{co-cca}}{f_{co}}\alpha(1+\alpha)6\Bigg(\frac{\lambda_{co-cca}}{f_{cca}}\Bigg)^2\Bigg(1-\frac{\lambda_{co-cca}}{f_{cca}}\Bigg)^2 + G_{co}\frac{\lambda_{co-cca}}{f_{co}}\alpha\Bigg(1-6\Bigg(\frac{\lambda_{co-cca}}{f_{cca}}\Bigg)^2\Bigg(1-\frac{\lambda_{co-cca}}{f_{cca}}\Bigg)^2\Bigg)\Bigg] + D_\alpha\nabla^2\alpha \quad (4.41e)$$

$$\frac{\partial \lambda_{co-ma}}{\partial t} = P_{cr}\lambda_{ma-ta} + P_{cr}\lambda_{ma-cca} - P_{cd}\lambda_{co-ma} + P_{ma}\lambda_{co-ta} - G_H H_{pop}\Bigg(\frac{\lambda_{co-ma}}{f_{ma}+f_{ta}}\Bigg) + 4\Bigg[G_{co}\lambda_{co-ma}(1-\eta)\Bigg(ag_{ma}-\frac{\lambda_{co-ma}}{f_{ma}}\Bigg) + G_{ma}\lambda_{co-ma}\eta\Bigg(ag_{co}-\frac{\lambda_{co-ma}}{f_{co}}\Bigg) + G_{co}\lambda_{co-ta}\frac{\lambda_{ma-ta}}{f_{ta}} + G_{co}\lambda_{co-cca}\frac{\lambda_{ma-cca}}{f_{cca}} + G_{ma}\lambda_{ma-ta}\frac{\lambda_{co-ta}}{f_{ta}} + G_{ma}\lambda_{ma-cca}\frac{\lambda_{co-cca}}{f_{cca}}\Bigg] + D_{CO-ma}(1-\eta)\nabla^2\lambda_{co-ma} + D_{co-MA}\eta\nabla^2\lambda_{co-ma} \quad (4.41f)$$

$$\frac{\partial \lambda_{co-ta}}{\partial t} = -P_{cr}\lambda_{co-ta} + P_{cr}f_{ta}ag_{ta} + P_{cr}\lambda_{ta-cca} - P_{cd}\lambda_{co-ta} - P_{ma}\lambda_{co-ta} + P_{tr}\lambda_{co-cca} - G_H H_{pop}\left(\frac{\lambda_{co-ta}}{f_{ma}+f_{ta}}\right) + 4\Bigg[G_{co}\lambda_{co-ta}\left(ag_{ta} - \frac{\lambda_{co-ta}}{f_{ta}}\right) + G_{co}\lambda_{co-ma}(1-\eta)\frac{\lambda_{ma-ta}}{f_{ma}} + G_{co}\lambda_{co-cca}\frac{\lambda_{ta-cca}}{f_{cca}} + G_{ta}\lambda_{ta-cca}\frac{\lambda_{co-cca}}{f_{cca}} - G_{ma}\lambda_{co-ma}\eta\frac{\lambda_{co-ta}}{f_{co}} - G_{ma}\lambda_{ma-ta}\frac{\lambda_{co-ta}}{f_{ta}}\Bigg] + D_{co-ta}\nabla^2\lambda_{co-ta} \quad (4.41g)$$

$$\frac{\partial \lambda_{co-cca}}{\partial t} = -P_{cr}\lambda_{co-cca} + P_{cr}f_{cca}ag_{cca} + P_{cr}\lambda_{ta-cca} + P_{cd}f_{co}ag_{co} + G_H H_{pop}\left(\frac{\lambda_{co-ma}}{f_{ma}+f_{ta}}\right) - P_{tr}\lambda_{co-cca} - P_{cd}\lambda_{co-cca} + G_H H_{pop}\left(\frac{\lambda_{co-ta}}{f_{ma}+f_{ta}}\right) + 4\Bigg[G_{co}\lambda_{co-cca}\left(ag_{cca} - \frac{\lambda_{co-cca}}{f_{cca}}\right) + G_{co}\lambda_{co-ma}(1-\eta)\frac{\lambda_{ma-cca}}{f_{ma}} + G_{co}\lambda_{co-ta}\frac{\lambda_{ta-cca}}{f_{ta}} - G_{ma}\lambda_{co-ma}\eta\frac{\lambda_{co-cca}}{f_{cca}} - G_{ma}\lambda_{ma-cca}\frac{\lambda_{co-cca}}{f_{cca}} - G_{ta}\lambda_{ta-cca}\frac{\lambda_{co-cca}}{f_{cca}}\Bigg] + D_{co-cca}\nabla^2\lambda_{co-cca} \quad (4.41h)$$

$$\frac{\partial \lambda_{ma-ta}}{\partial t} = -P_{cr}\lambda_{ma-ta} - P_{ma}\lambda_{ma-ta} + P_{ma}f_{ta}ag_{ta} + P_{tr}\lambda_{ma-cca} - 2G_H H_{pop}\left(\frac{\lambda_{ma-ta}}{f_{ma}+f_{ta}}\right) + 4\Bigg[G_{ma}\lambda_{ma-ta}\left(ag_{ta} - \frac{\lambda_{ma-ta}}{f_{ta}}\right) + G_{ma}\lambda_{co-ma}\eta\frac{\lambda_{co-ta}}{f_{co}} + G_{ma}\lambda_{ma-cca}\frac{\lambda_{ta-cca}}{f_{cca}} + G_{ta}\lambda_{ta-cca}\frac{\lambda_{ma-cca}}{f_{cca}} - G_{co}\lambda_{co-ma}(1-\eta)\frac{\lambda_{ma-ta}}{f_{ma}} - G_{co}\lambda_{co-ta}\frac{\lambda_{ma-ta}}{f_{ta}}\Bigg] + D_{ma-ta}\nabla^2\lambda_{ma-ta} \quad (4.41i)$$

$$\frac{\partial \lambda_{ma-cca}}{\partial t} = -P_{cr}\lambda_{ma-cca} + P_{cd}\lambda_{co-ma} + P_{ma}\lambda_{ta-cca} - P_{tr}\lambda_{ma-cca}$$
$$- G_H H_{pop}\left(\frac{\lambda_{ma-cca}}{f_{ma}+f_{ta}}\right) + G_H H_{pop}\left(\frac{f_{ma}ag_{ma}}{f_{ma}+f_{ta}}\right) + G_H H_{pop}\left(\frac{\lambda_{ma-ta}}{f_{ma}+f_{ta}}\right)$$
$$+ 4\Bigg[G_{ma}\lambda_{ma-cca}\left(ag_{cca} - \frac{\lambda_{ma-cca}}{f_{cca}}\right) + G_{ma}\lambda_{co-ma}\eta\frac{\lambda_{co-cca}}{f_{co}} + G_{ma}\lambda_{ma-ta}\frac{\lambda_{ta-cca}}{f_{ta}}$$
$$- G_{co}\lambda_{co-ma}(1-\eta)\frac{\lambda_{ma-cca}}{f_{ma}} - G_{co}\lambda_{co-cca}\frac{\lambda_{ma-cca}}{f_{cca}} - G_{ta}\lambda_{ta-cca}\frac{\lambda_{ma-cca}}{f_{cca}}\Bigg]$$
$$+ D_{ma-cca}\nabla^2\lambda_{ma-cca} \quad (4.41\text{j})$$

$$\frac{\partial \lambda_{ta-cca}}{\partial t} = -2P_{cr}\lambda_{ta-cca} + P_{cd}\lambda_{co-ta} - P_{ma}\lambda_{ta-cca} - P_{tr}\lambda_{ta-cca} + P_{tr}f_{cca}ag_{cca}$$
$$+ G_H H_{pop}\left(\frac{\lambda_{ma-ta}}{f_{ma}+f_{ta}}\right) - G_H H_{pop}\left(\frac{\lambda_{ta-cca}}{f_{ma}+f_{ta}}\right) + G_H H_{pop}\left(\frac{f_{ta}ag_{ta}}{f_{ma}+f_{ta}}\right)$$
$$+ 4\Bigg[G_{ta}\lambda_{ta-cca}\left(ag_{cca} - \frac{\lambda_{ta-cca}}{f_{cca}}\right) - G_{co}\lambda_{co-ta}\frac{\lambda_{ta-cca}}{f_{ta}} - G_{co}\lambda_{co-cca}\frac{\lambda_{ta-cca}}{f_{cca}}$$
$$- G_{ma}\lambda_{ma-ta}\frac{\lambda_{ta-cca}}{f_{ta}} - G_{ma}\lambda_{ma-cca}\frac{\lambda_{ta-cca}}{f_{cca}}\Bigg]$$
$$+ D_{ta-cca}\nabla^2\lambda_{ta-cca} \quad (4.41\text{k})$$

$$\frac{\partial H_{pop}}{\partial t} = a_{HA}H_{pop}(f_{ma}+f_{ta}) - (a_{HH} - \epsilon(1-f_{co}))H_{pop} + d_{hpop}\nabla^2 H_{pop}, \quad (4.41\text{l})$$

4.8 Figures

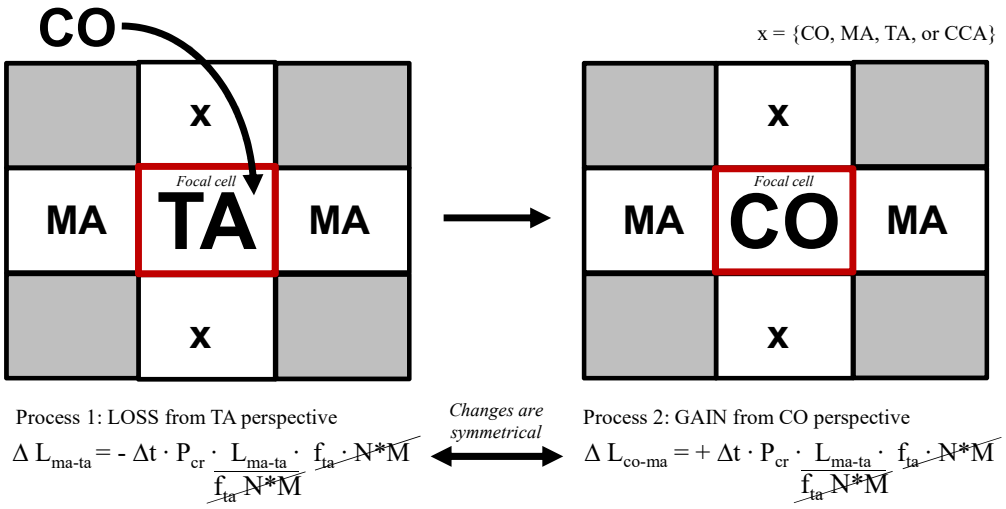

Figure 4.1: **Nondimensional boundary length term from process of CO recruiting to TA.**
CO recruiting to a TA cell decreases the total number of L_{ma-ta} boundaries (red), which in turn increases L_{co-ma} boundaries. Focusing in on one neighborhood, the CO recruitment event can be envisioned as processes that result in a set of negative changes to the number of boundaries, $Lma - ta$, and a symmetrical positive change to the number of L_{co-ma} boundaries.

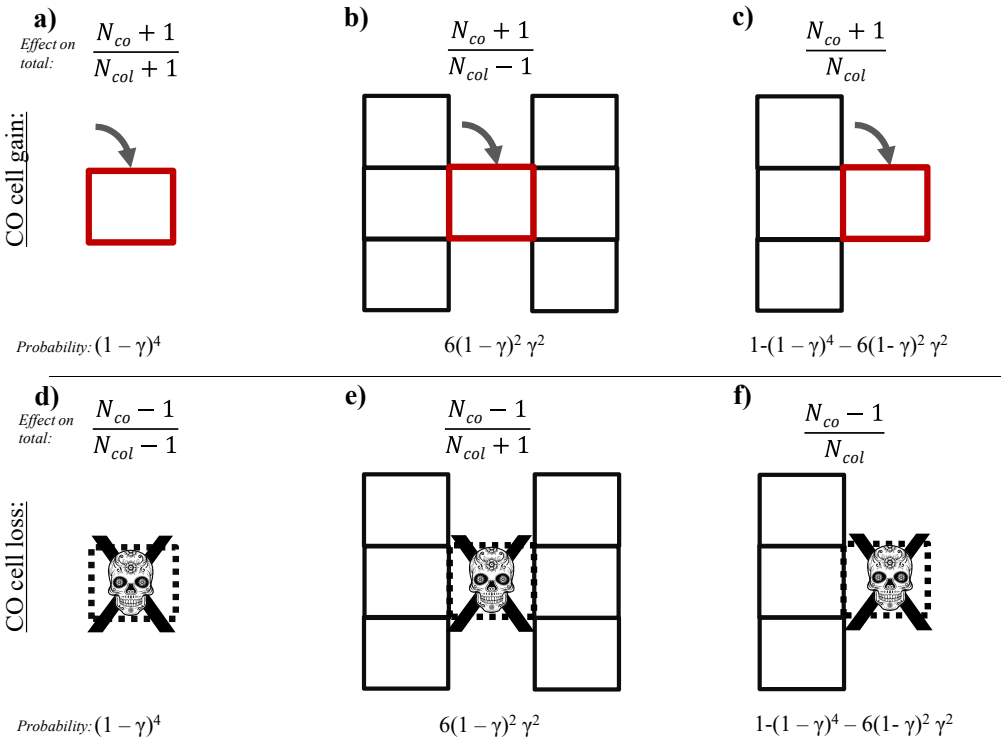

Figure 4.2: **Average colony size configurations and probabilities for CO cell gains and losses.**
Change in α is influenced by the cumulative effect of processes operating on three colony configurations. The top row, a - c, shows the configurations and the corresponding effect of a CO cell gain on N_{co}, the total number of CO cells, and N_{col}, the total number of CO colonies. Below each graphic is the associated probability of the configuration. Similarly, the bottom row shows the impact on α of a CO cell loss. γ is the probability of neighbors b of type c, or $\frac{\lambda_{b-c}}{f_c}$.

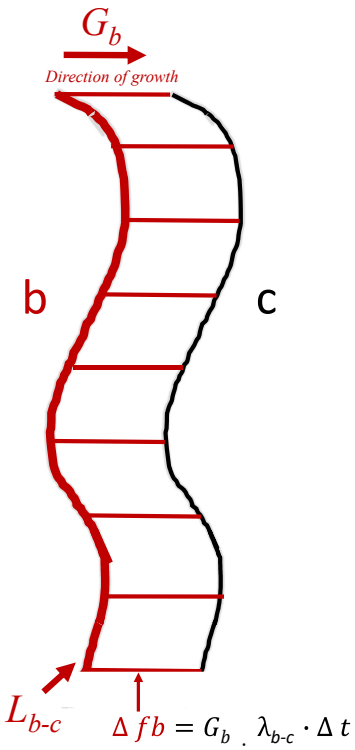

Figure 4.3: **Fractional cover overgrowth occurs along a front.**
The change in fractional cover, f_b, of functional type b overgrowing type c along a front of length, L_{b-c}: the rate of growth, G_b, times λ_{b-c} times Δt.

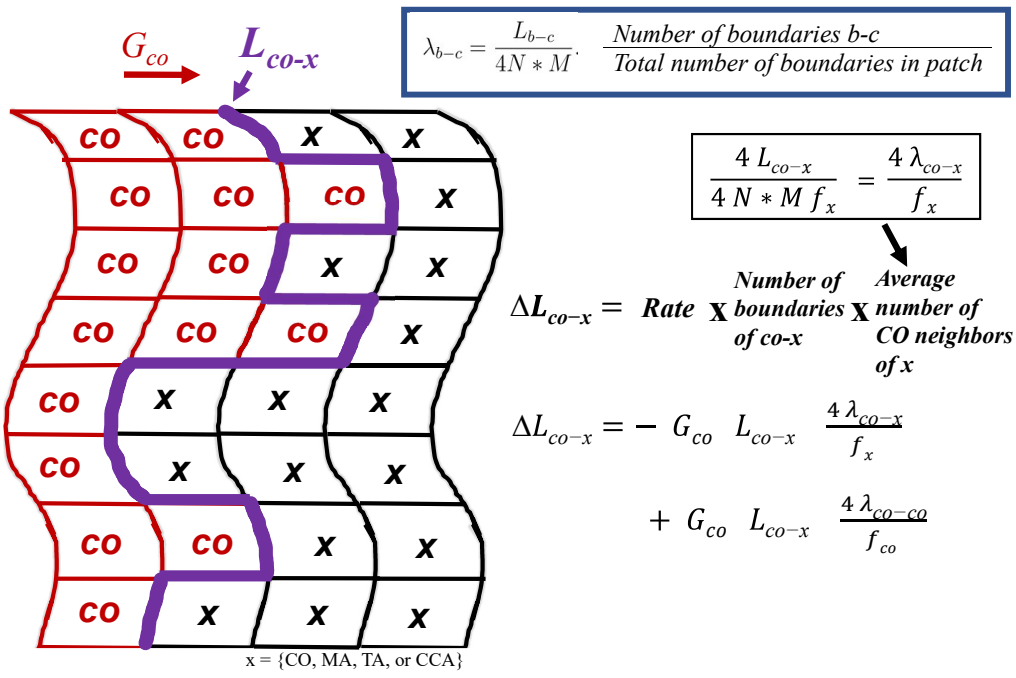

Figure 4.4: **Boundary length overgrowth occurs along a front.**
The change in boundary length, L_{co-x}, as functional type co overgrows type x along a front of length, L_{co-x}: the rate of growth, G_{co}, times L_{co-x} times $4\lambda_{co-x}/f_x$ times Δt.

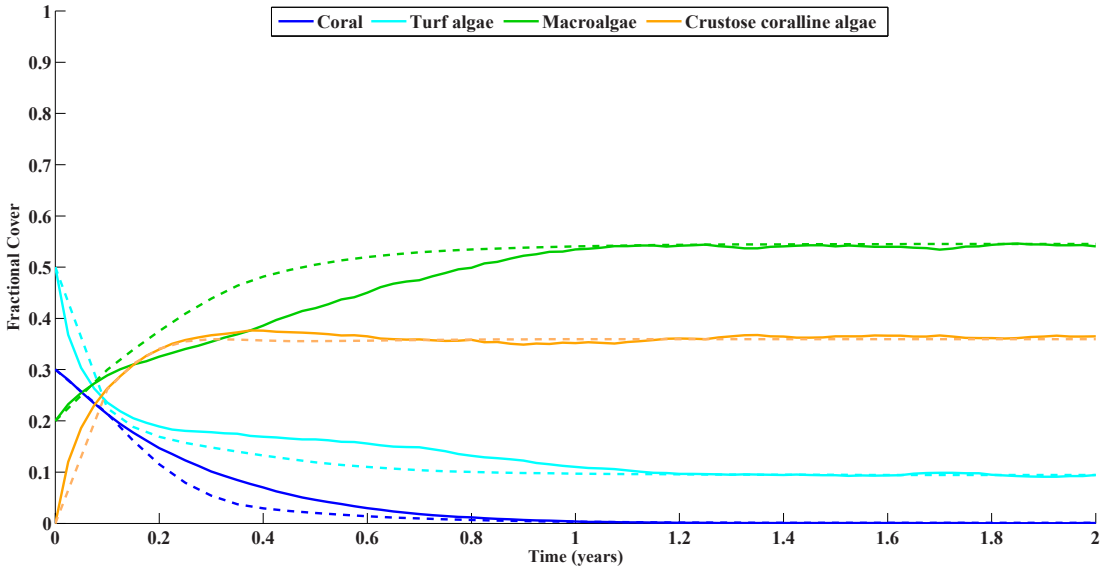

Figure 4.5: **Comparison of fractional cover between cellular model (bold lines) and continuum model (dotted lines) for MA attractor with adjusted parameters.**
The pathways between the two models are generally aligned, except for a possible difference in functional form for the decay to attractor.

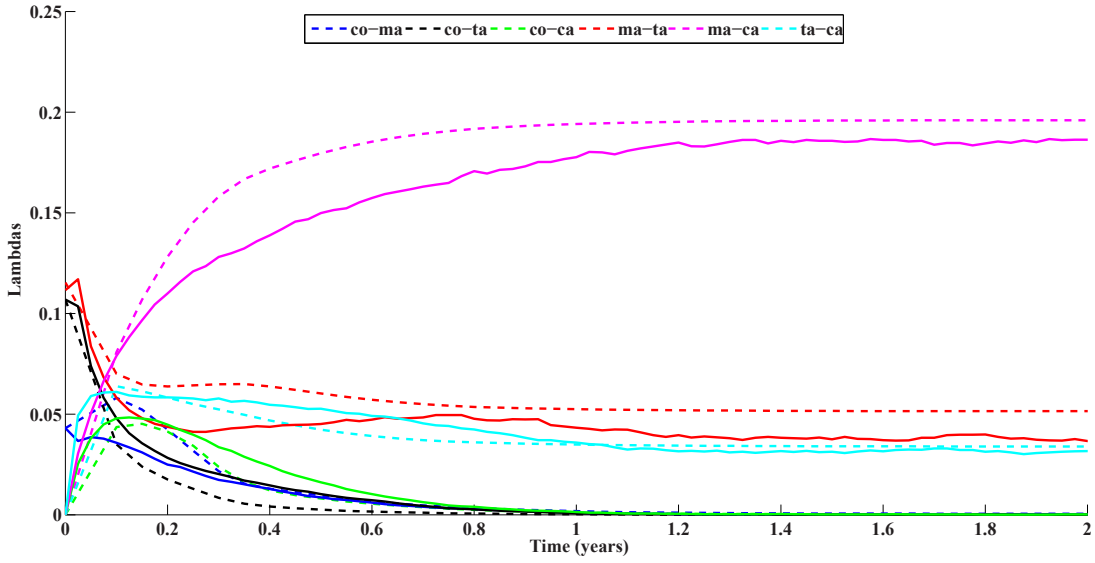

Figure 4.6: **Comparison of corresponding nondimensional boundary lengths between cellular (bold) and continuum (dotted) models for MA dominated attractor case with adjusted parameters.**
Discrepancies between the cellular and continuum models are markedly different for λ_{ma-ta} and λ_{ma-ca}

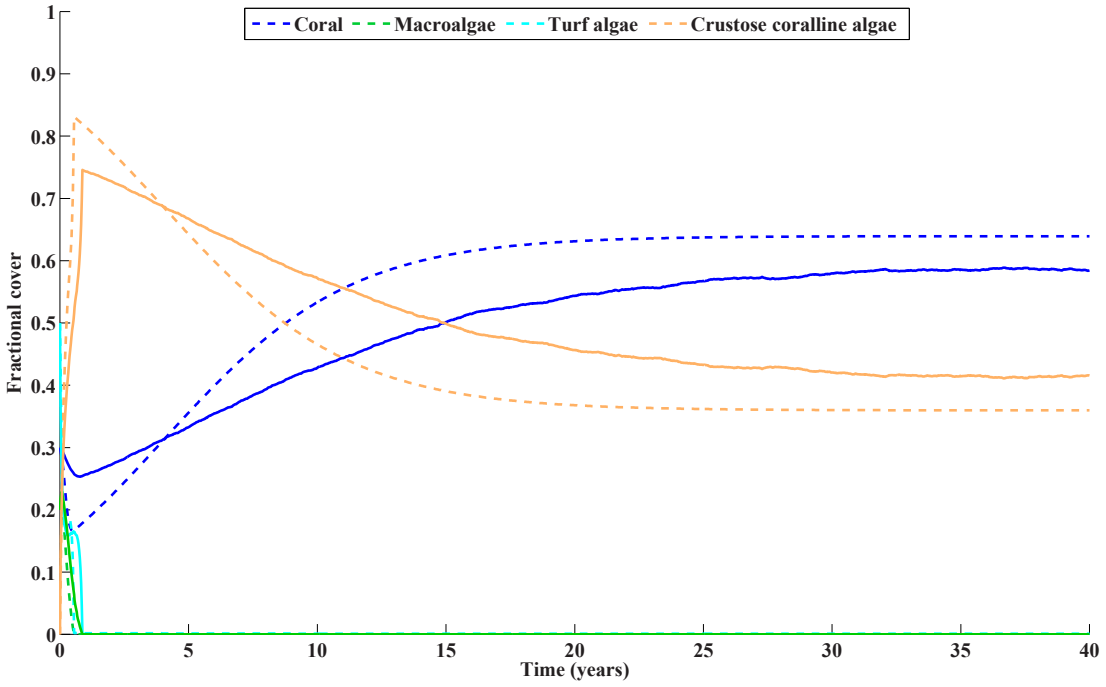

Figure 4.7: **Comparison of fractional cover between cellular model (bold lines) and continuum model (dotted lines) for CO attractor with adjusted parameters.**
The duration of the transients are comparable, but the differences between the decay time scales and attractor coral fractional cover persist.

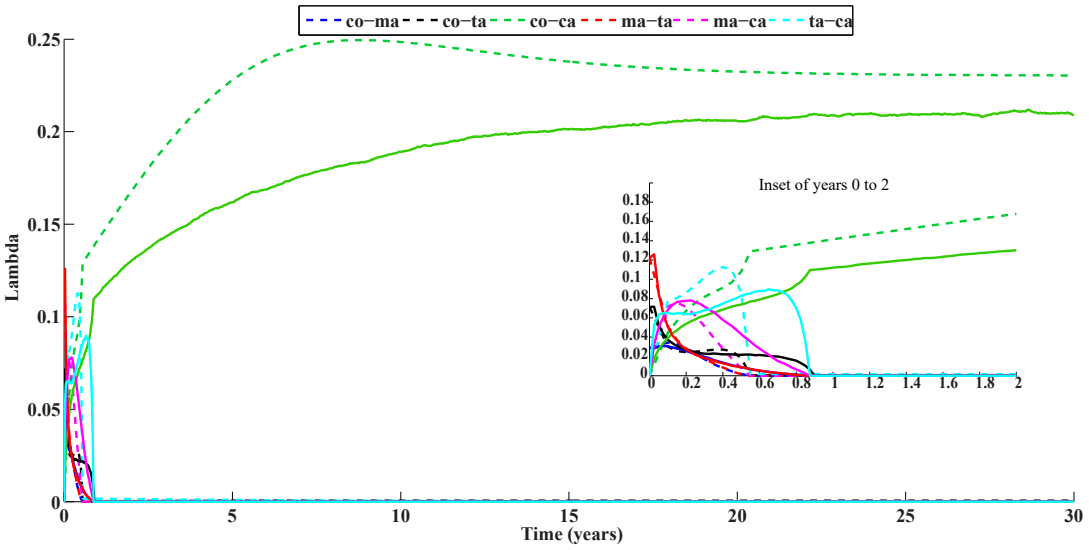

Figure 4.8: **Comparison of nondimensional boundary lengths between cellular (bold) and continuum (dotted) models for CO dominated attractor case with adjusted parameters.**
The attractor values of λ_{ma-ta} and λ_{ma-cca} are 5 and 20% larger, respectively, in the continuum model. The inset depicts the faster decay of the continuum model across all λs.

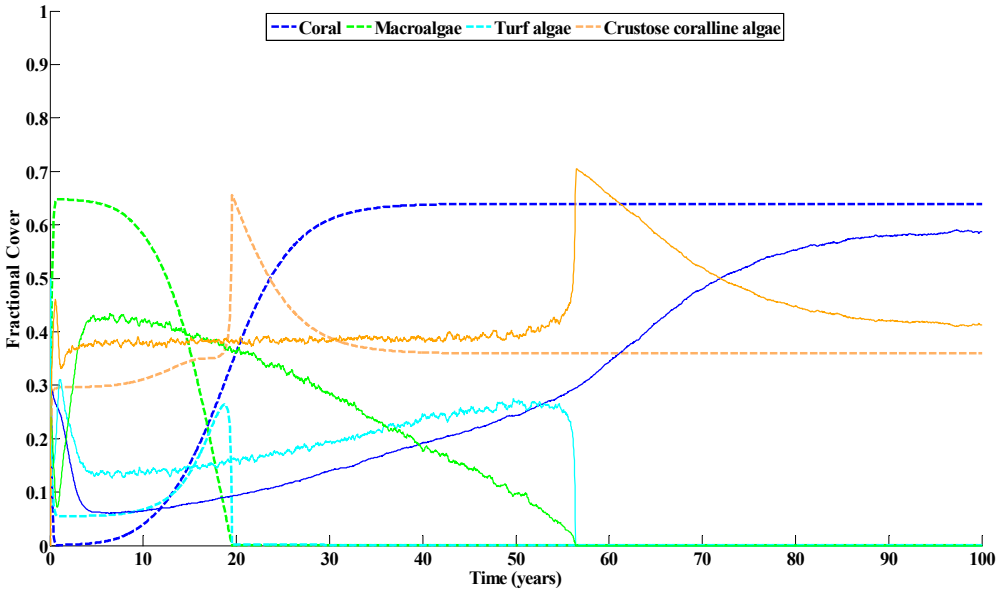

Figure 4.9: **Comparison between cellular model (bold lines) and continuum model (dotted lines) for CO attractor with long transient and adjusted parameters.**
Comparison of fractional cover model outputs for CO dominated case with long transient using adjusted parameters. As with the base parameter case, the general form of the behavior is similar, but the duration of the transient and associated time scales of the CO fractional cover are shorter and faster, respectively, for the continuum model.

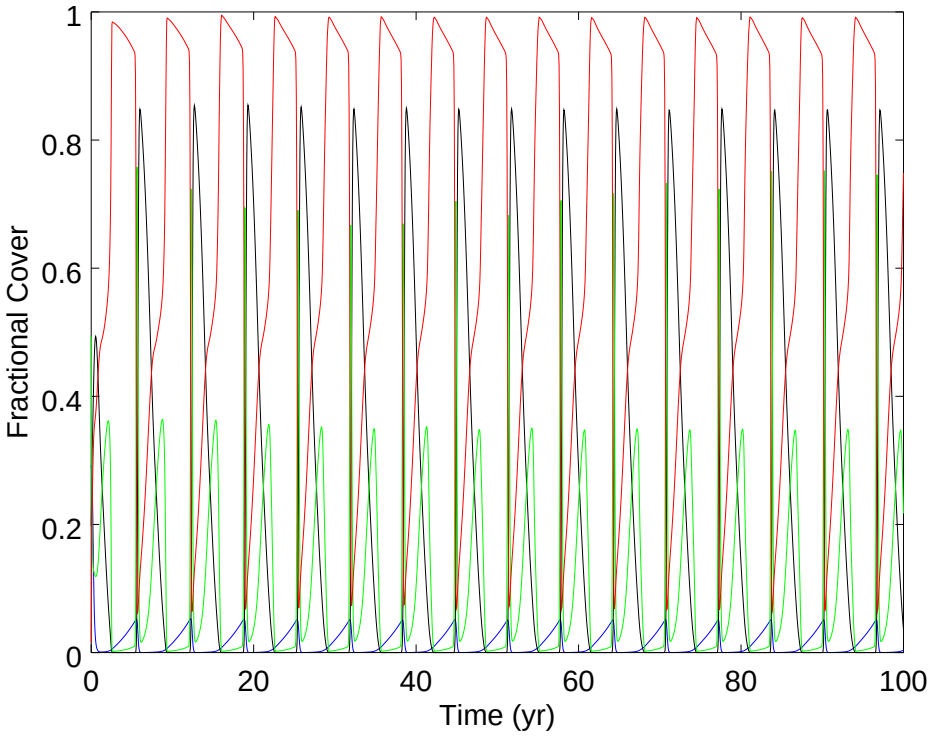

Figure 4.10: **Predator-prey oscillations in coupled reef-fish model.** Predator-prey oscillations in coupled reef-fish model (black = MA, green = TA, red = CCA, blue = CO). MA and TA exhibit a transient-like stage that is terminated by increases in fish population rather than increase in coral fractional cover, as for the CO dominated attractor cases.

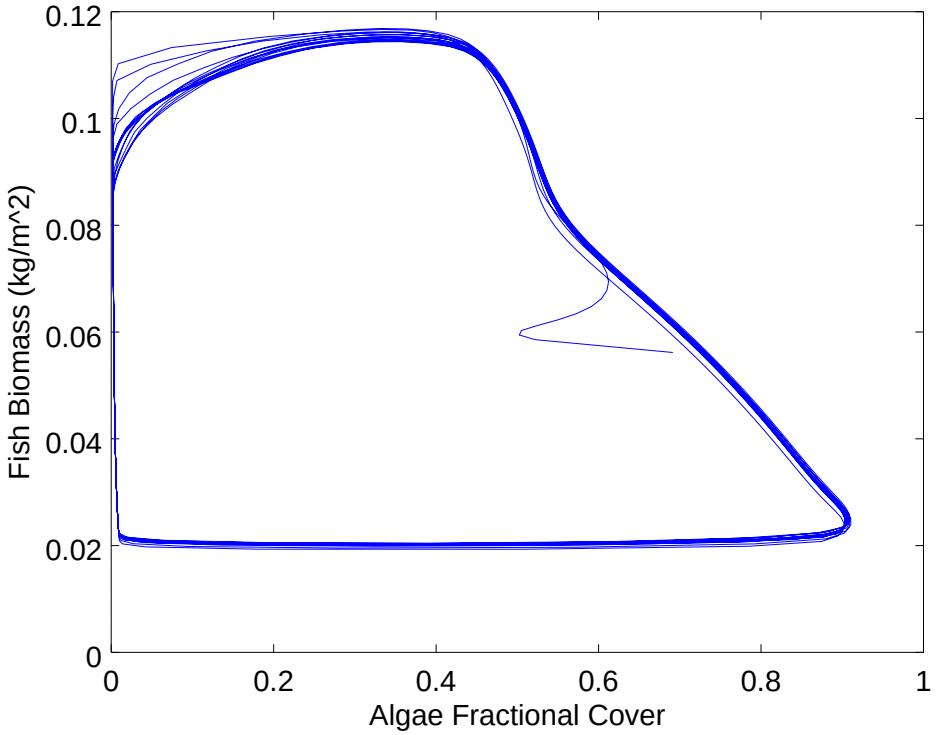

Figure 4.11: **Predator-prey oscillations cyclical attractor in phase space.** Fish and algae interactions evolve to a stable cyclical attractor over decades.

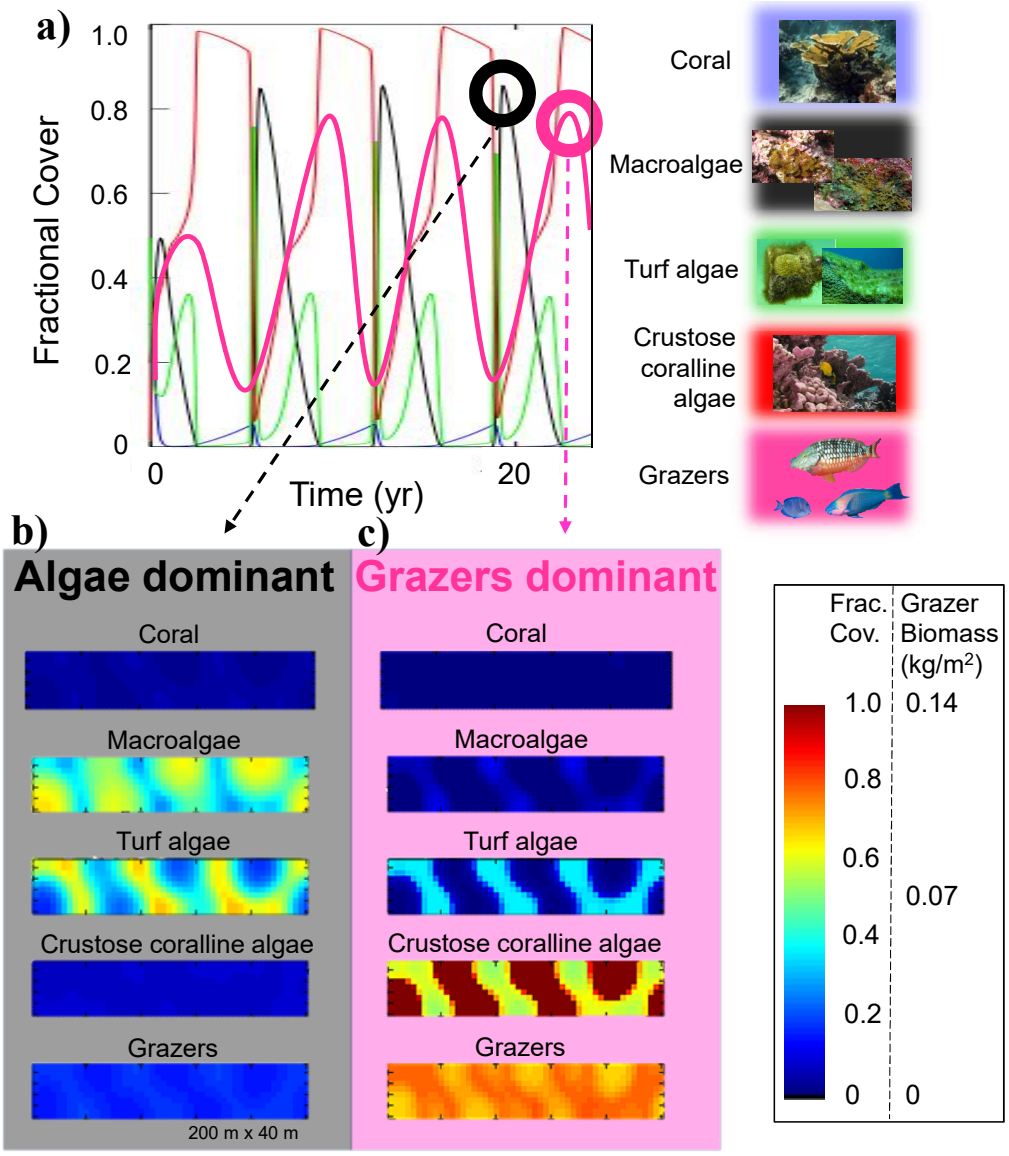

Figure 4.12: **Pathways for all groups and corresponding snapshots of continuum fields.**
Oscillating pathways of all functional groups with snapshots of corresponding continuum fields showing persistent reaction-diffusion type spatial patterns in the form of cross-shore stripes. a) pathways of all functional groups; b) continuum fields when algae is dominant: coral largely disappears and algae occurs in cross-shore striped pattern; c) continuum fields when grazers are dominant: coral largely absent while algae and grazers occur in cross-shore stripes.

4.9 Tables

Table 4.1: **Initial conditions for three example cases.**
Initial conditions for three example cases: MA dominated attractor, CO dominated attractor, and CO dominated attractor with long transient.

Variable	Symbol	MA dominated attractor	CO dominated attractor	CO dominated attractor with long transient
Fractional cover of CO	f_{co}	0.300	0.300	0.300
Fractional cover of MA	f_{ma}	0.200	0.200	0.200
Fractional cover of TA	f_{ta}	0.500	0.500	0.500
Fractional cover of CCA	f_{cca}	0.000	0.000	0.000
Aggregation of CO	ag_{co}	0.500	0.667	0.886
Aggregation of MA	ag_{ma}	0.227	0.246	0.279
Aggregation of TA	ag_{ta}	0.563	0.613	0.682
Aggregation of CCA	ag_{cca}	0.000	0.000	0
Non-dimensional boundary length co-ma	$\lambda_{co\text{-}ma}$	0.043	0.029	0.0097
Non-dimensional boundary length co-ta	$\lambda_{co\text{-}ta}$	0.107	0.071	0.0246
Non-dimensional boundary length co-cca	$\lambda_{co\text{-}cca}$	0.000	0.000	0
Non-dimensional boundary length ma-ta	$\lambda_{ma\text{-}ta}$	0.112	0.122	0.1346
Non-dimensional boundary length ma-cca	$\lambda_{ma\text{-}cca}$	0.000	0.000	0
Non-dimensional boundary length ta-cca	$\lambda_{ta\text{-}cca}$	0.000	0.000	0
Mean coral colony size	α	4	9	9
Herbivore biomass	H_{pop}	0.056	0.056	0.056

Table 4.2: **Continuum model base parameters and definitions.**
The base parameters are the converted values from the cellular model.
*For sources refer to [Sandin and McNamara, 2011, Kramer, 2008].

Parameter	Definition	Value	Units
P_{cr}	Probability of CO recruitment	0.01	per year
P_{tr}	Probability of TA recruitment	1.576	per year
P_{ma}	Probability of MA succession from TA	0.33	per year
P_{cd}	Probability of CO death	0.15	per year
G_{co}	Growth term for CO	0.1	m per year
G_{ma}	Growth term for MA	5	m per year
G_{ta}	Growth term for TA	10	m per year
a_{HH}	Mortality coefficient for herbivorous fish	1.77	
α_{th}	Threshold for CO size dominance	9	cells
G_H	Herbivore grazing rate	88.5	m^2 per kg

Table 4.3: **Continuum model adjusted parameters per example case.** The two adjusted parameters, threshold mean colony size and grazing, leading to closest results between continuum model and celllular model.

Case	Adjusted α_{th} value	Adjusted G_H value
MA dominated attractor	5	104.43
CO dominated attractor	7	119.475
CO dominated attractor with long transient	21	88.5

4.10 Supporting Information

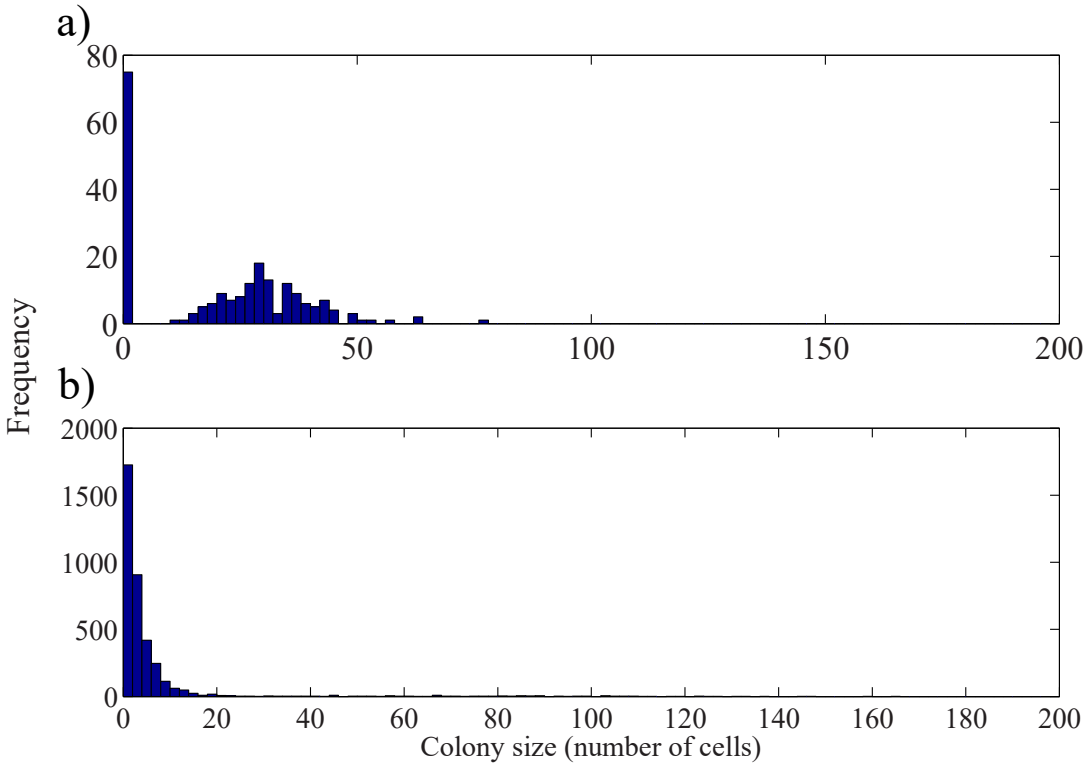

Figure 4.13: **Cellular model coral colony size distributions in the transient and attractor stages.**
Coral colony size distributions in the cellular model within the a) transient (year 25) and b) the attractor (year 95) for comparison to Poisson distribution assumption for colony sizes in continuum model.

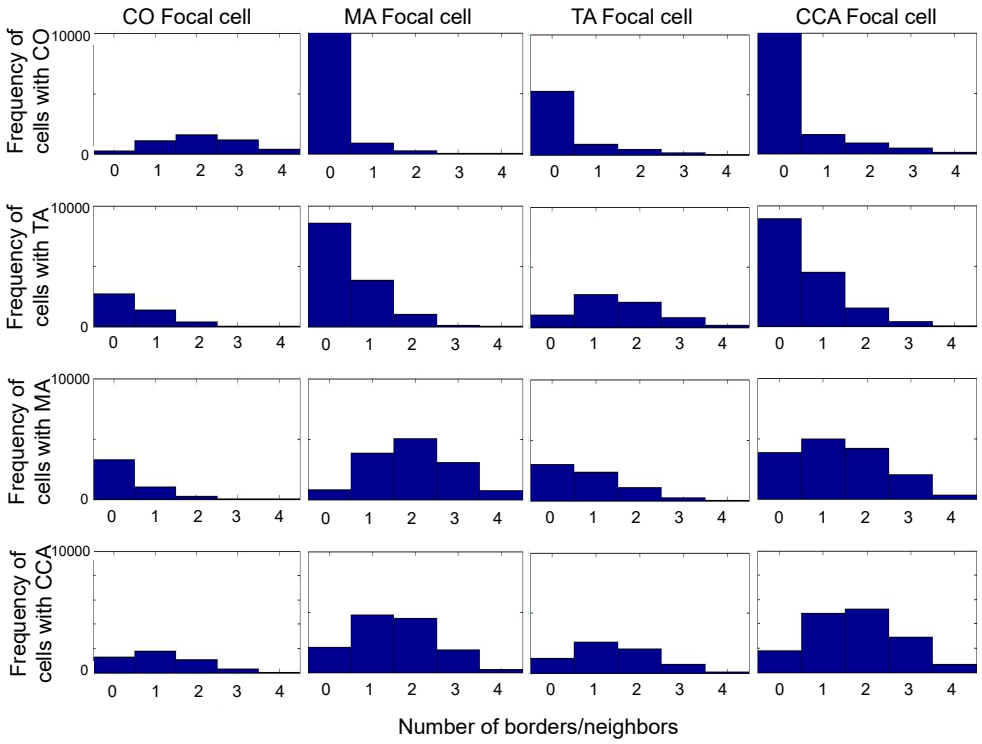

Figure 4.14: **Cellular model neighbors distributions per cell in the transient stage.**
Distributions of the number of borders of each central focal cell of a functional type (column) that neighbored each functional type (row) in the cellular model within the transient stage (year 25).

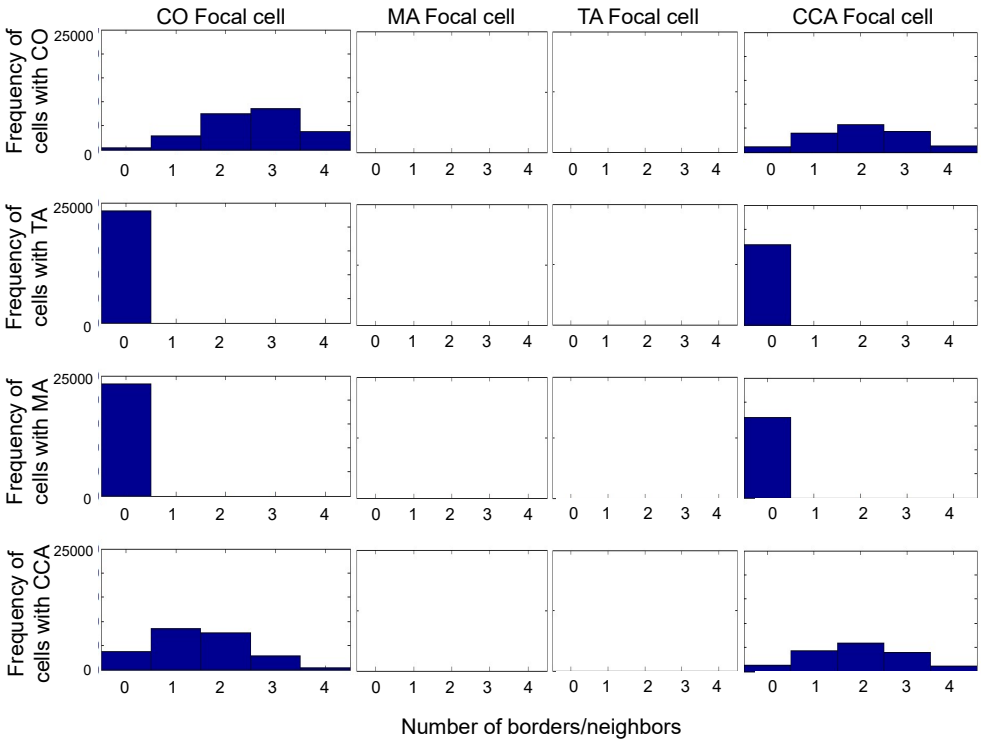

Figure 4.15: **Cellular model neighbors distributions per cell in the attractor stage.**
Distributions of the number of borders of each central focal cell of a functional type (column) that neighbored each functional type (row) in the cellular model within the attractor (year 95).

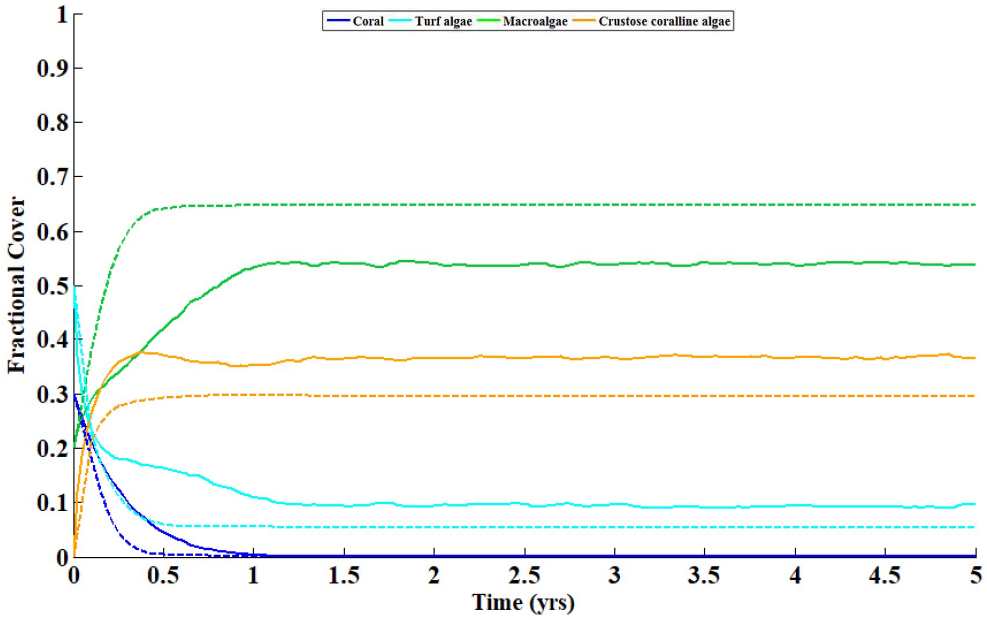

Figure 4.16: **Comparison between cellular model (bold lines) and continuum model (dotted lines) for MA attractor with base parameters.** All continuum model fractional cover pathways decay to the attractor faster than those in the cellular model. The attractor value for the dominant MA is higher in the continuum model by about 10%, with all other attractor values for the other functional types having discrepancies as well (except CO).

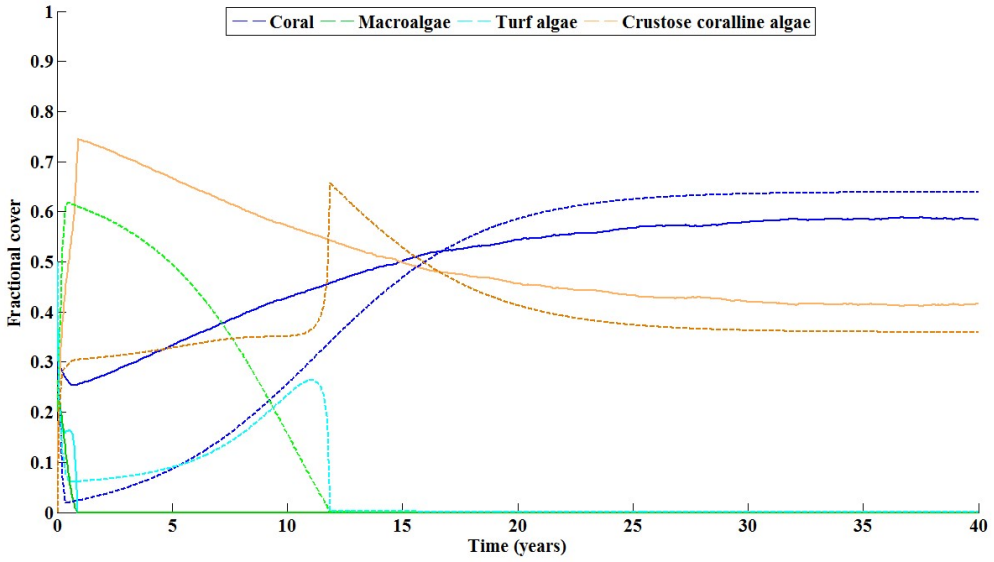

Figure 4.17: **Comparison between cellular model (bold lines) and continuum model (dotted lines) for CO attractor with base parameters.** The duration of the transient in the continuum model is twelve times that in the cellular model and the contiunnum model decays to the attractor about twice as fast, arriving at a value that is about 10 % higher.

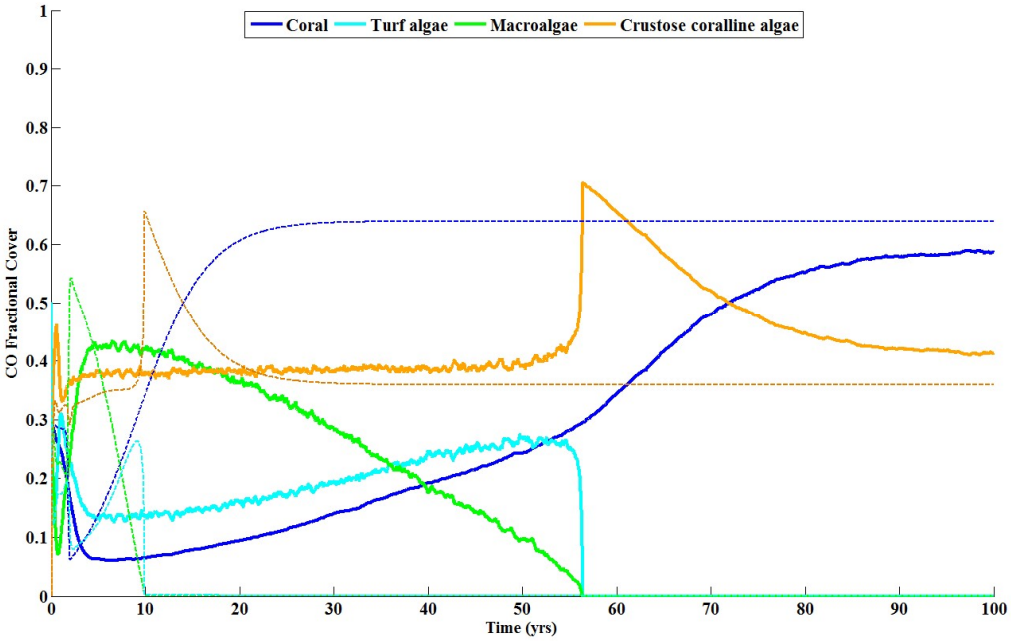

Figure 4.18: **Comparison of fractional cover between cellular model (bold lines) and continuum model (dotted lines) for CO attractor with long transient with base parameters.**
The general form of the behavior is similar in both models, but the duration of the transient (i.e., linked to time scale of CO) is more than five times as long as the transient in the continuum model and the value of coral fractional cover is 0.05 higher in the continuum model.

Chapter 5

Conclusions

"Our lives and the life of the sea are braided together . . . here we are islanders, we live because the sea lives." -Living Sea, 1995

The aim of my research has been to build the ecosystem model infrastructure that will allow the societal-coral reef system to be modeled over a duration sufficiently long that an attractor determined by two-way nonlinear interactions can develop. The preceding chapters describe investigations into multiple levels of the coral reef ecosystem, namely, small-scale coral colony level dynamics (Chapter 2), intermediate-scale consequences of coral aggregation patterns on decadal-scale reef evolution (Chapter 3), and integration of these aspects into an island-scale spatio-temporal continuum model (Chapter 4) that can be linked to coastal human societies.

Human societies interacting with coral reef ecosystems have been mostly characterized in the ecological academic literature as negative forces that threaten richly biodiverse coral reef habitats through fisheries resource over-exploitation, and in more contemporary times, through pollution from rapid urbanization and tourism [Maragos et al., 1996, Coll et al., 2008, Smith and Wishnie, 2000]. However, in traditional subsistence-based indigenous societies, the coupling between people and their environment has co-evolved over millennia to arrive at strong nonlinear connections that reverberate through all aspects of society, from basic sustenance to the formation of cultural and individual identities that view peo-

ple and the environment as one inseparable entity [Kealiikanakaoleohaililani and Giardina, 2015, Grim, 2001].

In this chapter, I give a broad overview of a subsistence-based Micronesian fishing society and conclude by describing an initial attempt to couple a representative fishing society to the island-scale continuum model developed in chapter 4. The chapter closes with identifying key challenges and knowledge gaps for future, more complete, model development and testing, as well as proposing future applications of the coupled model.

5.1 Coral Islanders and their relation to reefs

Coastal indigenous societal-reef relations vary across ocean basins with people depending upon coral reef resources to different degrees [Shackeroff et al., 2009]. In central Pacific Micronesian societies, people inhabit islands and atolls, or ring-shaped chains of small islands formed of coral, ranging in size and topographical elevation. In contrast to the larger, more horticulturally productive high islands, flatter, smaller island types, referred to as low islands, have limited land area available for cultivation [Alkire, 1978]. In general, smaller islands are characterized by more intensive interactions between people and the sea, and by more pronounced influences of the ocean on culture [Hau'ofa, 1998].

Subsistence-based Micronesian cultures emerged from the various combinations of challenging environmental conditions, including poor soils, few endemic species of flora or fauna, and susceptibility to storms and drought [Alkire, 1978]. These cultures are widely interconnected, cohesive fishing societies with deeply-rooted customs of resource sharing. Hierarchy and rank also are important aspects of Micronesian life but exist within a participatory context that allows for a significant degree of social mobility. The continual interplay between hierarchy and equality is best captured in the traditions of feasting, through which an individual's, household's, lineage's, or community's capacity for growing food, generosity, and commitment to community well-being are demonstrated. The emphasis on promoting general community welfare through sharing reinforces matrilineal clan

and inter-island social safety networks that play a central role in ameliorating the effects of natural catastrophes [Petersen, 2009b]. The communal nature of Micronesian life and strong kinship obligation is such that, at one point, there was strict prohibition of the selling of fish in the southern Line Islands and Tuvalu since it countered deeply rooted sharing customs [Ruddle and Johannes, 1984]. Strong customary tenure systems or lineage-based rights to cultivate specific lands and fish coral reefs are maintained through cultural and historical practices designed to regulate the use of, access to, and transfer of these 'resources' [Ruddle and Johannes, 1984, Aswani et al., 2007]. For example, a commonly practiced Micronesian cultural tradition involves temporarily closing (for variable periods of time) areas of the reef either in response to severely degraded reefs or in preparation for large celebratory feasts organized around significant life events [Johannes, 1981, Ruddle and Johannes, 1984, Petersen, 2009b]. These custom tenure systems and other strategies restricting access (e.g., social beliefs and taboos) serve to regulate fishing pressure on reefs.

Reef and lagoon tenure in Micronesian fishing societies broadly consists of lineage-based parcel allotment that stretches from land across the reef to just beyond the outer reef drop-off [Johannes, 1981]. Lineage households typically include a nuclear or extended family with three to fifteen or more individuals; the average house contains eight members spanning three to four generations [Alkire, 1978]. Fishing on the reef greatly contributes to the sustenance of household members and the clan communities to which they belong. Techniques for catching fish are highly variable, with reports of around forty-one different fishing methods in the southwest island of Tobi and thirty-three in Tamana [Johannes, 1981, Ruddle and Johannes, 1984]. Specialized fishing techniques involve different types of nets, hook and lines, spears, lures, nooses, traps, fences (weirs), poisoning, and gleaning. Communal fishing methods also abound, with the largest, most involved form being the *leaf sweep* method, a type of drive-in netting using interweaved palm fronds to encircle reef fish. In all instances, harvested reef and land 'resources' are shared within the lineage household, with neighbors, with the clan community at large, and seasonally between island communities.

By describing Micronesian culture and their relationship to coral reefs through fishing, I attempt to critically shift the nature of the ecological literature's predominant negative discourses of 'human-environment' relationships, while laying some groundwork for beginning to dissect historically-embedded power dynamics that decouple generally horizontal ontological relationships between people and reef environments.

5.2 Reef relationships in colonized societies

Iterative colonization by European, Japanese and American nation-states brought gradual and erratic changes to the coral islanders across Micronesia [Hezel, 2001, Hezel, 2003]. Coral islanders experienced severe depopulation from newly introduced diseases (e.g., tuberculosis, influenza, small pox, sexually transmitted diseases), enslavement and dispossession [Petersen, 2009b, Hanlon, 1994].

The eventual establishment of monetary exchange and connections to regional and global market economies had a significant weakening effect on the subsistence relationship between people and coral reefs [Clausen, 2005]. Fishing pressure on the reef was no longer driven just by family and communal need, but also by external market demand [Cinner et al., 2013, Rapaport, 1990]. The strong ethic of cooperation also eroded as wage based economies increasingly replaced traditional subsistence lifestyles, accentuating a trend towards individualization of land tenure, a shift to the nuclear family system, and urban/rural social distancing [Ward and Proctor, 1980, Hezel, 2001, Hezel, 2013]. The transition from traditional fishing vessels and gear to outboard motors, easily replaceable metal hooks, and flashlights for night fishing further exacerbated the decoupling between fishers and the coral reef environment [Dalzell et al., 1996]. More recently, power-imbalanced contractual agreements renouncing 'access rights' to external large-scale commercial fishing, mining and logging developments are damaging Pacific island resources and ways of life (from heavy metal pollution, deforestation, and water depletion from mining), although some successful cases of traditional clans closing their reefs to commercial fisheries have been reported [Mangubhai et al., 2012, Ruddle et al.,

1992, Dürr and Pascht, 2017].

In addition to outright land dispossession and exploitative resource extraction, the most insidious, long time-scale effects of colonialism are the erosion of the coupling between the reef ecosystem and people by diminishing the subsistence-based relationship, and the deliberate erasure of customary traditional knowledge deemed primitive and shameful in the minds of newly *educated* indigenous youth. The destruction of culture identities and the communal family structures that ensured social cohesion can have devastating consequences for people and local environments. For example, an extraordinarily high rate of suicide among adolescent boys (from age 15 to 24, 1 in 40) across urban centers in Micronesia coincided with disintegration of social support systems and economic roles traditionally reinforced in village men's houses [Rubinstein, 1995, Rubinstein, 2002] . Similar impacts have been documented in Native American communities, for example, with boarding schools, where widespread abuse was commonplace [Adams, 1995]. These examples capture the violence of setter colonialism in erasing and assimilating indigenous people and their traditional knowledge and environmental relationships developed over centuries [Teaiwa, 2008]. The impact of the cash economy, militarization, salaried work, and the dismantling of culturally-rooted dependence on reef ecosystems threatens continued decoupling of the links that bind people to their environment, with detrimental effects for both subsystems.

Despite the significant impacts of colonialism across the region, the characteristic Micronesian matrilineal clans and lineages have also exhibited a significant capacity for adaptation. Still relatively intact, the islanders' high regard for generosity and communal well-being and prioritization of 'resource' sharing (i.e., redistribution of concentrated wealth) is one of many traditional means of placing checks on abuses of power in their societies [Petersen, 2009b]. Because of the continued survival of communal customs (e.g., strong paternal ties, high rates of extended family child-rearing, customary tenure systems, and the organization of lineages into overarching clans) especially in the more rural islands, Micronesian societies continue to remain embedded in networks of social and environmental connections that provide them with profoundly adaptive social possibilities.

5.3 Quantitative characterizations of human societies

In the process of converting qualitative knowledge of human societies into quantitative dynamical representations, several considerations about model structure and individual and collective decision-making are warranted.

Representing humans as agents who demonstrate autonomous behavior, ability to sense their environment, ability to act upon their environment, and rationality, is one way of exploring which aspects of behavior are driving emergent patterns of interest [Shafer, 2007, Montes De Oca Munguia et al., 2009]. The idea is that collective effects of individual actions can elucidate the interactions resulting in the patterns seen in complex coupled human-landscape systems [Jager et al., 2000, Parker et al., 2003, Jager and Mosler, 2007]. However, agent-based modeling necessitates that actors be defined as discrete units, which has been argued to narrow the consideration and inclusion of collective-based behaviors in human systems [Sullivan and Haklay, 2000]. **Therefore, to capture collectively-driven processes in systems, one can explicitly build collective dynamics into the framework of agent-based models in a way that also allows for tracking the evolution of longer time-scale dynamics**.

Decision-making by agents is driven by underlying complex, multi-dimensional values that might change, depending upon the context. But the mechanics of how agents make decisions are typically represented using utility functions or formal logic-based methods, including heuristic decision-trees [Acevedo et al., 2008]. Utility functions characterize the value structure of each agent, so that the selected action decision optimizes expected utility. Logic-based methods specify a set of rules that define the actions to be taken by an agent. Acevedo ([Acevedo et al., 2008]) argued that the two approaches differ more in style and emphasis than substance, because logic-based approaches explicitly define decision rules, while implicitly defining value sets and utility, and utility functions explicitly define a value set, while implicitly defining a set of decision rules. In addition, using utility functions to describe behavior on multiple scale-separated levels of

description remains challenging, while heuristics, in many cases, do not respond to willing-based decision-making [Gigerenzer and Gaissmaier, 2011]. Societies often impose restrictions that are enforced through decision trees that might have only weak relationships to clearly defined goals (and that could form the basis for use of utility functions within an optimization scheme), such as the long-time scale mechanisms societies and resistance movements have developed for dispersing power [Graeber, 2001, Zibechi, 2010, Zibechi, 2012].

A comprehensive framework for analyzing coupled human-environmental systems would aid in unifying the foundational analyses that should be made to dynamically characterize coupled systems. Using a complexity approach, these elements, at a minimum, should include specification of the dominant times scales and levels of description, stability analyses to identify system attractors, bifurcation analyses, quantification of intrinsic time scales of the system using perturbations, and identification of the role of feedbacks on emergent patterns across the coupled system [Werner and McNamara, 2007, Mena et al., 2011]. For example, I expect that for Micronesian societal-reef systems, the direct connection between between fisher families and the reef ecosystem that allows for reef health evaluation will act as a critical feedback for the stability of the coupled system.

*

5.4 Coupling indigenous societies to coral reef ecosystems

Here, I summarize an initial attempt to couple the continuum coral reef ecosystem model to a human society parameterized loosely around Micronesian societies. Previous model representations of coupled human-reef systems have focused largely on exploring case study scenarios of human over-exploitation without comprehensively characterizing the nonlinearities (e.g., reciprocal feedbacks), intrinsic timescales of the different levels of the system, and the interactions linked to emergent large-scale patterns, nor interrogating who is the 'human' in these systems and the historical legacies that molded the power structures in which they are

embedded [Gray et al., 2006, Kramer, 2008, Little et al., 2007, Melbourne-Thomas et al., 2011b, Ruiz Sebastián and McClanahan, 2013, Shafer, 2007, Nietschmann, 1997].

The overall coupled human-reef model is comprised of two dynamical subsystems: the coral reef ecosystem model and the human societal model. At this early stage, the coupled human-reef model developed here is not designed to be representative of any particular reef or human society. Instead I am endeavoring to develop a general but reasonable representation of a coral reef system and an end-member human society tied to the reef through fishing. The coral reefscape model includes the novel continuum model developed in chapter 4, while the human societal model is an agent-based model broadly representing a traditional Micronesian subsistence-based fishing society. The fishing society is coupled to the coral reef benthic community in two ways: via a fish population and by the continual evaluation of the health of the reef by fisher families having a deep relationship with the coastal ocean. The societal model is composed of fisher family agents and community agents. The need of each fishing family is the projected food requirement, plus a supplementary fraction for storage or sharing, referred to as personal stores. The overall community can undertake fishing activities in preparation for upcoming celebratory feasts, or to maintain community food stores to which all members have access. Agent decision-making behavior is represented heuristically using decision-trees that can evolve slowly and be bounded by long-time-scale characteristics of the society (Fig. 5.1). This approach is appropriate for societies that emphasize collective long- time-scale decisions over individual short- time-scale decisions [Werner, 2012].

A customary tenure system of equally allotted reef parcels provides the cultural context for the subsistence functioning of the fishing society. An area of the reef is subject to closure (restricted from fishing) and reopening based on the community's collective decision tree process (Fig. 5.1). At each timestep, the community first asks whether a reef closure is necessary and proceeds to check whether the current state of reef health is above or below the 10 % coral fractional cover threshold. If reef health is severely degraded, the community then closes part

of the reef, regardless of whether there is a celebratory feast event or community-wide food stores are below the defined threshold. The reef closure stays in place only until the reef recovers and then the closure is lifted if community stores are below a defined thresold or a celebratory feast is scheduled. When reef closures are imposed, 20 % of the reef is closed and the remaining reef parcels are divided equally amongst the families in the community. In a similar fashion, fisher families and community fishing agents make decisions about whether to pursue fishing activities, simulating drop-line or spear fishing for fisher families and communal leaf sweep fishing for community agents. Celebratory feasts occur, on average, every six months.

The fishing society is dynamically coupled to the reef ecosystem via the fish population and the direct evaluation of the reef condition by the community. The order of processes is such that each of N fisher families makes a decision about whether to fish and where to fish, they fish, the biology of the system updates, and then fishers reevaluate the reef and decide whether and where to fish in the next timestep. Coupling the societal model to the reef ecosystem model also calls for synchronizing the time scale of fishing decisions to the scale of coral reefscape ecological dynamics. Additional characteristics of fisher behavior can be explored by deviating from the rational expectations assumption, where all fishers have access to all knowledge, by introducing uncertainty and risk into decision-making or differentially constraining the behaviors of fishers to simulate adaptive harvesting. Broadly, representing human societies as autonomous agents capable of sensing their environment and responding to it, can inform which aspects of human behavior are related to emergent spatial patterns unfolding across the reefscape and the overall coupled system.

The nearly complete coupled model is being built to be expandable (e.g., the current global fish population can be expanded into functional types: herbivores and piscivores) and adaptable to treating evolving representations of island societies. The coupled model will be used to investigate how the dynamics of the coupled system change in response to societal integration into market economies, effects of cultural erosion from colonization on the inheritance of traditional knowl-

edge, societal cohesion, and the connection to the reef. In the context of accelerating climate change, the adaptive capacity of the coupled system can be quantified to inform historical and predicted system responses to slow and rapid shifts in climate. The characterization of the adaptive capacity inherent in these subsistence-based coupled systems along with deciphering the cultural characteristics that underlie it can provide a metric for gauging other societies and assessing current efforts aimed at adaptation to global warming. For example, current climate change discourse and conservation efforts have mostly promoted: government imposed no-take natural areas without including affected peoples in decision-making processes [Adams et al., 2004, Ferse et al., 2010], and/or alternative economic livelihoods that sever historical and cultural connections to ecosystems [King and Stewart, 1996]. Using the coupled indigenous societal-reef model, future research will be aimed at exploring how societal resilience can be encouraged by maintaining strong links between people and environmental systems and the traditional customs that underlie cohesive societies. In particular, the question of how resilience in western societies might be bolstered by investing in spaces that maintain interconnected practices and traditions will be addressed.

5.5 Figures

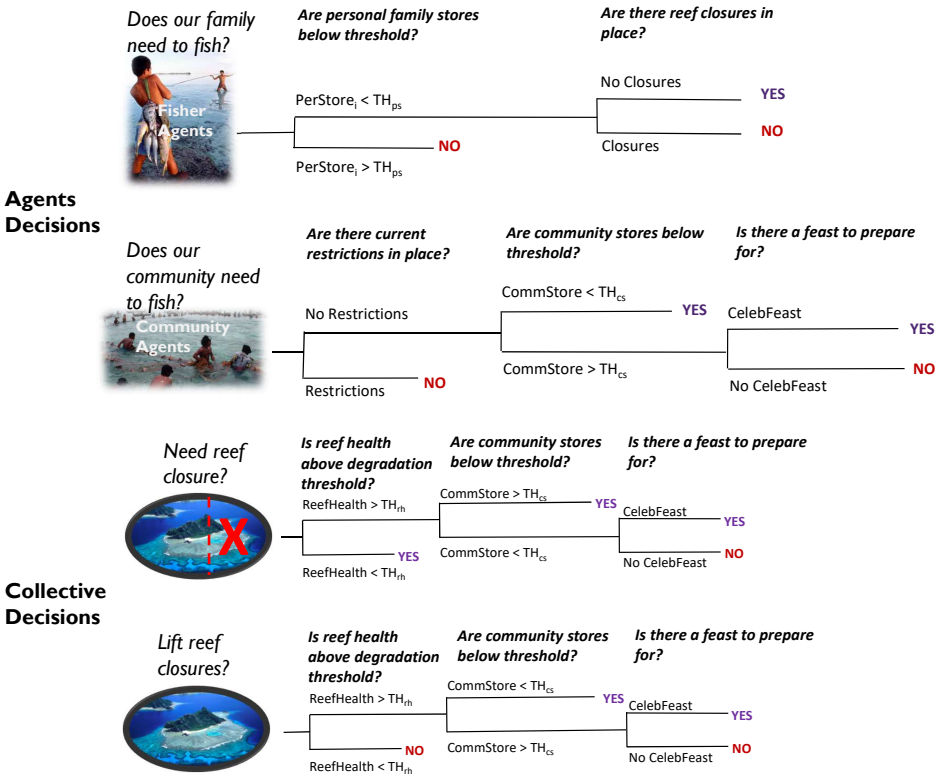

Figure 5.1: **Heuristic decision trees used by agents to make fishing and reef closure decisions.**
Fisher agents based there decision on whether to fish or not on the level of two types of stores, personal and community, which could be above or below a defined threshold, TH. The community collectively decides whether the reef is above or below a certain reef health threshold and whether an area of the reef will be closed to allow for recovery.

Bibliography

[Acevedo et al., 2008] Acevedo, M. F., Baird Callicott, J., Monticino, M., Lyons, D., Palomino, J., Rosales, J., Delgado, L., Ablan, M., Davila, J., Tonella, G., Ramírez, H., and Vilanova, E. (2008). Models of natural and human dynamics in forest landscapes: Cross-site and cross-cultural synthesis. *Geoforum*, 39(2):846–866.

[Acton, 1970] Acton, F. (1970). *Numerical methods that work*. Harper & Row, New York, NY.

[Adams, 1995] Adams, D. (1995). *Education for Extinction: American Indians and the Boarding School Experience, 1875-1928*. University Press of Kansas, Lawrence, KS.

[Adams et al., 2004] Adams, W. M., Aveling, R., Brockington, D., Dickson, B., Elliott, J., Hutton, J., Roe, D., Vira, B., and Wolmer, W. (2004). Biodiversity conservation and the eradication of poverty. *Science (New York, N.Y.)*, 306(5699):1146–9.

[Alkire, 1978] Alkire, W. (1978). *Coral Islanders (Worlds of Man)*. AHM Publishing Corporation, Arlington Heights, IL.

[Alvarez-Noriega et al., 2016] Alvarez-Noriega, M., Baird, A. H., Dornelas, M., Madin, J. S., Cumbo, V. R., and Connolly, S. R. (2016). Fecundity and the demographic strategies of coral morphologies. *Ecology*, 97(12):3485–3493.

[Anthony et al., 2002] Anthony, K., Connolly, S., and Willis, B. (2002). Comparative analysis of energy allocation to tissue and skeletal growth in corals. *Limnology and oceanography*, 47(5):1417–1429.

[Arias-González et al., 2011] Arias-González, J. E., Johnson, C., Seymour, R. M., Perez, P., and Aliño, P. (2011). Scaling up Models of the Dynamics of Coral Reef Ecosystems: An approach for Science-Based Management of Global Change. In Dubinsky, Z. and Stambler, N., editors, *Coral Reefs: An Ecosystem in Transition*, number Wilkinson 2008, pages 373–388. Springer Netherlands, Dordrecht.

[Aswani et al., 2007] Aswani, S., Albert, S., Sabetian, a., and Furusawa, T. (2007). Customary management as precautionary and adaptive principles for protecting coral reefs in Oceania. *Coral Reefs*, 26(4):1009–1021.

[Babcock, 1991] Babcock, R. C. (1991). Comparative Demography of Three Species of Scleractinian Corals Using Age- and Size-Dependent Classifications. *Ecological Monographs*, 61(3):225.

[Bak, 1976] Bak, R. (1976). The growth of coral colonies and the importance of crustose coralline algae and burrowing sponges in relation with carbonate accumulation. *Netherlands Journal of Sea Research*, 10(3):285–337.

[Barnes, 1973] Barnes, D. J. (1973). Growth in colonial scleractinians. *Bulletin of Marine Science*, 23(2):280–298.

[Barott et al., 2011] Barott, K. L., Rodriguez-Mueller, B., Youle, M., Marhaver, K. L., Vermeij, M. J. a., Smith, J. E., and Rohwer, F. L. (2011). Microbial to reef scale interactions between the reef-building coral Montastraea annularis and benthic algae. *Proceedings of the Royal Society B: Biological Sciences*, 279:1655–1664.

[Baums et al., 2006] Baums, I. B., Miller, M. W., and Hellberg, M. E. (2006). Geographic Variation in Clonal Structure in a Reef- Building Caribbean Coral , Acropora Palmata. *Ecological Monographs*, 76(4):503–519.

[Bell and Galzin, 1984] Bell, J. and Galzin, R. (1984). Influence of live coral cover on coral-reef fish communities. *Mar. Ecol. Prog. Ser*, 15:265–274.

[Bruno, 1998] Bruno, J. F. (1998). Fragmentation in Madracis mirabilis (Duchassaing and Michelotti): How common is size-specific fragment survivorship in corals? *Journal of Experimental Marine Biology and Ecology*, 230(2):169–181.

[Bruno and Edmunds, 1997] Bruno, J. F. and Edmunds, P. J. (1997). Clonal variation for phenotypic plasticity in the coral Madracis mirabilis. *Ecology*, 78(7):2177–2190.

[Buddemeier and Kinzie III, 1976] Buddemeier, R. W. and Kinzie III, R. A. (1976). Coral growth. *Oceanographic Marine Biology Annual Review*, 14:183–225.

[Cai, 1988] Cai, L.-D. (1988). *Some notes on repeated averaging smoothing*, pages 597–605. Springer Berlin Heidelberg, Berlin, Heidelberg.

[Carilli, 2014] Carilli, J. E. (2014). Equatorial Pacific coral geochemical records show recent weakening of the Walker Circulation. *Paleoceanography*, 29:1–15.

[Chornesky, 1991] Chornesky, E. A. (1991). The ties that bind: Inter-clonal cooperation may help a fragile coral dominate shallow high-energy reefs. *Marine Biology*, 109(1):41–51.

[Cinner et al., 2013] Cinner, J. E., Graham, N. A. J., Huchery, C., and Macneil, M. A. (2013). Global Effects of Local Human Population Density and Distance to Markets on the Condition of Coral Reef Fisheries. *Conservation Biology*, 27(3):453–458.

[Clausen, 2005] Clausen, R. (2005). The Metabolic Rift and Marine Ecology: An Analysis of the Ocean Crisis Within Capitalist Production. *Organization & Environment*, 18(4):422–444.

[Coll et al., 2008] Coll, M., Libralato, S., Tudela, S., Palomera, I., and Pranovi, F. (2008). Ecosystem overfishing in the ocean. *PloS one*, 3(12):e3881.

[Crabbe, 2010] Crabbe, M. J. C. (2010). Topography and spatial arrangement of reef-building corals on the fringing reefs of North Jamaica may influence their response to disturbance from bleaching. *Marine environmental research*, 69(3):158–62.

[Dalzell et al., 1996] Dalzell, P., Adams, T., and Polunin, N. (1996). Coastal fisheries in the Pacific Islands. *Oceanography and Marine Biology: an annual review.*, 34:395–531.

[Darling et al., 2012] Darling, E. S., Alvarez-Filip, L., Oliver, T. A., Mcclanahan, T. R., and Cote, I. M. (2012). Evaluating life-history strategies of reef corals from species traits. *Ecology Letters*, 15(12):1378–1386.

[Dickie, 2005] Dickie, R. a. (2005). Indigenous Traditions and Sacred Ecology in the Pacific Islands. *Oceania*, pages 1–9.

[Dieckmann et al., 2000] Dieckmann, U., Law, R., and Metz, J. (2000). *The geometry of ecological interactions: simplifying spatial complexity*. University Press, Cambridge, UK.

[Dizon and Yap, 2006] Dizon, R. T. and Yap, H. T. (2006). Understanding coral reefs as complex systems : degradation and prospects for recovery. *Scientia Marina*, 70(2):219–226.

[Done, 1999] Done, T. J. (1999). Coral Community Adaptability to Environmental Change at the Scales of Regions , Reefs and Reef Zones. *American Zoologist*, 39(1):66–79.

[Dornelas et al., 2017] Dornelas, M., Madin, J. S., Baird, A. H., and Connolly, S. R. (2017). Allometric growth in reef-building corals. *Proceedings of the Royal Society B: Biological Sciences*, 284(1851):20170053.

[Dürr and Pascht, 2017] Dürr, E. and Pascht, A., editors (2017). *Environmental Transformations and Cultural Responses Ontologies, Discourses, and Practices in Oceania*. Palgrave Macmillan US.

[Edmunds, 1999] Edmunds, P. J. (1999). The role of colony morphology and substratum inclination in the success of Millepora alcicornis on shallow coral reefs. *Coral Reefs*, 18(2):133–140.

[Edwards et al., 2017] Edwards, C., Eynaud, Y., Williams, G., Pedersen, N., Zgliczynski, B., Gleason, A., Smith, J., and Sandin, S. (2017). Large-area imaging reveals biologically-driven non-random spatial patterns of corals at a remote reef. *Coral Reefs*.

[Elahi and Edmunds, 2007] Elahi, R. and Edmunds, P. J. (2007). Consequences of fission in the coral Siderastrea siderea: growth rates of small colonies and clonal input to population structure. *Coral Reefs*, 26(2):271–276.

[Eynaud et al., 2016] Eynaud, Y., McNamara, D. E., and Sandin, S. A. (2016). Herbivore space use influences coral reef recovery. *Royal Society Open Science*, 3:160262.

[Fabricius, 2005] Fabricius, K. (2005). Effects of terrestrial runoff on the ecology of corals and coral reefs: Review and synthesis. *Mar Pollut Bull*, 50(2):125–146.

[Ferrari et al., 2012] Ferrari, R., Gonzalez-Rivero, M., and Mumby, P. (2012). Size matters in competition between corals and macroalgae. *Marine Ecology Progress Series*, 467:77–88.

[Ferse et al., 2010] Ferse, S. C., Máñez Costa, M., Máñez, K. S., Adhuri, D. S., and Glaser, M. (2010). Allies, not aliens: increasing the role of local communities in marine protected area implementation. *Environmental Conservation*, 37(01):23–34.

[Friedlander and Parrish, 1998] Friedlander, A. M. and Parrish, J. D. (1998). Habitat characteristics affecting fish assemblages on a Hawaiian coral reef. *Journal of Experimental Marine Biology and Ecology*, 224(1):1–30.

[Fung, 2009] Fung, T. (2009). *Local scale models of coral reef ecosystems for scenario testing and decision support*. Doctoral, University College London.

[Fung et al., 2011] Fung, T., Seymour, R. M., and Johnson, C. R. (2011). Alternative stable states and phase shifts in coral reefs under anthropogenic stress. *Ecology*, 92(4):967–82.

[Furby et al., 2017] Furby, K. A., Smith, J. E., and Sandin, S. A. (2017). Porites superfusa mortality and recovery from a bleaching event at Palmyra Atoll, USA. *PeerJ*.

[Garvie, 2007] Garvie, M. R. (2007). Finite-difference schemes for reaction-diffusion equations modeling predator-prey interactions in Matlab. *Bulletin of Mathematical Biology*, 69(3):931–956.

[Gigerenzer and Gaissmaier, 2011] Gigerenzer, G. and Gaissmaier, W. (2011). Heuristic Decision Making. *Annual Review of Psychology*, 62(1):451–482.

[Gove et al., 2013] Gove, J. M., Williams, G. J., McManus, M. A., Heron, S. F., Sandin, S. A., Vetter, O. J., and Foley, D. G. (2013). Quantifying climatological ranges and anomalies for pacific coral reef ecosystems. *PloS one*, 8(4):e61974.

[Graeber, 2001] Graeber, D. (2001). *Toward An Anthropological Theory of Value: The false coin of our own dreams*. Palgrave, New York, NY.

[Gray et al., 2006] Gray, R., Fulton, E., Little, R., and Scott, R. (2006). CSIRO North West Shelf Joint Environmental Management Study: Ecosystem model specification within an agent based framework. Technical Report 16, CSIRO North West Shelf Joint Environmental Management Study, Australia.

[Grim, 2001] Grim, J. A. (2001). *Indigenous Traditions and Ecology*. Harvard University Press, Cambridge, MA.

[Grimes et al., 2015] Grimes, D. J., Cortale, N., Baker, K., and McNamara, D. E. (2015). Nonlinear forecasting of intertidal shoreface evolution. *Chaos*, 25(10):1–9.

[Guin et al., 2015] Guin, L. N., Chakravarty, S., and Mandal, P. K. (2015). Existence of spatial patterns in reaction - diffusion systems incorporating a prey refuge. *Nonlinear Analysis: Modelling and Control*, 20(4):509–527.

[Hanlon, 1994] Hanlon, D. (1994). Patterns of Colonialism in Micronesia to 1942. In *The History of the Pacific Islands in the Twentieth Century*, pages 93–118. University of Hawai'i Press, Honolulu, howe, kerr edition.

[Harrington et al., 2004] Harrington, L., Fabricius, K., De'ath, G., and Negri, A. (2004). Recognition and selection of settlement substrata determine post-settlement survival in corals. *Ecology*, 85:3428–3437.

[Hart and Marshall, 2009] Hart, S. P. and Marshall, D. J. (2009). Spatial arrangement affects population dynamics and competition independent of community composition. *Ecology*, 90(6):1485–1491.

[Hastings, 2004] Hastings, A. (2004). Transients: the key to long-term ecological understanding? *Trends in ecology & evolution*, 19(1):39–45.

[Hastings, 2010] Hastings, A. (2010). Timescales, dynamics, and ecological understanding. *Ecology*, 91(12):3471–3480.

[Hastings and Higgins, 1994] Hastings, A. and Higgins, K. (1994). Persistence of transients in spatially structured ecological models. *Science*, 263(1992):1992–1995.

[Hatcher, 1997] Hatcher, B. G. (1997). Coral reef ecosystems: how much greater is the whole than the sum of the parts? *Coral Reefs*, 16:S77–S91.

[Hau'ofa, 1998] Hau'ofa, E. (1998). The Ocean in Us. *The Contemporary Pacific*, 10(2):391–410.

[Hezel, 2001] Hezel, F. (2001). *The New Shape of Old Island Cultures*. University of Hawai'i Press, Honolulu.

[Hezel, 2003] Hezel, F. (2003). *Strangers in Their Own Land: A Century of Colonial Rule in the Caroline and Marshall Islands*. University of Hawai'i Press, Honolulu.

[Hezel, 2013] Hezel, F. X. (2013). *Making Sense of Micronesia: The Logic of Pacific Island Culture*. University of Hawai'i Press, Honolulu.

[Highsmith, 1982] Highsmith, R. (1982). Reproduction by fragmentation in corals. *Ecol. Prog. Ser.*, 7:207–226.

[Hilborn and Mangel, 1997] Hilborn, R. and Mangel, M. (1997). *The ecological detective: confronting models with data*. Princeton University Press, Princeton, New Jersey, USA.

[Hixon, 1991] Hixon, M. (1991). Predation as a process structuring coral reef fish communities. In Sale, P., editor, *The Ecology of Fishes on Coral Reefs*, pages 475–508. Academic Press, Inc., San Diego.

[Hughes, 1984] Hughes, T. (1984). Population dynamics based on individual size rather than age: a general model with a reef coral example. *American Naturalist*, 123(6):778–795.

[Hughes, 1994] Hughes, T. (1994). Catastrophes, phase shifts, and large-scale degradation of a Caribbean coral reef. *Science*, 77(September 1994):1547–1551.

[Hughes, 1996] Hughes, T. (1996). Demographic approaches to community dynamics: a coral reef example. *Ecology*, 77(7):2256–2260.

[Hughes et al., 2003] Hughes, T., Baird, A., Bellwood, D., Card, M., Connolly, S., Folke, C., Grosberg, R., Hoegh-Guldberg, O., Jackson, J. B. C., Kleypas, J., Lough, J. M., Marshall, P., Palumbi, S. R., Pandolfi, J. M., Rosen, B., and Roughgarden, J. (2003). Climate change, human impacts, and the resilience of coral reefs. *Science*, 301(5635):929–933.

[Hughes et al., 2000] Hughes, T., Baird, A., Dinsdale, E., Moltschaniwskyj, N., Pratchett, M., Tanner, J., and Willis, B. (2000). Supply-side ecology works both ways: the link between benthic adults, fecundity, and larval recruits. *Ecology*, 81(8):2241–2249.

[Hughes and Jackson, 1985] Hughes, T. and Jackson, J. (1985). Population dynamics and life histories of foliaceous corals. *Ecological monographs*, 55(2):141–166.

[Hughes and Jackson, 1980] Hughes, T. and Jackson, J. B. C. (1980). Do Corals Lie About Their Age? Some Demographic Consequences of Partial Mortality, Fission, and Fusion. *Science*, 209:713–715.

[Hughes et al., 1992] Hughes, T. P., Ayre, D., and Connell, J. H. (1992). The evolutionary ecology of corals. *Trends in Ecology and Evolution*, 7(9):292–295.

[Humann and Deloach, 2001] Humann, P. and Deloach, N. (2001). *Reef Coral Identification*. New World Publications, 2 edition.

[Idjadi and Karlson, 2007] Idjadi, J. A. and Karlson, R. H. (2007). Spatial arrangement of competitors influences coexistence of reef-building corals. *Ecology*, 88(10):2449–54.

[Iwamura et al., 2016] Iwamura, T., Lambin, E. F., Silvius, K. M., Luzar, J. B., and Fragoso, J. M. V. (2016). Socio-environmental sustainability of indigenous lands: Simulating coupled human-natural systems in the Amazon. *Frontiers in Ecology and the Environment*, 14(2):77–83.

[Jackson and Coates, 1986] Jackson, J. and Coates, A. (1986). Life cycles and evolution of clonal (modular) animals. *Philosophical Transactions of the Royal Society of London B: Biological Sciences*, 313:7–22.

[Jackson, 1977] Jackson, J. B. C. (1977). Competition on marine hard substrata: the adaptive significance of solitary and colonial strategies. *American Naturalist*, 111:743–767.

[Jager et al., 2000] Jager, W., Janssen, M. A., De Vries, H. J. M., De Greef, J., and Vlek, C. A. J. (2000). The human actor in ecological-economic models: Behaviour in commons dilemmas: Homo economicus and Homo psychologicus in an ecological-economic model. *Ecological Economics*, 35:357–379.

[Jager and Mosler, 2007] Jager, W. and Mosler, H. (2007). Simulating human behavior for understanding and managing environmental resource use. *Journal of Social Issues*, 63(1):97–116.

[Johannes, 1981] Johannes, R. E. (1981). *Words of the lagoon: fishing and marine lore in the Palau District of Micronesia*. University of California Press, Berkeley.

[Kareiva and Wennergren, 1995] Kareiva, P. and Wennergren, U. (1995). Connecting landscape patterns to ecosystem and population processes. *Nature*, 373:299–302.

[Karlson et al., 2007] Karlson, R. H., Cornell, H. V., and Hughes, T. P. (2007). Aggregation influences coral species richness at multiple spatial scales. *Ecology*, 88(1):170–7.

[Kayal et al., 2015] Kayal, M., Vercelloni, J., Wand, M. P., and Adjeroud, M. (2015). Searching for the best bet in life-strategy: A quantitative approach to individual performance and population dynamics in reef-building corals. *Ecological Complexity*, 23:73–84.

[Kealiikanakaoleohaililani and Giardina, 2015] Kealiikanakaoleohaililani, K. and Giardina, C. P. (2015). Embracing the sacred: an indigenous framework for tomorrow's sustainability science. *Sustainability Science*, 11(1):57–67.

[Kennel et al., 1992] Kennel, M. B., Brown, R., and Abarbanel, H. D. I. (1992). Determining embedding dimension for phase-space reconstruction using a geometrical construction. *Physical Review A*, 45(6):3403–3411.

[Kim and Lasker, 1998] Kim, K. and Lasker, H. R. (1998). Allometry of Resource Capture in Colonial Cnidarians and Constraints on Modular Growth. *Functional Ecology*, 12(4):646–654.

[King and Stewart, 1996] King, D. a. and Stewart, W. P. (1996). Ecotourism and commodification: protecting people and places. *Biodiversity and Conservation*, 5:293–305.

[Kittinger et al., 2012] Kittinger, J. N., Finkbeiner, E. M., Glazier, E. W., and Crowder, L. B. (2012). Human Dimensions of Coral Reef Social-Ecological Systems. *Ecology and Society*, 17(4):17.

[Kittinger et al., 2011] Kittinger, J. N., Pandolfi, J. M., Blodgett, J. H., Hunt, T. L., Jiang, H., Maly, K., McClenachan, L. E., Schultz, J. K., and Wilcox, B. A. (2011). Historical reconstruction reveals recovery in Hawaiian coral reefs. *PLoS ONE*, 6(10).

[Klausmeier, 1999] Klausmeier, C. (1999). Regular and Irregular Patterns in Semiarid Vegetation. *Science*, 284(5421):1826–1828.

[Knowlton and Jackson, 2008] Knowlton, N. and Jackson, J. B. C. (2008). Shifting baselines, local Impacts, and global change on coral reefs. *PLoS biology*, 6:e54.

[Kramer, 2008] Kramer, D. B. (2008). Adaptive Harvesting in a Multiple-Species Coral-Reef Food Web. *Ecology and Society*, 13(1).

[Langmead and Sheppard, 2004] Langmead, O. and Sheppard, C. (2004). Coral reef community dynamics and disturbance: a simulation model. *Ecological Modelling*, 175(3):271–290.

[Lehman and Tilman, 1997] Lehman, C. L. and Tilman, D. (1997). Competition in Spatial Habitats. In Tilman, D. and Kareiva, P., editors, *Spatial Ecology: the role of space in population dynamics and interspecific competition. Monographs*

in Population Biology, chapter 8, pages 185–203. Princeton University Press, Princeton, New Jersey.

[Little et al., 2007] Little, L., Punt, A., Mapstone, B., Pantus, F., Smith, A., Davies, C., and McDonald, A. (2007). ELFSim - A model for evaluating management options for spatially structured reef fish populations: An illustration of the larval subsidy effect. *Ecological Modelling*, 205(3-4):381–396.

[Liu et al., 2007] Liu, J., Dietz, T., Carpenter, S. R., Alberti, M., Folke, C., Moran, E., Pell, A. N., Deadman, P., Kratz, T., Lubchenco, J., Ostrom, E., Ouyang, Z., Provencher, W., Redman, C. L., Schneider, S. H., and Taylor, W. W. (2007). Complexity of coupled human and natural systems. *Science (New York, N.Y.)*, 317(5844):1513–6.

[Liu et al., 2014] Liu, Q.-X., Herman, P. M. J., Mooij, W. M., Huisman, J., Scheffer, M., Olff, H., and van de Koppel, J. (2014). Pattern formation at multiple spatial scales drives the resilience of mussel bed ecosystems. *Nature communications*, 5:5234.

[MacArthur, R. H. & Wilson, 1967] MacArthur, R. H. & Wilson, E. O. (1967). *The Theory of Island Biogeography*. Princeton Univ. Press, Princeton, New Jersey.

[Mangubhai et al., 2012] Mangubhai, S., Erdmann, M. V., Wilson, J. R., Huffard, C. L., Ballamu, F., Hidayat, N. I., Hitipeuw, C., Lazuardi, M. E., Muhajir, Pada, D., Purba, G., Rotinsulu, C., Rumetna, L., Sumolang, K., and Wen, W. (2012). Papuan Bird's Head Seascape: Emerging threats and challenges in the global center of marine biodiversity. *Marine Pollution Bulletin*, 64(11):2279–2295.

[Maragos et al., 1996] Maragos, Crosby, and McManus (1996). Coral Reefs and Biodiversity: A Critical and Threatened Relationship. *Oceanography*, 9(1):83–99.

[McClanahan, 1995] McClanahan, T. (1995). A coral reef ecosystem-fisheries model: impacts of fishing intensity and catch selection on reef structure and processes. *Ecological Modelling*, 80(1):1–19.

[McNamara and Werner, 2008] McNamara, D. E. and Werner, B. T. (2008). Coupled barrier island-resort model: 1. Emergent instabilities induced by strong human-landscape interactions. *Journal of Geophysical Research*, 113(F1):F01016.

[Melbourne-Thomas et al., 2011a] Melbourne-Thomas, J., Johnson, C. R., Fung, T., Seymour, R. M., Chérubin, L. M., Arias-González, J. E., and Fulton, E. a. (2011a). Regional-scale scenario modeling for coral reefs: a decision support tool to inform management of a complex system. *Ecological applications*, 21(4):1380–98.

[Melbourne-Thomas et al., 2011b] Melbourne-Thomas, J., Johnson, C. R., Perez, P., Eustache, J., Fulton, E. A., and Cleland, D. (2011b). Coupling Biophysical and Socioeconomic Models for Coral Reef Systems in Quintana Roo , Mexican Caribbean. *Ecology and Society*, 16(3):23.

[Mena et al., 2011] Mena, C. F., Walsh, S. J., Frizzelle, B. G., Xiaozheng, Y., and Malanson, G. P. (2011). Land Use Change on Household Farms in the Ecuadorian Amazon: Design and Implementation of an Agent-Based Model. *Applied geography (Sevenoaks, England)*, 31(1):210–222.

[Meron, 2016] Meron, E. (2016). Pattern formation - A missing link in the study of ecosystem response to environmental changes. *Mathematical Biosciences*, 271:1–18.

[Michener et al., 2003] Michener, W., Baerwald, T., Firth, P., Palmer, M., Rosenberger, J., and Sandlin, E. (2003). Defining and unraveling biocomplexity. *Bioscience*, 51(12):1018–1023.

[Mistr and Bercovici, 2003] Mistr, S. and Bercovici, D. (2003). A Theoretical Model of Pattern Formation in Coral Reefs. *Ecosystems*, 6(1):0061–0074.

[Montes De Oca Munguia et al., 2009] Montes De Oca Munguia, O., Harmsworth, G., Young, R., and Dymond, J. (2009). The Use of an Agent-Based Model to Represent Maori Cultural Values. In *18th World IMACS / MODSIM Congress*, number July, pages 2849–2855, Cairns, Australia.

[Mumby and Dytham, 2006] Mumby, P. and Dytham, C. (2006). Metapopulation dynamics of hard corals. In Kritzer, J. and Sale, P., editors, *Marine metapopulations*, chapter 5. Academic Press.

[Mumby, 2006] Mumby, P. J. (2006). The impact of exploiting grazers (Scaridae) on the dynamics of Caribbean coral reefs. *Ecological applications*, 16(2):747–69.

[Mumby et al., 2007] Mumby, P. J., Hastings, A., and Edwards, H. J. (2007). Thresholds and the resilience of Caribbean coral reefs. *Nature*, 450(7166):98–101.

[Murawski et al., 2007] Murawski, S., Methot, R., and Tromble, G. (2007). Commentary: Biodiversity Loss in the Ocean : How Bad Is It? *Science*.

[Murdoch, 2007] Murdoch, T. (2007). *A Functional Group Approach for Predicting the Composition of Hard Coral Assemblages in Florida and Bermuda*. Phd dissertation, University of South Alabama, Alabama.

[Murdoch and Aronson, 1999] Murdoch, T. J. T. and Aronson, R. B. (1999). Scale-dependent spatial variability of coral assemblages along the Florida Reef Tract. *Coral Reefs*, 18(4):341–351.

[Murrell et al., 2001] Murrell, D. J., Purves, D. W., and Law, R. (2001). Uniting pattern and process in plant ecology. *Trends in Ecology and Evolution*, 16(10):529–530.

[Nicolis, 1995] Nicolis, G. (1995). *Introduction to Nonlinear Science*. Cambridge University Press, Cambridge.

[Nietschmann, 1997] Nietschmann, B. (1997). Protecting Indigenous Coral Reefs and Sea Territories, Miskito Coast, RAAN, Nicaragua. In Stevens, S., editor, *Conservation through Cultural Suvival*, chapter 7. Island Press, Washington, DC.

[Nyström et al., 2000] Nyström, M., Folke, C., and Moberg, F. (2000). Coral reef disturbance and resilience in a human-dominated environment. *Trends in ecology & evolution*, 15(10):413–417.

[Okubo and Levin, 2001] Okubo, A. and Levin, S. A. (2001). *Diffusion and Ecological Problems: Modern Perspectives*, volume 82.

[Osinga et al., 2011] Osinga, R., Schutter, M., Griffioen, B., Wijffels, R. H., Verreth, J. a. J., Shafir, S., Henard, S., Taruffi, M., Gili, C., and Lavorano, S. (2011). The biology and economics of coral growth. *Marine Biotechnology*, 13(4):658–71.

[Pandolfi, 2002] Pandolfi, J. (2002). Coral community dynamics at multiple scales. *Coral reefs*, 21(1):13–23.

[Parker et al., 2003] Parker, D. C., Manson, S. M., Janssen, M. a., Hoffmann, M. J., and Deadman, P. (2003). Multi-Agent Systems for the Simulation of Land-Use and Land-Cover Change: A Review. *Annals of the Association of American Geographers*, 93(2):314–337.

[Parlitz and Merkwirth, 2000] Parlitz, U. and Merkwirth, C. (2000). Prediction of spatiotemporal time series based on reconstructed local states. *Physical review letters*, 84(9):1890–1893.

[Parrott, 2002] Parrott, L. (2002). Complexity and the limits of ecological engineering. *Transactions of the ASAE*, 45(5):1697–1702.

[Pearson, 1993] Pearson, J. E. (1993). Complex patterns in a simple system. *Science*, 261(July):9–12.

[Petersen, 2009a] Petersen, G. (2009a). Household and Family , Land and Labor. In *Traditional Micronesian Societies: Adaptation, Integration, and Political Organization in the Central Pacific*, chapter 5. University of Hawai'i Press.

[Petersen, 2009b] Petersen, G. (2009b). *Traditional Micronesian Societies: Adaptation, Integration, and Political Organization*. University of Hawai'i Press, Honolulu.

[Pizzirani, 2016] Pizzirani, S. M. (2016). *A culturally-focused life cycle sustainability assessment: Analysis of forestry value chain options with Maori land owners*. Phd, Massey University.

[Pratchett et al., 2015] Pratchett, M. S., Anderson, K. D., Hoogenboom, M. I. a. O., Widman, E., Baird, A. H., Pandolfi, J. M., Edmunds, P. J., and Lough, J. M. (2015). Spatial, temporal and taxonomic variation in coral growth - implications for the structure and function of coral reef ecosystems. *Oceanography and Marine Biology: An Annual Review*, 53(October):215–296.

[Preece and Johnson, 1993] Preece, A. L. and Johnson, C. R. (1993). Recovery of model coral communities: Complex Behaviours from Interaction of Parameters Operating at different spatial scales. In Green, D. G. and Bossomaier, T., editors, *Complex Systems: from biology to computation*, pages 69–81.

[Rapaport, 1990] Rapaport, M. (1990). Population pressure on coral atolls: Trends and approaching limits. *Atoll Research Bulletin*, (340).

[Raymundo, 2001] Raymundo, L. J. (2001). Mediation of growth by conspecific neighbors and the effect of site in transplanted fragments of the coral Porites attenuata Nemenzo in the Central Philippines. *Coral Reefs*, 20(3):263–272.

[Raymundo and Maypa, 2004] Raymundo, L. J. and Maypa, A. P. (2004). Getting Bigger Faster : Mediation of Size-Specific Mortality Via Fusion in Juvenile Coral Transplants. *Ecological Applications*, 14(1):281–295.

[Reif, 1965] Reif, F. (1965). Elementary kinetic theory of transport processes. In *Fundamentals of statistical and thermal physics*, chapter 12, pages 461–490. McGraw-Hill, New York.

[Rietkerk and van de Koppel, 2008] Rietkerk, M. and van de Koppel, J. (2008). Regular pattern formation in real ecosystems. *Trends in ecology & evolution*, 23(3):169–75.

[Rinkevich, 1995] Rinkevich, B. (1995). Restoration strategies for coral reefs damaged by recreational activities: the use of sexual and asexual recruits. *Restoration Ecology*, 3:241–251.

[Rivera-Collazo et al., 2015] Rivera-Collazo, I., Winter, A., Scholz, D., Mangini, A., Miller, T., Kushnir, Y., and Black, D. (2015). Human adaptation strategies to abrupt climate change in Puerto Rico ca. 3.5 ka. *Holocene*, 25(4):627–640.

[Rothman and Zaleski, 1997] Rothman, D. and Zaleski, S. (1997). *Lattice-Gas Cellular Automata: Simple Models of Complex Hydrodynamics*. Cambridge University Press, New York, NY.

[Rubinstein, 1995] Rubinstein, D. H. (1995). Alcohol is complex factor in changing social ecology of Micronesian families. *Journal of the Pacific Society*, 18(1).

[Rubinstein, 2002] Rubinstein, D. H. (2002). Youth Suicide and Social Change in Micronesia.

[Ruddle, 1988] Ruddle, K. (1988). Social Principles Underlying Traditional Inshore Fishery Management Systems in the Pacific Basin. *Marine Resource Economics*, 5(4):351–363.

[Ruddle et al., 1992] Ruddle, K., Hviding, E., and Johannes, R. E. (1992). Marine Resources Management in the Context of Customary Tenure. *Marine Resource Economics*, 7(4):249–273.

[Ruddle and Johannes, 1984] Ruddle, K. and Johannes, R. E. (1984). Traditional Resource Management in the Pacific Basin: An Anthology.

[Ruiz Sebastián and McClanahan, 2013] Ruiz Sebastián, C. and McClanahan, T. R. (2013). Description and validation of production processes in the coral reef ecosystem model CAFFEE (Coral-Algae-Fish-Fisheries Ecosystem Energetics) with a fisheries closure and climatic disturbance. *Ecological Modelling*, 263:326–348.

[Sandin and McNamara, 2011] Sandin, S. A. and McNamara, D. E. (2011). Spatial dynamics of benthic competition on coral reefs. *Oecologia*, 168:1079–1090.

[Schmitz, 2010] Schmitz, O. J. (2010). Spatial dynamics and ecosystem functioning. *PLoS biology*, 8(5):e1000378.

[Sebens, 1987] Sebens, K. (1987). The Ecology Of Indeterminate Growth In Animals. *Annual Review of Ecology and Systematics*, 18(1):371–407.

[Shackeroff et al., 2009] Shackeroff, J., Hazen, E., and Crowder, L. (2009). The oceans as peopled seascapes. In McLeod, K. and Leslie, H., editors, *Ecosystem-based management for the oceans: resilience approaches.*, chapter 3. Island Press, Washington, DC.

[Shafer, 2007] Shafer, J. (2007). *Agent-based simulation of a recreational coral reef fishery: linking ecological and social dynamics*. Doctoral, University of Hawai'i.

[Silvertown et al., 1992] Silvertown, J., Holtier, S., Johnson, J., and Dale, P. (1992). Cellular automaton models of interspecific competition for space - the effect of pattern on process. *Journal of Ecology*, 80:527–534.

[Sleeman et al., 2005] Sleeman, J. C., Boggs, G. S., Radford, B. C., and Kendrick, G. A. (2005). Using Agent-Based Models to Aid Reef Restoration: Enhancing Coral Cover and Topographic Complexity through the Spatial Arrangement of Coral Transplants. *Restoration Ecology*, 13(4):685–694.

[Smith and Wishnie, 2000] Smith, E. A. and Wishnie, M. (2000). Conservation and Subsistence in Small -Scale Societies. *Annual Review of Anthropology*, 29:493–524.

[Spalding et al., 2001] Spalding, M., Ravilious, C., and Green, E. (2001). *World Atlas of Coral Reefs*. University of California Press, Berkely, USA.

[Stearns, 1992] Stearns, S. C. (1992). *The Evolution of Life Histories*. Oxford University Press, London.

[Stoll and Prati, 2001] Stoll, P. and Prati, D. (2001). Intraspecific aggregation alters competitive interactions in experimental plant communities. *Ecology*, 82(2):319–327.

[Sugihara and May, 1990] Sugihara, G. and May, R. (1990). Nonlinear forecasting as a way of distinguishing chaos from measurement error in time series. *Nature*, 344(6268):734–741.

[Sullivan and Haklay, 2000] Sullivan, D. O. and Haklay, M. (2000). Agent-based models and individualism. pages 1–20.

[Tanner, 2000] Tanner, J. (2000). Stochastic density dependence in population size of a benthic clonal invertebrate: the regulating role of fission. *Oecologia*, 122:514–520.

[Tanner, 2001] Tanner, J. (2001). The influence of clonality on demography: patterns in expected longevity and survivorship. *Ecology*, 82(7):1971–1981.

[Tarnita et al., 2017] Tarnita, C. E., Bonachela, J. A., Sheffer, E., Guyton, J. A., Coverdale, T. C., Long, R. A., and Pringle, R. M. (2017). A theoretical foundation for multi-scale regular vegetation patterns. *Nature*, 541(7637):398–401.

[Teaiwa, 2008] Teaiwa, T. K. (2008). Globalizing and Gendered Forces: The Contemporary Militarization of Pacific/Oceania. In Ferguson, K. E. and Mironescu, M., editors, *Gender and Globalization in Asia and the Pacific*, pages 318–332. University of Hawai'i Press, Honolulu.

[Trygonis and Sini, 2012] Trygonis, V. and Sini, M. (2012). photoQuad: A dedicated seabed image processing software, and a comparative error analysis of four photoquadrat methods. *Journal of Experimental Marine Biology and Ecology*, 424-425:99–108.

[Upadhyay et al., 2008] Upadhyay, R. K., Kumari, N., and Rai, V. (2008). Wave of Chaos and Pattern Formation in Spatial Predator-Prey Systems with Holling Type IV Predator Response. *Mathematical Modelling of Natural Phenomena*, 3(4):71–95.

[Van Duyl, 1985] Van Duyl, F. C. (1985). *Atlas of the Living Reefs of Curacao and Bonaire (Netherland Antilles)*. PhD thesis.

[van Woesik et al., 2012] van Woesik, R., Franklin, E., O'Leary, J., McClanahan, T., Klaus, J., and Budd, A. (2012). Hosts of the Plio-Pleistocene past reflect modern-day coral vulnerability. *Proc. R. Soc. Lond., Ser. B: Biol. Sci.*, 279:2448–2456.

[Vermeij, 2012] Vermeij, M. (2012). The current state of Curacao's Coral Reefs. Technical report, CARMABI, Willemstad.

[Vermeij and Sandin, 2008] Vermeij, M. and Sandin, S. (2008). Density-dependent settlement and mortality structure the earliest life phases of a coral population. *Ecology*, 89:1994–2004.

[Ward and Proctor, 1980] Ward, R. and Proctor, A. (1980). The political context. In *South Pacific aqriculture: Choices and constraints, South Pacific aqricultural survey*, pages 137–156. ANU, Canberra, Australia.

[Wells, 1957] Wells, J. (1957). Corals. *Geological Society of America Memoirs*, 67:1087–1104.

[Werner, 1999] Werner, B. (1999). Complexity in natural landform patterns. *Science*, 284(April):102–104.

[Werner, 2003] Werner, B. (2003). Modeling landforms as self-organized, hierarchical dynamical systems. *Prediction in geomorphology*, pages 133–150.

[Werner, 2012] Werner, B. (2012). Complexity and culture (SIO190).

[Werner and Hicks, 2014] Werner, B. T. and Hicks, D. E. (2014). Mexico-US Border as a Complex System.

[Werner and McNamara, 2007] Werner, B. T. and McNamara, D. E. (2007). Dynamics of coupled human-landscape systems. *Geomorphology*, 91(3-4):393–407.

[Zibechi, 2010] Zibechi, R. (2010). *Dispersing Power: Social Movements as Anti-state Forces*. AK Press, Oakland, CA.

[Zibechi, 2012] Zibechi, R. (2012). *Territories in Resistance*. AK Press, Oakland, CA.

[Zilberberg and Edmunds, 2001] Zilberberg, C. and Edmunds, P. (2001). Competition among small colonies of Agaricia: the importance of size asymmetry in determining competitive outcome. *Marine Ecology Progress Series*, 221:125–133.